NBSIR 79-1598

Models for the Migration of Paraffinic Additives in Polyethylene

L. E. Smith, I. C. Sanchez, S. S. Chang, and F. L. McCrackin

Polymer Science and Standards Division
Center for Materials Science
National Bureau of Standards
Washington, D.C. 20234

Annual Report for the Period
October 1, 1977 - September 30, 1978

Issued January 1979

NBSIR 79-1598

MODELS FOR THE MIGRATION OF PARAFFINIC ADDITIVES IN POLYETHYLENE

L. E. Smith, I. C. Sanchez, S. S. Chang, and F. L. McCrackin

Polymer Science and Standards Division
Center for Materials Science
National Bureau of Standards
Washington, D.C. 20234

Annual Report for the Period
October 1, 1977 - September 30, 1978

Issued January 1979

U.S. DEPARTMENT OF COMMERCE, Juanita M. Kreps, *Secretary*

Jordan J. Baruch, *Assistant Secretary for Science and Technology*

NATIONAL BUREAU OF STANDARDS, Ernest Ambler, *Director*

ABSTRACT

General physical models of the migration of low molecular weight species in polymer matrices are needed to provide a basis for the efficient regulation of plastics used in food contact applications. This report presents the first year's progress on a project containing both theoretical and experimental elements aimed at producing such models. Using a modified equation of state approach, models have been developed for estimating the equilibrium partitioning of a diffusant in a polymer at a temperature above its glass transition in contact with a finite volume of solvent. Some possible new approaches to a diffusion theory based on volume fluctuations were outlined. Model calculations using diffusion equations have been made for the extraction of additives from polymers with concomitant solvent absorption and for finding a constant extraction temperature equivalent to migration under varying temperature conditions. The migration of an oligomer, ^{14}C-labeled octadecane, from high density linear polyethylene into various solvents at different temperatures was measured in order to elucidate the effects of thickness, temperature, concentration and solvent. Deviations from ideal Fickean kinetics in the experimental results may be attributed to the strong influence of swelling of the polymer on the migration rates and to the possible incorporation of a small portion of the oligomer in the crystalline phase of the polymer.

TABLE OF CONTENTS

iii

I. INTRODUCTION

This report covers progress during the first year of an FDA-sponsored project on additive migration in plastics. The objectives of this project is the elucidation of the physical principles underlying the transport of small molecules in polymers and the development of general material-related models for the prediction of additive migration in food contact applications. Our semi-annual report issued in July, 1978, gave a preliminary evaluation of existing physical models and tabulated available migration data directly applicable to this problem. The current program consists of two separate, but interacting, parts reflected in the major division of this report into theoretical and experimental sections. The theoretical work is aimed at developing and applying current models and concepts to the prediction of the equilibrium and transport properties of polymer-migrant systems. The emphasis has been placed on the most general descriptions of the broadest possible classes of systems in order to elucidate the fundamental physical principles underlying these properties. These theoretical models use basic physical property measurements of the constituent polymers and additives to predict the partitioning and diffusion observed in direct experiments. Other theoretical work applies phenomenological models to the analysis of data from particular experimental configurations, e.g., solution of diffusion equations using boundary conditions applicable to a given geometry.

The second major part of this project uses a series of carefully designed and executed experiments to guide theoretical developments by providing reliable data on well controlled systems. In addition, the experimental program attempts to explore significant deviations from idealized behavior and explore the physical basis for these exceptions. In spite of the recognized importance of migration phenomena, the number of well-studied systems with significant amounts of available data is surprisingly small. This was not only our conclusion following the evaluation of the literature presented in our semi-annual report, but it was also expressly stated in a recent review on migration phenomena in food packaging done for the European Economic Community.*

In order to have the widest possible application, our work has initially focused on polyethylene, the food packaging material used in largest volume. Migration of small molecules through this semi-crystalline polymer occurs almost exclusively through the amorphous regions which are well above their glass transition at any realistic use temperature. We have therefore not dealt as yet with diffusion in the glassy state and its attendant difficulties. Also, food contact is almost always simplified to mean contact with * so-called food simulating solvents. We have followed in this assumption. The validity of this simplification, i.e. the correlation of migration into food stuffs with migration into solvents, is the subject of a Food and Drug Administration contract with the Arthur D. Little Corporation and so will not be considered here.

* G. Haesen and A. Schwarze, "Migration Phenomena in Food Packaging", Commission of the European Communities, Community Reference Bureau, Brussels-Luxembourg, 1978.

II. THEORETICAL MODELS OF ADDITIVE MIGRATION

Migration of minor constituents from a polymeric film to a food or food simulating solvent is controlled by both transport and thermodynamic factors. A valid physical model of migration requires a knowledge of migrant's transport and thermodynamic properties in both polymer and solvent phases. These requisite properties are often very difficult to measure (e.g., diffusion constants). A useful model of migration theoretically predicts these requisite physical parameters from known or easily measurable properties of the polymer/migrant/solvent system.

The general approach that we have adopted in our modeling studies is to first consider migration in "simple systems". In a simple system migration satisfies Fick's two laws of diffusion. Based on the accumulated experience of many others, this type of simple migration occurs in lightly crosslinked amorphous polymers and in semi-crystalline polymers at temperatures above their respective glass transition temperatures, T_g. Simple systems have two distinct advantages: First, since the diffusion is Fickian, one needs only to specify the boundary conditions to solve the diffusion problem. Second, the amorphous polymer or the amorphous component of a semi-crystalline polymer can be treated as an equilibrium liquid. The latter is an important prerequisite for the calculation of the chemical potential of the migrant in the polymer.

The more tractable aspect of the migration problem is the thermodynamic or equilibrium one. As a result most of our effort has been concentrated in this area during the past year. In the first of three theoretical sections, the equilibrium properties of the polymer/migrant/solvent system are addressed. The main objective is to theoretically calculate the equilibrium partitioning of a migrant between polymer and solvent phases. In the second section a new molecular theory of diffusion is outlined. The validity of this theory remains as yet untested. In the third and last section some phenomological aspects of migration in simple systems is considered.

EQUILIBRIUM PARTITIONING

Consider a polymer that initially contains M_o grams of a diffusant in contact with a solvent of finite volume V_s. At long diffusion times, M_∞ grams of diffusant are transferred to the solvent. Using mass balance yields

$$M_\infty / M_o = \alpha / (1 + \alpha) \tag{1}$$

$$\alpha = (V_s / V_p) K \tag{2}$$

$$K = C^s / C^p \tag{3}$$

where C^s and C^p are the __equlibrium__ concentrations (mass/unit volume) of the diffusant in solvent and polymer phases, respectively, K is the equilibrium partition coefficient, V_p is the volume of the amorphous material (it is assumed that the diffusant is excluded from crystalline domains) and C^p refers to the diffusant concentration within the amorphous regions. (Superscripts s and p are used to designate solvent and polymer phases and subscripts are used, only when necessary, to designate species.

At equilibrium, the thermodynamic activity of the diffusant in the polymer a^p will equal the activity a^s of the diffusant in the solvent:

$$a^p = a^s \tag{4}$$

$$\gamma^p \phi^p = \gamma^s \phi^s \tag{5}$$

where γ^s and γ^p are the respective volume fraction activity coefficients. The partition coefficient is defined as

$$K \equiv \phi^s / \phi^p = \gamma^p / \gamma^s \tag{6}$$

Usually the diffusant will be present in low concentrations. In dilute solutions all concentration units (mole fractions, volume fraction, molarity, etc.) are proportional to one another, therefore

$$K = \phi^s / \phi^p = C^s / C^p = \gamma^p(\infty) / \gamma^s(\infty) \tag{7}$$

$$\gamma(\infty) \equiv \lim_{\phi \to 0} \gamma \tag{8}$$

Partitioning with Negligible Solvent Absorption.

According to the well-known Flory-Huggins theory of solutions[1,2] the activity and volume fraction activity coefficient of component 1 in a binary mixture of 1 and 2 are given by

$$\ln a_1 = \ln \phi_1 + (1 - r_1/r_2) \phi_2 + r_1 X_{12} \phi_2^2 \tag{9}$$

$$\ln \gamma_1 = (1 - r_1/r_2) \phi_2 + r_1 X_{12} \phi_2^2 \tag{10}$$

4

where $\phi_1 = 1 - \phi_2$ is the site or volume fraction of component 1, r^1 and r^2 are the respective number of lattice sites occupied by the components, and χ_{12} is a dimensionless, and symmetrical ($\chi_{12} = \chi_{21}$) parameter that characterizes the interaction between the two components. Usually, r_1/r_2 is equated to the ratio of molar volumes and the product $r_1 \chi_{12}$ (designated as χ_1 in reference 1) is treated as an empirical parameter.

For dilute solutions

$$\ln \gamma^p(\infty) = 1 + r_d \chi_p^\infty \tag{11}$$

$$\ln \gamma^s(\infty) = 1 - r_d/r_s + r_d \chi_s^\infty \tag{12}$$

where the subscripts p, s, and d refer to polymer, solvent, and diffusant, respectively; χ_p^∞ and χ_s^∞ are the infinite dilution values of polymer-diffusant and solvent-diffusant interaction parameters. The term r_d/r_p is absent in Eq. (11) because r_p, a parameter proportional to the molecular weight of the polymer, approaches infinity for a crosslinked polymer.

Combining Eqs. (7), (11), and (12) yields

$$\ln K_o = r_d \left(1/r_s + \chi_p^\infty - \chi_s^\infty\right) \tag{13}$$

A zero subscript has been attached to K to remind us that Eq. (13) is only valid when solvent is not absorbed by the polymer.

Partitioning with Solvent Absorption

When solvent is absorbed by the polymer, the polymer phase becomes a ternary solution; the activity of the diffusant in the polymer phase can be written as

$$\ln a^p = \ln \phi_d + (1 - r_d/r_s) \phi_s + \phi_p + r_d (\phi_s \chi_s + \phi_p \chi_p - \phi_s \phi_p \chi_{sp}) \tag{14}$$

where, of course,

$$\phi_d + \phi_s + \phi_p = 1 \tag{15}$$

and χ_{sp} is the solvent-polymer interaction parameter for a solvent concentration of ϕ_s. We will assume that the concentrations ϕ_s and ϕ_p are much larger than the diffusant concentration ϕ_d so that χ_s and χ_p can be replaced by χ_s^∞ and χ_p^∞. In this limit

$$\ln \gamma^p(\infty) = (1 - r_d/r_s) \phi_s + \phi_p + r_d (\phi_s \chi_s^\infty + \phi_p \chi_p^\infty - \phi_s \phi_p \chi_{sp}) \tag{16}$$

Combining Eqs. (7, (12), and (16) yields

$$\ln K = (1 - \phi_s) [\ln K_o - \phi_s r_d \chi_{sp}] \tag{17}$$

Absorption of solvent causes the polymer to swell. Within a swollen polymer, the pressure acting on the solvent is greater than the atmospheric pressure, P_o. The excess pressure π caused by the elastic forces of a crosslinked polymer (crystalline domains act as effective crosslinks) raises the chemical potential of the solvent μ_s within the polymer phase. The condition of equilibrium is

$$\mu_s^o = \mu_s(P_o + \pi) = \mu_s(P_o) + \int_{P_o}^{P_o + \pi} \frac{\partial \mu_s}{\partial P} dP \simeq \mu_s(P_o) + \pi \overline{V}_s \tag{18}$$

where μ_s^o is the chemical potential of pure solvent at P_o and $\overline{V}_s$ is the partial molar volume of the solvent. Since, by definition

$$\ln a_s(P_o) \equiv [\mu_s(P_o) - \mu_s^o] / RT \tag{19}$$

we have by Eq. (9)

$$\ln \phi_s + \phi_p + r_s \chi_{sp} \phi_p^2 = -\pi \overline{V}_s / RT \tag{20}$$

As can be seen from the derivation of Eq. (20), the swelling pressure π is equivalent to the osmotic pressure developed by a non-crosslinked polymer solution of the same concentration. In the absence of significant swelling, this pressure will be relatively small and to a good approximation the right hand side of Eq. (20) can be set equal to zero. Thus, a measurement of the equilibrium absorption of solvent (ϕ_s) yields an approximate experimental value of χ_{sp}:

$$r_s \chi_{sp} \simeq - [\ln \phi_s + \phi_p] / \phi_p^2 \tag{21}$$

If the swelling is appreciable, as it might be for a very good solvent, corrections can be made to Eq. (21) for both crosslinked amorphous polymers[3] and semi-crystalline polymers[4],[5].

Substitution of Eq. (21) into (17) yields

$$\ln K = \ln K_o - \phi_s \left\{ \ln K_o + (r_d / r_s) \left[1 + \ln (1/\phi_s)/(1 - \phi_s) \right] \right\} \tag{22}$$

where it is understood that ϕ_s is the equilibrium amount of absorbed solvent. Notice that $K \to K_0$ as $\phi_s \to 0$ and $K \to 1$ as $\phi_s \to 1$ as it should.

A further check of the self-consistency of Eq. (22) is obtained by considering the partitioning of a diffusant in which the diffusant is radiolabeled (RL) solvent. In this case $\chi_s^\infty = 0$, and $r_d = r_s$. Substituting these results into Eq. (22) or (17) yields

$$\ln K = - \ln \phi_s \qquad (23)$$

The RL solvent should partition exactly as the non-RL solvent. The partition coefficient for the non-RL solvent, K_s, is equal to the volume fraction of the bulk solvent in the solvent phase (unity) divided by the volume fraction of the solvent in the polymer phase (ϕ_s) or

$$K_s = 1/\phi_s \qquad (24)$$

which agrees with the result obtained from Eq. (22) for the RL solvent.

Interaction Parameters

In the original formulation of the Flory-Huggins theory[1], χ_{ij} was strictly an energetic parameter that was proportional to the energy required to form an i-j bond from a i-i and j-j bond. It also had a simple $1/T$ temperature dependence and was independent of solution composition. Experimentally, χ_{ij} often has a large positive entropic component which arises, according to the Flory[6-9] and lattice fluid (LF)[10-13] theories, from differences in the equation of state properties of the pure components.

Both the Flory and LF theories require three equation of state parameters for each pure component which are determined from PVT data. Each component satisfies a theoretical equation of state; the LF equation of state is

$$\tilde{\rho}^2 + \tilde{P} + \tilde{T} \left[\ln(1 - \tilde{\rho}) + (1 - 1/r) \tilde{\rho} \right] = 0 \qquad (25)$$

where $\tilde{T}$, $\tilde{P}$ and $\tilde{\rho}$ are the <u>reduced</u> temperature, pressure, and density. Three equation of state parameters, T^*, P^*, and ρ^*, are used to reduce the experimental temperature, pressure, and mass density of the fluid; r is the number of lattice sites occupied by a molecule and is proportional to its molecular weight, M:

$$r = (P^*/RT^*\rho^*) M \qquad (26)$$

For the LF, equation of state parameters have been tabulated for about 60 low molecular weight fluids[10] and the ten different polymers[12]. Methods for determining these parameters are discussed in the Appendix A.

From the LF theory, the interaction parameters χ_s^∞ and χ_0^∞ required in Eqs. (13) and (22) are given by [13]

$$\chi_s^\infty = \tilde{\rho}_s \Delta P_s^* / P_d^* \tilde{T}_d + (\tilde{\rho}_d - \tilde{\rho}_s) / \tilde{T}_d + \ln(\tilde{\rho}_s / \tilde{\rho}_d) / r_d \qquad (27)$$

$$+ (1 - \tilde{\rho}_s) \ln(1 - \tilde{\rho}_s) / \tilde{\rho}_s - (1 - \tilde{\rho}_d) \ln(1 - \tilde{\rho}_d) / \tilde{\rho}_d$$

and a similar expression holds for $\widetilde{C}_p$ (replaces s by p). The parameter ΔP_S^* which has units of pressure is the only unknown parameter in Eq. (27). All other quantities are calculable from the equation of state properties of the pure components. The physical meaning of ΔP_S^* is that it is a measure of the net change in the energetics that occurs upon mixing solvent and diffusant at the absolute zero of temperature. At absolute zero, the sign of ΔP^* determines the sign of the heat of mixing.

In both the Flory and LF theories, the cohesive energy density of a fluid at absolute zero equals its characteristic pressure, P^*. It is, therefore, convenient to define a dimensionless parameter Δ_s in terms of the characteristic pressures of the pure components:

$$\Delta_s \equiv \Delta P_s^* / (P_s^* + P_d^*); \qquad \Delta_p \equiv \Delta P_p^* / (P_p^* + P_d^*) \qquad (28)$$

Combining Eqs. (13, (27) and (28) yields

$$\ln K_o = r_d \Bigg\{ \Big[\widetilde{\rho}_s [1 - \Delta_s (P_s^* / P_d^* + 1)] - \widetilde{\rho}_p [1 - \Delta_p (P_p^* / P_d^* + 1)] \Big] \widetilde{T}_d^{-1} \qquad (29)$$

$$+ (1 - \widetilde{\rho}_p) \ln (1 - \widetilde{\rho}_p) / \widetilde{\rho}_p - (1 - \widetilde{\rho}_s) \ln (1 - \widetilde{\rho}_s) / \widetilde{\rho}_s + r_d^{-1} \ln (\widetilde{\rho}_p / \widetilde{\rho}_s) + r_s^{-1} \Bigg\}$$

where r_d and r_s are defined by Eq. (26) and $\widetilde{\rho}_s$ and $\widetilde{\rho}_p$ are calculated from the equation of state (25).

Sample Calculations

In principle the diffusant-solvent or the diffusant-polymer interaction parameter can be empirically determined from a single solution datum such as a heat of mixing, a critical temperature, a solution density, etc. However, in some systems intelligent choices of Δ_s and Δ_p can be made from limited data. An example of this kind is the partitioning of the n-alkanes between linear polyethylene (PE) and n-heptane. In Table I, the partition coefficients K_o and K are calculated from Eqs. (29) and (22) for selected n-alkanes at 25°C. Equation of state parameters required in the calculations were obtained from references 8 and 9. For PE, the equilibrium amount of n-heptane absorbed is $\phi_s = 0.26$. Entries enclosed within parentheses are K values and those without are K_o values. Entries that are crossed out with solid lines are considered unlikely values of the partition coefficient; those with broken lines are considered more probable than those crossed out with solid lines, but less probable than the clear entries.

The rationale for selecting Δ_p in the range between 0.01 and 0.03 is based on the calculation of Δ_p for polyisobutylene (PIB) solutions of the n-alkanes from heats of mixing and the experimental result that $K = K_s = 1/0.26 = 3.8$ for n-heptane. For PIB, $\Delta_p = 0.016$ for n-pentane and decreased monotonically with chain length to $\Delta_p = 0.002$ for n-decane[13]. Since PIB and PE are chemically very similar, it is not unreasonable to expect that Δ_p values in the PE/n-alkanes are similar to those in PIB/n-alkanes. Selection of $\Delta_s = 0$ is certainly correct for n-heptane (assumed to be radiolabeled n-heptane) and is probably an excellent approximation for the n-alkanes between pentane and decane. Of course, as the chain length of the n-alkane increases, $\Delta_s \to \Delta_p$ and $\Delta_p \to 0$, which explains the choice of Δ_s and Δ_p values for the partitioning of PE of molecular weight 10^4. Because the partition coefficient is proportional to the chain length of the diffusant [see Eqs. (13) and (22)], the calculated values of the partition coefficient become more uncertain as chain length increases.

In Table II calculated values of K_o are shown for the partitioning of some n-alkanes between linear PE and ethanol. Here the estimates of Δ_s, and consequently K_o, are much more uncertain. However, we have some crude guidelines to go by. We know that the n-alkanes exhibit limited miscibility in ethanol which is qualitatively indicative of a large, positive Δ_s value. Also, because ethanol is polar and PE and the diffusants are non-polar, we can reasonably expect that $\Delta_p < \Delta_s$.

diffusant	0	0.04	0.03	0.02	0.01	0	0.01	0.02	0.03	0.04
n-pentane	9.1 (4.3)	7.0 (3.5)	5.3 (2.9)	4.1 (2.4)	3.1 (1.9)					
n-heptane	13.6 (5.6)	9.6 (4.3)	6.8 (3.3)	4.7 (2.6)	3.3 (2.0)					
n-decane	24.9 (8.3)	15.5 (6.1)	9.7 (4.3)	6.0 (3.0)	3.8 (2.2)					
n-heptadecane		40.4 (11.5)	19.2 (6.6)	9.2 (3.8)	4.4 (2.2)					
linear PE $M = 10^4$					2.5x10^{15} (9.3x10^2)		1.3x10^3 (7.5x10^{-7})	6.7x10^{-10} (6.1x10^{-16})	3.5x10^{-22} (4.9x10^{-25})

Table I   Calculated partition coefficients, K and K, for selected n-alkanes between linear polyethylene and n-heptane at 25° C.

| diffusant | 0.1 | 0.075 | 0.05 | $\leftarrow \Delta_s$ |
	0.025	0.025	0.025	$\leftarrow \Delta_p$
n-pentane	6.1×10^{-2}	1.8×10^{-1}	5.3×10^{-1}	
n-heptane	1.8×10^{-2}	7.5×10^{-2}	3.1×10^{-1}	
n-decane	3.1×10^{-3}	2.1×10^{-2}	1.5×10^{-1}	
n-heptadecane	5.2×10^{-5}	1.1×10^{-3}	2.3×10^{-2}	

Table II Calculated partition coefficients, K_0, for selected n-alkanes between linear polyethylene and ethanol at 25^0 C.

Inspection of Eq. (22) reveals that if $K_O > 1$; i.e., if partitioning favors the solvent phase, absorption of solvent lowers the partition coefficient ($K < K_O$) as is illustrated for the partitioning of the n-alkanes between PE and n-heptane in Table I. This effect on partitioning is best understood by imagining the partitioning to occur in two steps. In the first step the diffusant partitions in the absence of solvent absorption preferentially toward the solvent phase. In the second step, solvent containing some of the diffusant is absorbed by the polymer. Thus, the diffusant is reabsorbed literally on the "coattails" of the solvent.

When $K_O < 1$, Eq. (22) suggests that it is possible for solvent absorption to increase the partition coefficient ($K > K_O$). The exact conditions for this to occur are

$$\chi_s^\infty > 1/r_s + \chi_p^\infty + \phi_p \chi_{sp} = \chi_p^\infty + \ln(1/\phi_s)/r_s(1 - \phi_s) \tag{30}$$

Under these conditions we have a reverse coattail effect. It can be understood as follows: A small K_O implies a poor solvent-diffusant interaction (large positive χ_s^∞) and the diffusant prefers to remain in the polymer phase in the absence of solvent absorption. When solvent is absorbed, the diffusant now "sees" a thermodynamic environment in the polymer phase that is similar to the one in the solvent phase, neither of which it likes. Since the disparity in thermodynamic environments is reduced by solvent absorption, the diffusant tends to redistribute itself more evenly between the two phases.

11

DIFFUSION THEORY

Self-Diffusion

Consider a system of N molecules in a system of macroscopic volume V. The average volume per molecule $\bar{v} = V/N$; the average distance between molecular centers is $\bar{v}^{1/3}$. In the liquid state we can imagine that each molecule in the system is confined to a "cage" formed by neighboring molecules. This cage has an average size of $\bar{v}^{1/3}$ and average volume $\bar{v}$. The cage fluctuates in size with time as is schematically illustrated below:
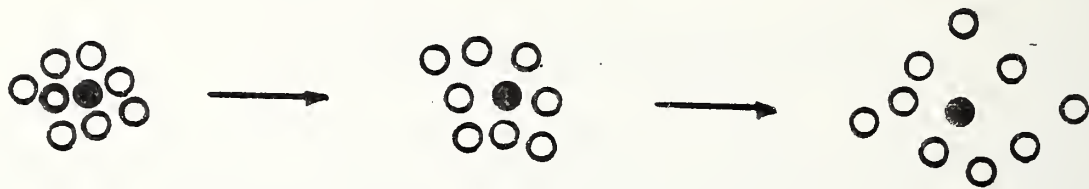
The hypothesis is invoked that a molecule is confined to its cage until the cage volume exceeds a certain critical value v^*. If the cage is larger than v^* the molecule "escapes". Escape followed by capture (collision) constitutes a successful diffusive displacement. This physical picture of diffusion is one in which a molecule spends an average residence time τ in its cage before it escapes and travels a mean distance ℓ before it is captured. The time required for the molecule to travel a distance ℓ is assumed to be much smaller than τ. While confined to its cage, a molecule suffers many molecular collisions and is constantly being displaced, but its average location remains the same in the time interval τ. Below we schematically trace the diffusing path of a molecule. Each straight line segment represents a mean free path; ℓ is the average of the indicated ℓ_i
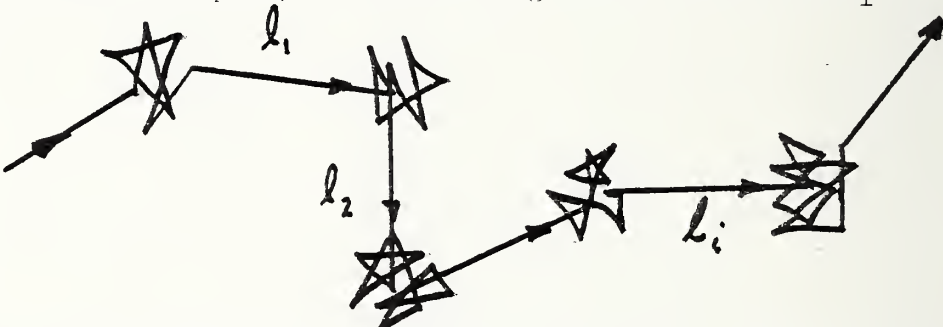
This physical picture of diffusion in liquids is not novel. Cohen and Turnbull[15] have used a very similar physical description in their theory of diffusion.

Let $P(v)dv$ equal the probability that a molecule has a cage volume between v and $v + dv$; $P(v)$ possesses the following properties:

$$\int_0^\infty P(v)dv = 1 \qquad (31)$$

$$\int_0^\infty vP(v)dv = \bar{v} \qquad (32)$$

The probability that the cage volume exceeds v* is

$$P(v > v^{\cdot}) = \int_{v^{\cdot}}^{\infty} P(v) dv \qquad (33)$$

Now radiolabel a very small number of the molecules in the system. Call these N* and their density $\rho^* = N^*/V$. Suppose that their distribution is non-uniform in the x-direction as illustrated below:
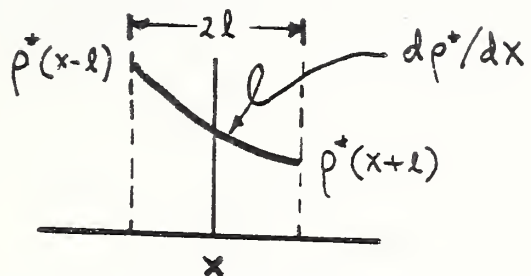
All labeled molecules within a distance l of the plane at x are capable of crossing that plane when they undergo a diffusive displacement. The average velocity $\bar{u}$ of a molecule of mass m at a temperature T is

$$\bar{u} = (kT/m)^{1/2} \qquad (34)$$

by virtue of the equipartition theorem. Roughly 1/3 of the molecules will be moving in the x-direction; 1/6 will be moving in the positive direction, and 1/6 will be moving in the negative direction, but only P(v>v*) of these molecules will be executing diffusive displacements of average length l. The mean number of labeled molecules which in unit time cross a unit area of the plane from the left is

$$J_x = \bar{u} P(v > v^{\cdot}) \left[\rho^{\cdot}(x - l) - \rho^{\cdot}(x + l) \right] / 6 \qquad (35)$$

but

$$\rho^{\cdot}(x - l) \simeq \rho^{\cdot}(x) - \frac{d\rho^{\cdot}}{dx} l$$

$$\rho^{\cdot}(x + l) \simeq \rho^{\cdot}(x) + \frac{d\rho^{\cdot}}{dx} l \qquad (36)$$

and therefore

$$J_x = -D d\rho^{\cdot}/dx \qquad (37)$$

$$D = \bar{u} l P(v > v^{\cdot})/3 \qquad (38)$$

13

That is, the net flux of labeled molecules passing through the plane at x is proportional to the concentration gradient at that point (Fick's first law of diffusion). The proportionality constant D is the diffusion coefficient.

The numerical coefficient of 1/3 in Eq. (38) should not be taken too seriously since our estimate of the number of molecules with velocity components in the x-direction is very crude.

The primary problem is to calculate $P(v)$ and $P(v>v*)$. Cohen and Turnbull[15] assumed that a multinomial distribution of volumes exist in a liquid and proceeded to calculate $P(v)$ from this hypothesis. The disadvantage of this approach is that the calcualted $P(v)$ is not easily related to the physical properties of the liquid. The approach that we adopt is to use classical fluctuation theory to calculate $P(v)$. Bueche[14] has used a similar approach to describe self-diffusion in polymeric liquids. According to fluctuation theory, the distribution of volumes is a Gaussiam function given by

$$P(v) = (2\pi\sigma^2)^{-1/2} \exp\left[-\frac{(v-\bar{v})^2}{2\sigma^2}\right] \qquad (39)$$

$$\sigma^2 = kT\bar{v}\,\beta/N \qquad (40)$$

where β is the isothermal compressibility of the medium. The mean square volume fluctuation equals σ^2. Notice the σ^2 varies inversely with the number of molecules N in the system. We are interested in volume fluctuations on the microscopic scale; i.e., fluctuations associated with a single molecule (N=1). The derivation of Eq. (39) becomes highly approximate for N=1. Nevertheless, we shall employ Eqs. (39) and (40) for $P(v)$ fully aware of its shortcomings.

For N=1, the volume fluctuations predicted by Eq. (40) are still relatively small. For example, for the typical liquid values of T=300K, $\beta=10^{-4}$ bar^{-1} and $\bar{v}=100$ cm^3/mole, $\sigma/\bar{v}$ equals about 0.15 or the volume fluctuations are about 15% of the average molecular volume. Because the distribution is relatively narrow, we can safely extend the limits of integration (for the purposes of normalization) from 0 to ∞ to $-\infty$ to ∞ without introducing appreciable error.

We now have by Eq. (33)

$$P(v>v*) = \left\{1-\text{erf}\left[\frac{v*-\bar{v}}{\sqrt{2}\sigma}\right]\right\}/2$$

$$P(v>v*) = \text{erfc}\left[\frac{v*-\bar{v}}{\sqrt{2}\sigma}\right]/2 \qquad (41)$$

where erf x and erfc x are the error and complementary error functions, respectively. Notice that for

$$v*=\bar{v} \qquad P(v>v*)=1/2 \qquad (42)$$

To complete the calculation of the self-diffusion coefficient we must specify the mean distance ℓ that a molecule travels during a diffusive displacement. One approximation is to assume that $\ell = (v^*)^{1/3}$, but other approximations are possible. One can argue that ℓ should be a unique function of $\bar{v}$ and the molecular collision cross-section σ. Dimensional analysis then suggests that $\ell \sim \bar{v}/\sigma$. This is the functional form for the mean free path of a gas molecule that is calculated from the classical kinetic theory of gases. Using the kinetic theory result ($\ell = \bar{v}/2^{\frac{1}{2}}\sigma$) has the virtue of yielding the correct diffusion coefficient for a gas in the limit $\bar{v} \gg v^* (D = u\ell/3)$.

Diffusion of a Small Molecule in a Polymer

Now consider a system comprised of a polymeric liquid and a trace amount of a small molecule diffusant. The effective volume of the diffusant molecule in the polymer is the diffusant's partial molar volume at infinite dilution $\bar{v}^\infty$. If N_d is the number of diffusant molecules then $\bar{v}^\infty$ is given by

$$\bar{v}^\infty = \lim_{N_d \to 0} \left(\frac{\partial v}{\partial N_d} \right) \tag{43}$$

where V is the volume of polymer + diffusant.

The volume fluctuations that are occurring in this system are characteristic of those occurring in the pure polymer. If we focus attention on a small volume within the polymer of size $\bar{v}^\infty$, the volume fluctuations about this volume would be approximately given by

$$\sigma^2 = kT\beta\bar{v}^\infty \tag{44}$$

where β, of course, is the isothermal compressibility of the polymer liquid. The distribution of volumes about $\bar{v}^\infty$ would be approximately Gaussian with a variance given by Eq. (44). Thus, we can assume that the volume fluctuations that a diffusant molecules "sees" in diffusing through the polymer are those given by Eq. (44) and its diffusion coefficient is

$$D = u(v^*)^{1/3}\,\mathrm{erfc}\left[\frac{v^* - \bar{v}^\infty}{(2kT\beta\bar{v}^\infty)^{1/2}}\right]/6 \tag{45}$$

where ℓ has been taken to be equal to $(v^*)^{1/3}$

Equation (45) embodies all of the physical factors judged important for diffusion in polymers through $v^*, \bar{v}^\infty$, and β; v^* is a unique property of the shape and size of the diffusant; $\bar{v}^\infty$ is the property which depends sensitively on the polymer-diffusant intermolecular interaction; and β is a characteristic property of the polymer.

EXTRACTION OF ADDITIVES WITH SOLVENT ABSORPTION

The rate of migration of an additive from a plastic in contact with a liquid is often increased by simultaneous migration of the liquid in the plastic, that is, by extraction by the liquid. The migration curves for extraction cannot be found by analytical formulas. Therefore, the diffusion equation for extraction has been solved by a finite difference method. The calculated migration curves will first be qualitatively compared with the experimental extraction curve. Later, they will be fit to experimental extraction curves and applied to studies of extraction from plastic containers in use.

Graphical Results

First, the symbols that are used will be defined. Let the diffusion coefficient of the liquid in the plastic be D_ℓ and the diffusion coefficient of the additive be given by

$$D = D_O + k \, c \tag{46}$$

where D_O is the initial diffusion coefficient, k is a constant and c is the concentration of the liquid in the plastic. Because c depends on the position in the plastic and time, D also depends on position and time.

Let c_∞ be the concentration of the liquid in the plastic at infinite time, the equilibrium concentration, and let D_∞ be the corresponding diffusion coefficient of the additive. Then

$$D_\infty = D_O + k \, c_\infty \tag{47}$$

The diffusion coefficient of the additive varies from D_O to D_∞ during its migration.

The migration curves for $D_\ell/D_O = 2$, that is, the liquid diffuses twice as fast as the initial rate for the additive are shown in Fig. 1. The amount of additive, M_t, that has migrated from the plastic to the liquid at time t over the initial amount, M_∞, of additive in the plastic is plotted versus the square root of the reduced time. ℓ is one-half the thickness of the plastic sheet. Curves are given for 4 values of D_∞/D_O. The solid curve for $D_\infty/D_O = 1$ corresponds to zero increase of diffusion of the additive due to liquid absorption. The amount of additive migrated out of the plastic is seen to increase linearly with the square root of time for the first 60% of the migration of the additive. For increasing values of D_∞/D_O, corresponding to increasing diffusion of the additive due to liquid absorption, the migration of the additive increases, as expected. However, the shape of the migration curve does not markedly change; the migration still increases linearly for the first 60% of the migration of the additive.

Fig. 2 shows the migration curves when the liquid diffuses at 10 times the rate of the initial rate of the additive. The migration is somewhat larger for this case, but the migration curves are similar to those of Fig. 1.

The preceeding analysis considered the migration of the liquid in the plastic to be ideal with a constant diffusion coefficient D_ℓ. However, for some systems D_ℓ is expected to increase with increasing concentrations, C_ℓ, of the liquid in the plastic. When D_ℓ is very dependent on concentration, the diffusion of the liquid at a position in the plastic will be very small until the plastic has been "opened up" by the first penetrating liquid. Therefore, the plastic will contain an essentially unswollen region and a highly swollen region, separated by a well defined front. The penetration depth of this front will be proportional

Fig. 1. Amount of migration from a plastic sheet when the surrounding liquid migrates in the sheet at twice the rate of the additive. The curves, reading from the lower to the upper curves, are for D_∞/D_O of 1, 1.5, 2 and 5.
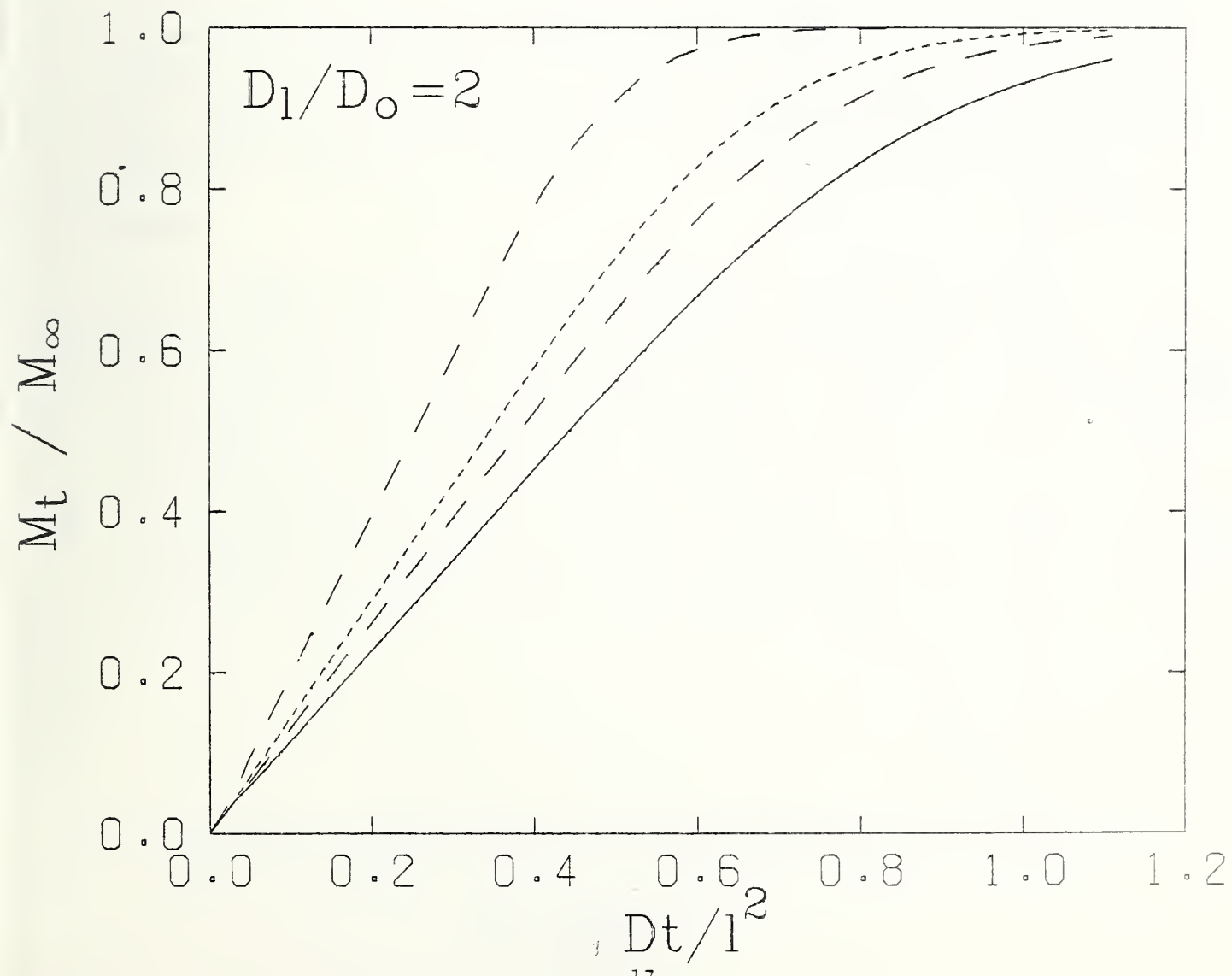
Fig. 2. Amount of migration from a plastic sheet when the surrounding liquid migrates in the sheet at ten times the rate of the additive. The curves, reading from the lower to the upper curves, are for D_∞/D_o of 1, 1.5, 2 and 5.
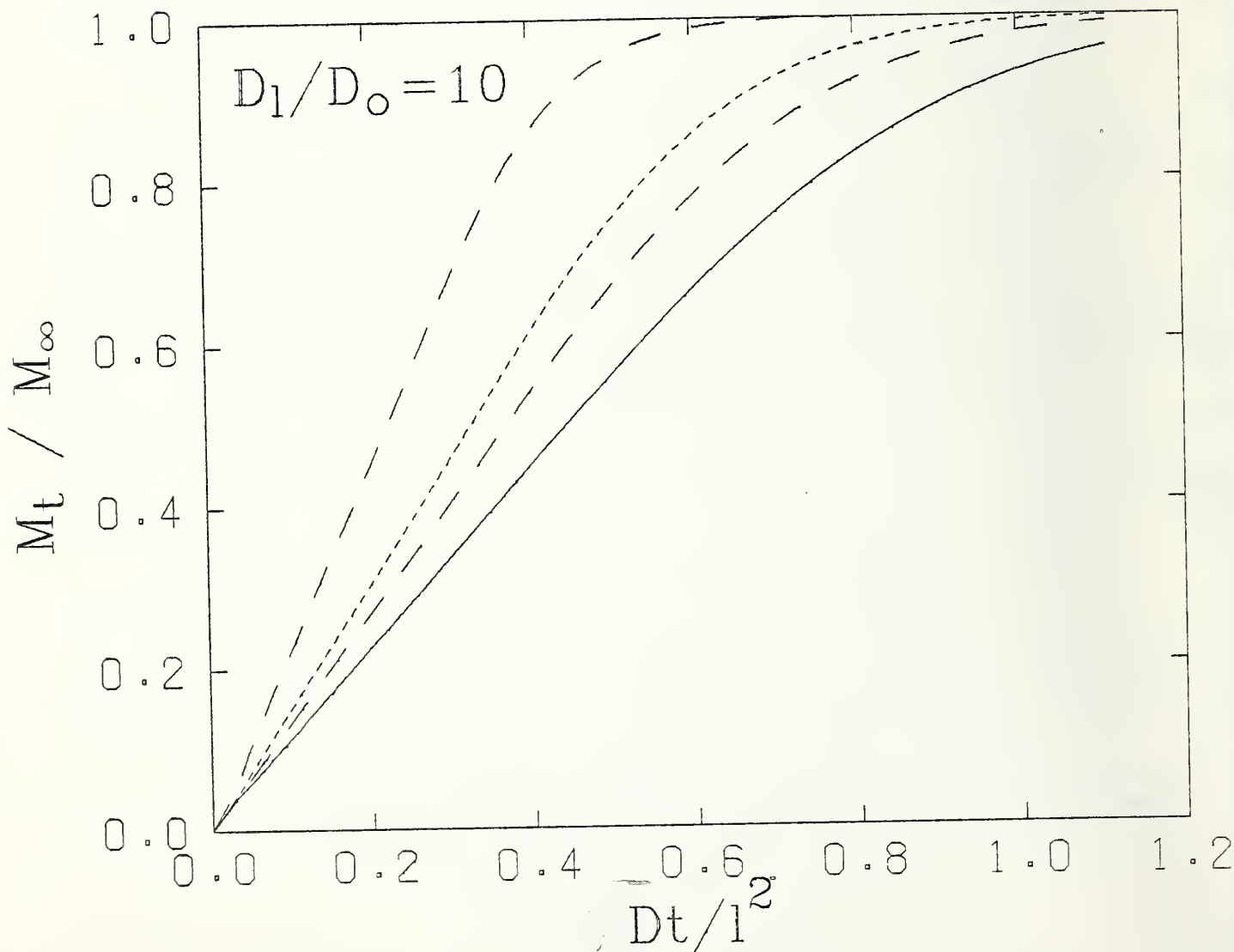
to the square root of time. Fig. 3 shows schematically the concentration distribution of the liquid for three equally spaced times.

The penetration depth of the front is taken to be $w\sqrt{t}$. Fig. 4 shows the migration curves for the additive for this concentration-dependent diffusion of the liquid. The lower solid curve corresponds to zero increase of the additive due to absorption of liquid by the plastic, and is included for comparison with the other curves. The other curves are for $D_\infty/D_0 = 5$ and for values of the reduced parameter $w/\sqrt{D_0}$ of 0.05, 0.1, 0.2 and 0.5, the upper curves correspond to larger values of $w/\sqrt{D_0}$.

The migration at a given time is seen to increase for increasing velocities of the front of the liquid diffusion, corresponding to larger values of w. However, the shape of the migration curve does not change markedly; the curves remain linear for small times.

The effect of non-uniform initial distribution of the additive in the plastic sheet was also calculated. The increase of migration of the additive due to absorption of the surrounding liquid was not included in these calculations.

The three initial distributions of the additive shown in Fig. 5 were considered. The solid line represents a uniform distribution; the dashed line represents a concentration of the additive near the sides of the sheet that is one-half the concentration in the center of the sheet; and the dotted line represents a concentration that increases linearly from zero at the sides of the sheet to a maximum value at the center of the sheet. These distributions were chosen so that they all have the same average concentration.

The migration curves calculated for these distributions are shown in Fig. 6. The amount of migration is proportional to $\sqrt{t}$ for the uniform distribution, as has been previously observed. However, the migration for low concentration of additive at the sides, shown by the dashed curve, is smaller and shows an inflection point for small times. This is similar to some of the experimentally observed migration curves. The migration curve for the dotted triangular distribution shows a pronounced decrease at small times.

Summary

The migration curves of an additive from a plastic have been computed for the case there the rate of migration is increased by the surrounding liquid migrating into the plastic. The migration curves have been computed both for a constant liquid diffusion coefficient and for a liquid diffusion coefficient strongly dependent on the concentration of the liquid in the plastic. Although the rate of migration of the additive was increased by migration of the extracting liquid, the shapes of the migration curves were not markedly different from the case where the migration of the additive in the plastic is not affected by migration of the surrounding liquid into the plastic.

The migration curves have also been calculated for a non-uniform initial concentration distribution of additive in the plastic. The shapes of the migration curves were found to depend on the additive distribution, showing inflection points similar to those observed in some of the experimental migration curves.

Fig. 3. The concentration distribution for three equally spaced times of the
liquid in the plastic for the case that the diffusion of the liquid
is very concentration dependent. The front of penetration of liquid
in the plastic moves a distance $w \sqrt{t}$ in time t.
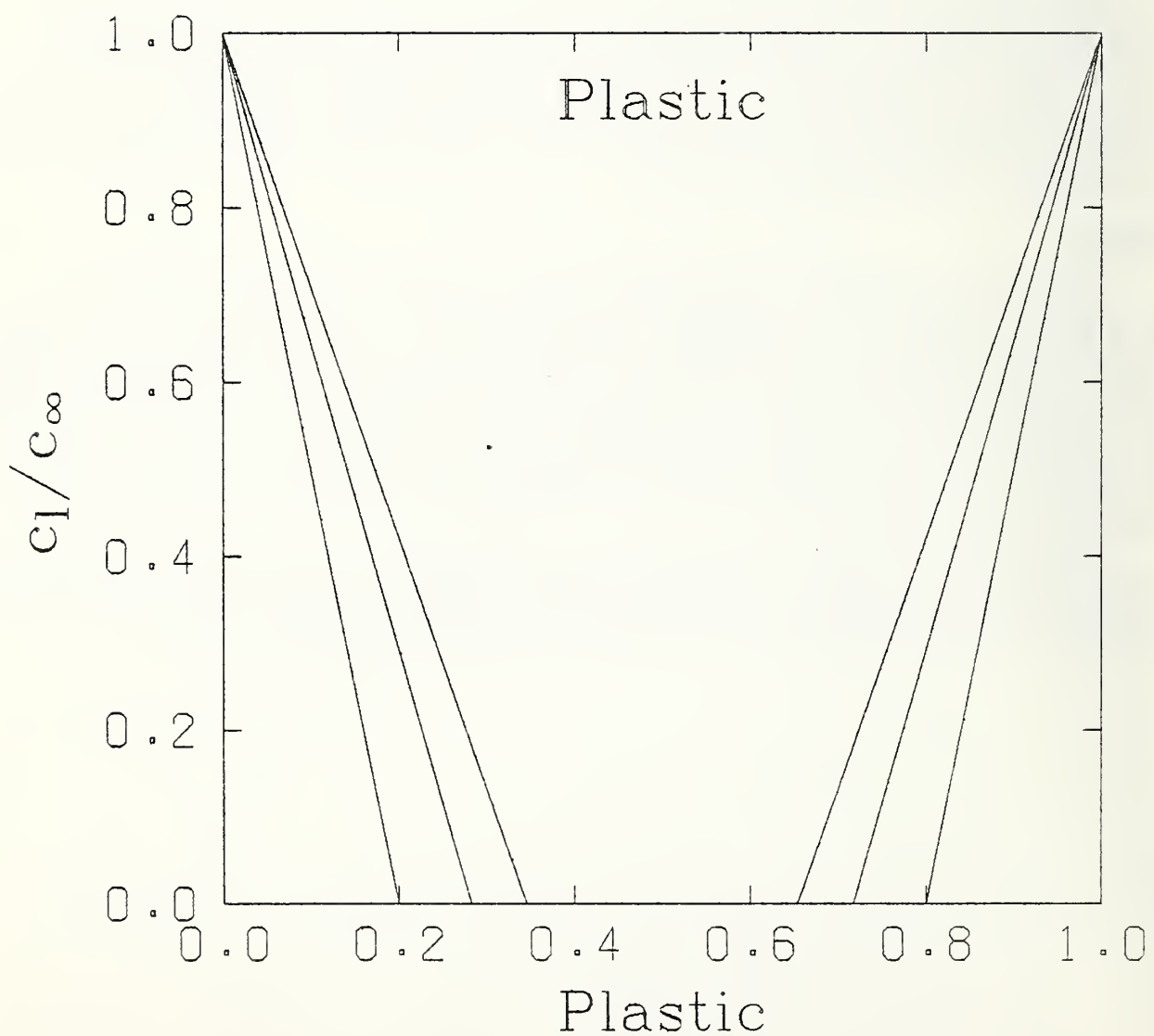
Fig. 4. The migration curves for the additive when the concentration distribution of the liquid in the plastic is that shown in fig. 3. The curves, reading from the lower to upper curve, are for values of $w/\sqrt{D_o}$ of 0, 0.05, 0.1, 0.2, and 0.5.
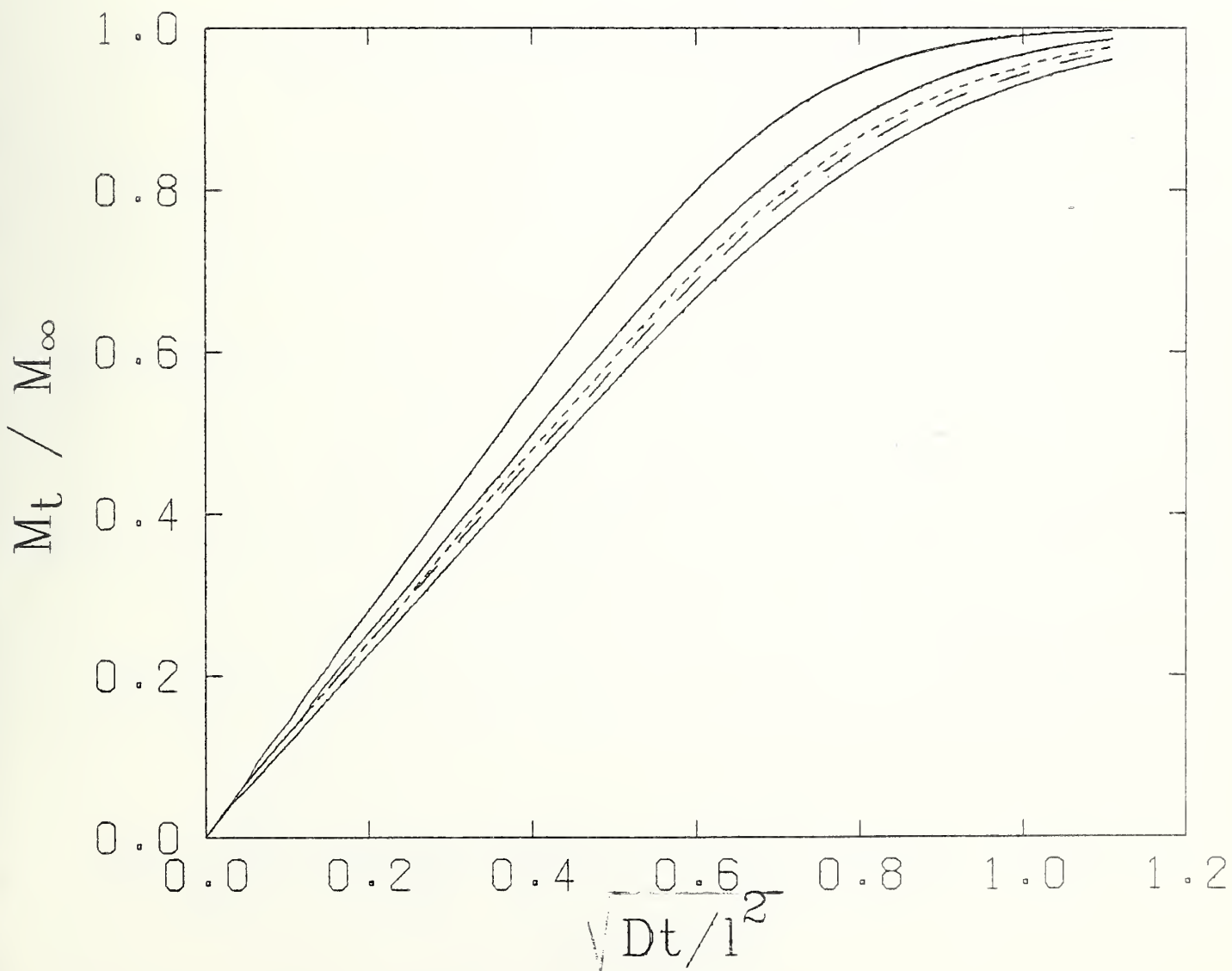
Fig. 5. Three assumed initial distributions of the concentration, c_o, of the additive in the plastic sheet.
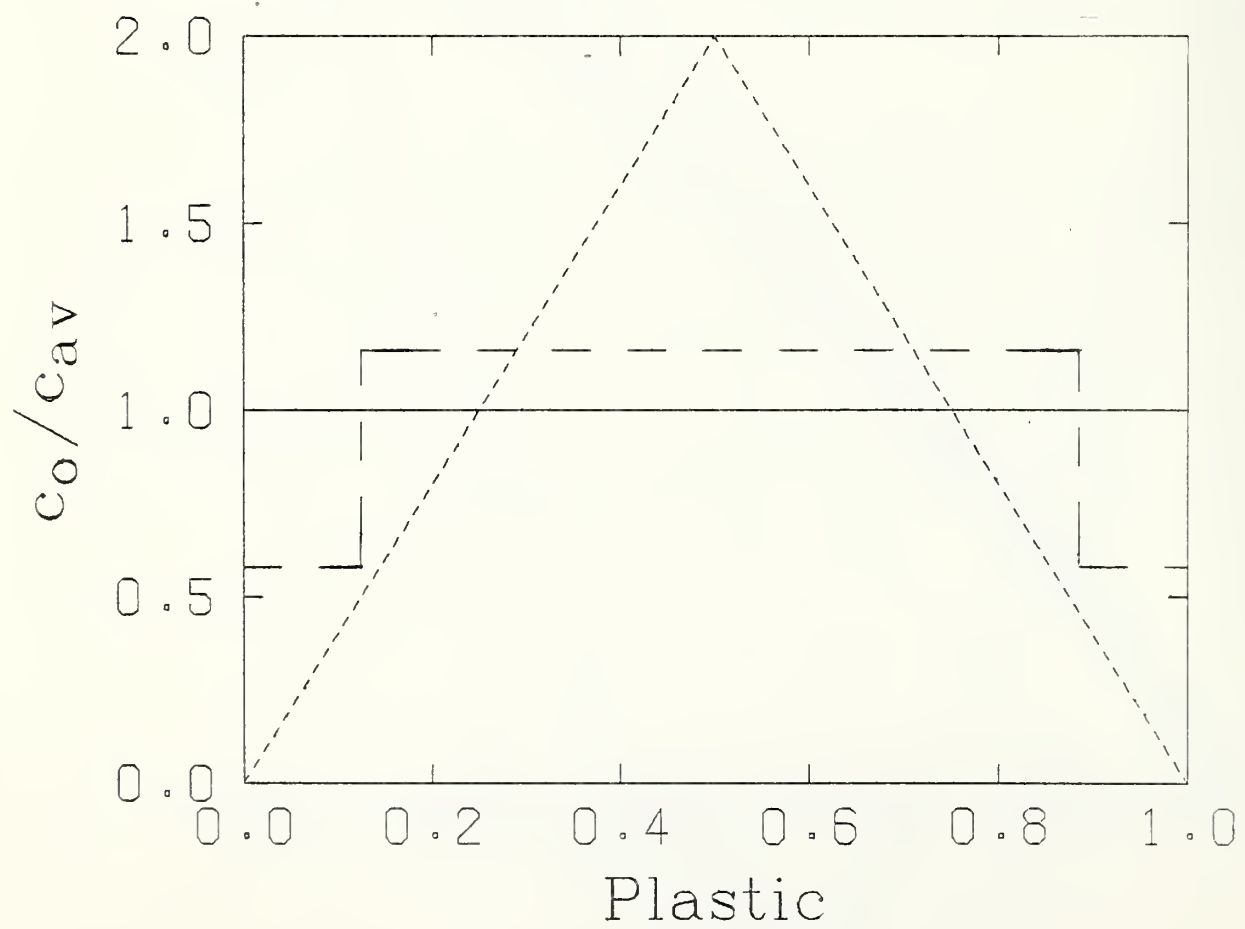
Fig. 6.   The migration curves for the distributions shown in fig. 5.

$$M_t \,/\, M_\infty$$

$$Dt/l^2$$
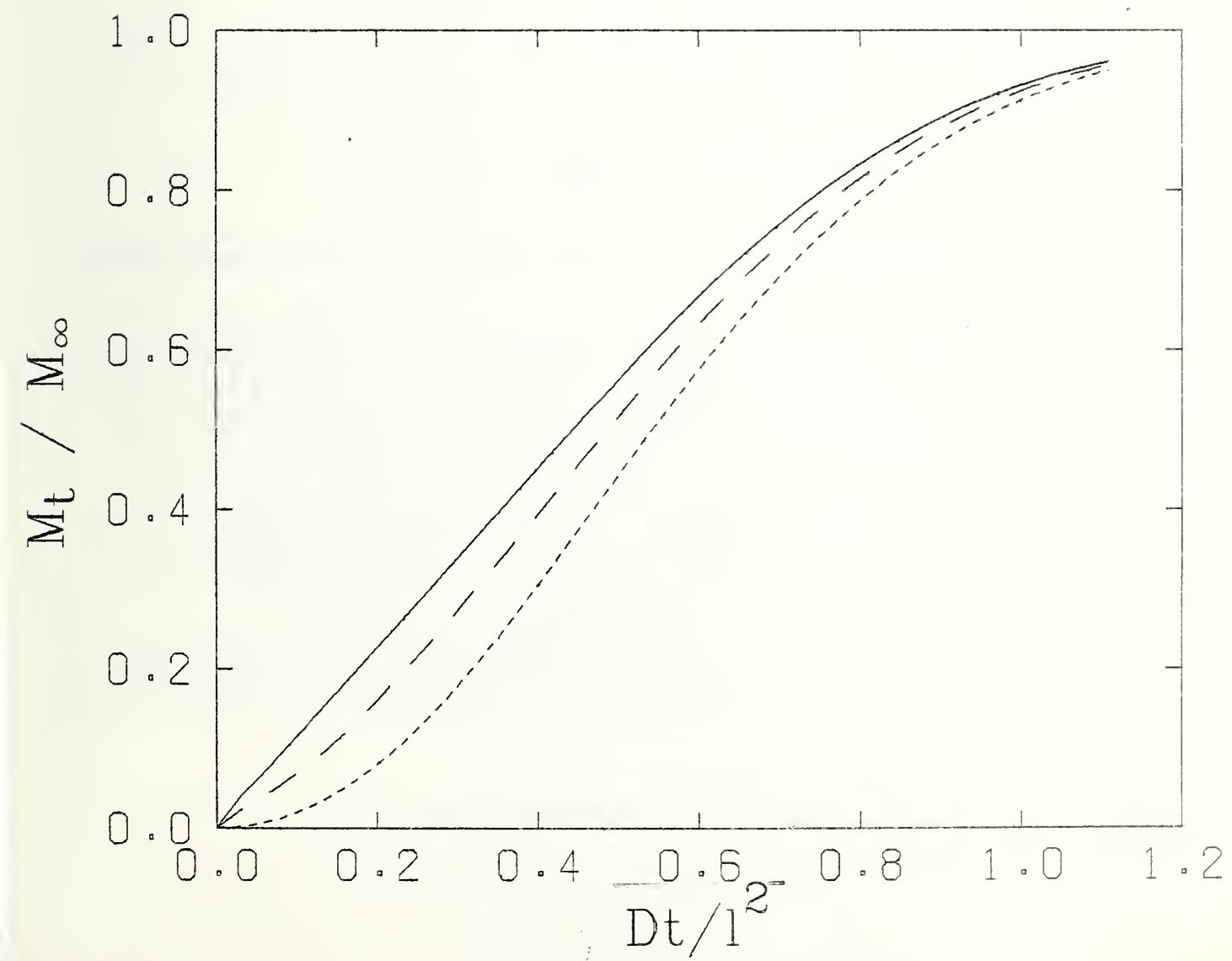
EQUIVALENT EXTRACTION TEMPERATURES
FOR SIMULATION OF ADDITIVE MIGRATION
IN POLYMERS SUBJECT TO VARYING TEMPERATURES

A polymer in use is exposed to a range of temperatures. Migration of an additive in the polymer will vary with the temperature, being greatest at the highest temperature. On the other hand, tests of the migration of additives are generally performed at a constant temperature. In this section, an equivalent test temperature, Te, is derived such that the migration of an additive in a test of temperature Te is the same as the migration of the additive at the range of temperatures of the polymer in use.

The diffusion constant, D, of the additive in the polymer will vary with temperature, T, according to the relationship

$$D = D_0 \exp(-E/RT) \tag{48}$$

where E is the activation energy of diffusion and R is the gas constant.

Consider first the simple case that the polymer in use is exposed to a temperature T_1 a fraction f of the time, and is exposed to a temperature T_2 the remaining fraction (1-f) of the time. Then the equivalent test temperature is shown in Appendix D to be given by

$$T_e = \frac{-E/R}{\text{Log}_e[f \exp(-E/RT_1) + (1-f)\exp(-E/RT_2)]} \tag{49}$$

For the general case in which the polymer is exposed to any variation of temperature T with time, t, the equivalent test temperature is shown in Appendix D to be given by

$$T_e = \frac{-E/R}{\text{Log}_e[(1/t) \int_0^t \exp(-E/RT)dt]} \tag{50}$$

If the activation energy E is known for a polymer-additive system, the equivalent test temperature, T_e, corresponding to any variation of temperature may be computed by Eq. 49 or 50.

The diffusion of the ultraviolet stabilizer 2,4-dihydroxybenzophenone in polyolefins has been measured by Westlake and Johnson. The measured values of the activation energies, E_1, of diffusion are 18, 23 and 34 kcal/mole for low-density polyethylene, high-density polyethylene and polypropylene, respectively. As these values are probably typical for activation energies, calculations of equivalent test temperatures were performed for activation energies of 15 and 30 kcal/mole. The calculations were performed for temperatures varying from 20 to 75°C for variations of the temperature with time shown in Figs. 7, 8, and 9. For Fig. 7, the test temperature is 20°C for half the time and 75°C for the other half of the time. For Figs. 8 and 9, the temperature varies between 20 and 75°C in a manner that is more realistic. The equivalent test temperatures calculated by Eqs. 49 and 50 are shown in Table 3.

Fig. 10 shows the equivalent test temperatures for the time variation shown in Fig. 7 except that varying amounts of time are spent at the high temperature of 75°C. The solid line is for an activation energy E of 15 kcal/mole and the dashed line is for E of 30 kcal/mole.
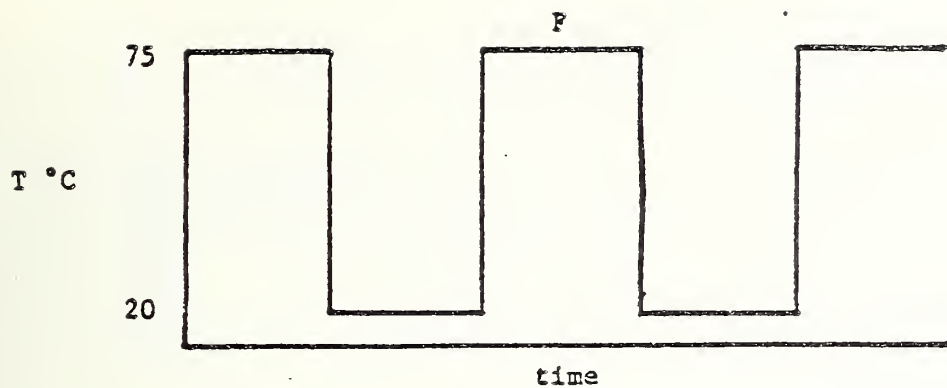
Figure 7

Assumed time variation of temperature of plastic.
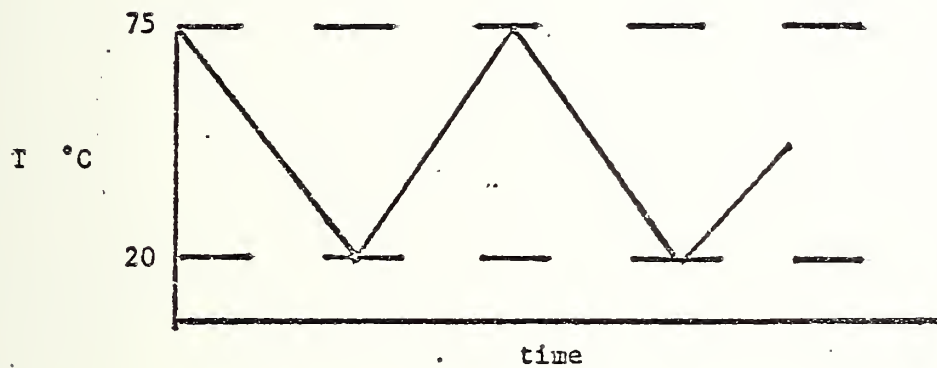
Figure 8

Assumed time variation of temperature of plastic.
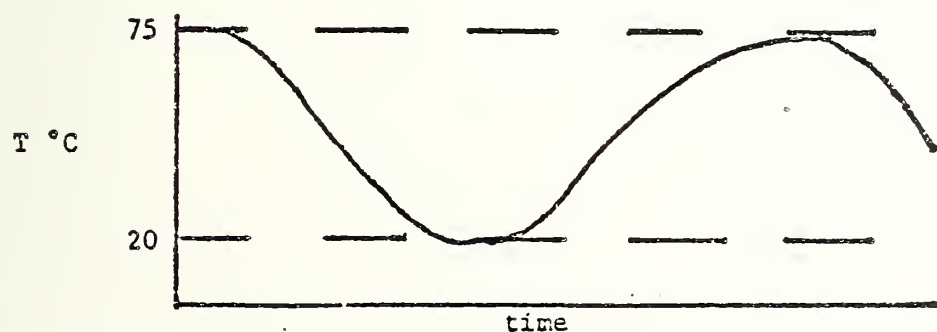
Figure 9

Assumed time variation of temperature of plastic.

25

TABLE 3

Equivalent Test Temperatures in $^{\circ}$C for Temperatures
Varying Between 20 to 75°C

Variation of Temperature given by	Activation Energy of Diffusion, E, kcal/mole	
	15	30
Fig. 1	64.5	69.5
Fig. 2	54.9	60.0
Fig. 3	54.8	59.3

Equivalent test temperature for a plastic subjected to the time variation shown in Fig. 7 between 20 and 75°C versus the percentage of the time the specimen is at 75°C.

f, % of time specimen is at 75 C

T_e

27
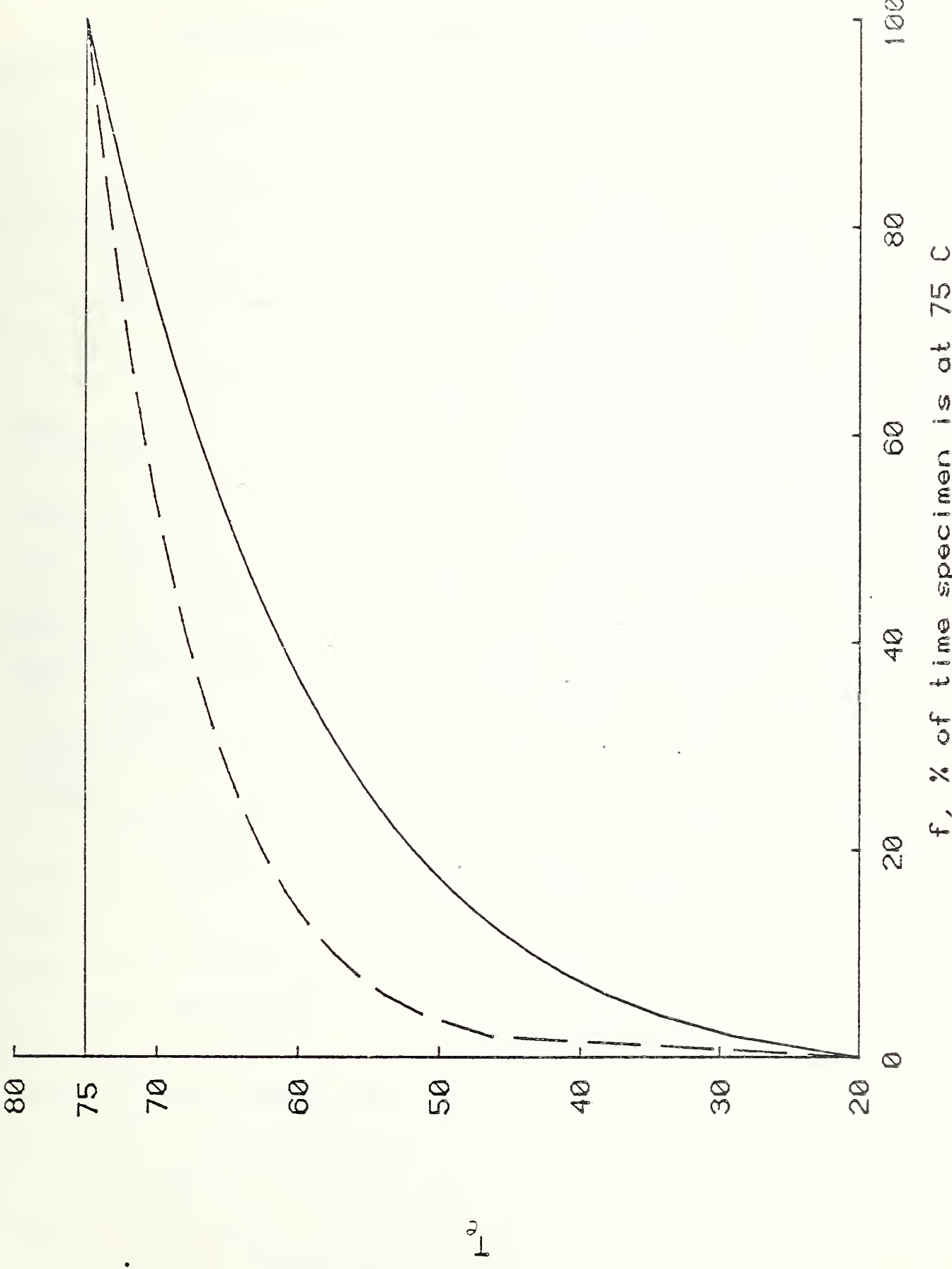
III. EXPERIMENTAL MEASUREMENTS OF ADDITIVE MIGRATION

Polyethylene

There are a number of reasons for the choice of polyethylene as the polymer substrate for migration studies. As the largest volume packaging material, there are a wide variety of commercial resins and formulations available so general physical models would have broad application and case by case testing would be tedious. The commercial importance of polyethylene and the simplicity of its chemical structure have prompted enough scientific investigation that a great deal is already known about the detailed structure and morphology of the solid state. There is a wide range of crystallinities available with different resins and the crystallinity in a given resin is controllable within limits by well known thermal treatments. This presents a challenge to any theoretical model and another variable to control and alter in experiments. Finally, polyethylene is relatively stable chemically. It does not degrade thermally under usual processing conditions and can be adequately protected from oxidation.

The first migrating species to be considered are the polyethylene oligomers. Some octadecane migration results are presented in this report. Further data including other oligomers will be presented in the next report as well as initial experiments with polar additives.

MATERIALS

Polymers

The basic polymer used for the extraction experiment is the National
Bureau of Standards Standard Reference Material (NBS-SRM) 1475, Linear Poly-
ethylene Whole Polymer. This SRM is well characterized and certified[18] for
its molecular weights, molecular weight distribution, density, melt-flow rate,
viscosity and heat capacity. The weight averaged molecular weight of SRM 1475
is 52,000.

When the FDA extraction procedure (Code of Federal Regulations, Title 21,
Chapter I, Part 177.1520) was applied to the SRM 1475 sample in pellet form,
the hexane extractives at $50^\circ C$ are in the order of 0.05 to 0.1%, either by
weighing the residue from hexane extract or by the weight loss of the sample
pellets. Additional experiments with heptane at $50^\circ C$ on a 0.2 mm film made
from SRM 1475 yielded a weight loss figure about 0.2%.

Future polymeric materials will include NBS-SRM 1476, Branched Polyethylene
Whole Polymer, and other polyethylenes of commercial grade especially those used
for bottling purposes.

Additives

The low molecular weight paraffinic hydrocarbons are oligomers of linear
polyethylene. We have now on hand ^{14}C-labeled decane, octadecane and dotriacon-
tane with total activities of about 5 mCi (millicuries) each. Labeled hexadecane
is also readily available in small quantities as NBS-SRM 4222.

We have chosen octadecane as the first hydrocarbon for the migration study
because of its relatively low volatility (b.p. $316^\circ C$). The molecules of octade-
cane are still small enough to have relatively large diffusion coefficient, so
that the experiments may be completed in reasonable time scale.

n-Octadecane-1-^{14}C was obtained from commercial source as hexane solution
sealed in glass ampules. The specific activity in one of the ampule was stated
as 13.3 mCi/g, but was found to be 12.2 mCi/g. The total activity is

29

1.65 mCi in 135 mg of $C_{13}H_{38}$ dissolved in hexane. The entire content of the ampule was diluted into 50 ml (33 μCi/ml). One ml of this solution is further diluted into 50 ml (0.66 μCi/ml). These dilutions provide much easier handling of the labeled compound. Further isotopic dilution by unlabeled octadecane may be desirable in some cases to reduce unneccessary waste of radioactive materials. The amount of dilution depends upon the minimum detection level desired and the concentration of the additives in the polymer.

The FDA's extraction procedures for the determination of total non-volatile extractives (Code of Federal Regulations, Title 21, Chapter I, Part 177.1010) uses a ratio of 10 ml of solvent per square inch of plastic surface for a sample of 5 in^2 of surface area. The extractives in parts per million are then obtained as 100 times the weight of extractives in milligrams per square inch of plastic surface. Strickly speaking this expression for extractives is expressed in terms of micrograms per milliliter of solvent or per 0.1 in^2 of the plastic surface.

If we desire a detection limit of 10 ppb (10 ng/ml) for the extractives in food simulating solvents, we are required to detect the presence of 100 ng of the extractives in 10 ml of solvent or from each square inch of the plastic surface. By assuming a minimum counting rate at twice the background rate as the instrumental detection limit, then this requirement amounts to a minimum activity in the order of 25 pCi. Therefore the minimum specific activity of the extractives should be about 0.25 mCi/g. However if we desire to have a 1% precision of the data at the 10 ppb level, then a minimum activity of 2.5 nCi or about 5000 dpm in the 10 ml solvent would be more desirable.

SAMPLE PREPARATION

Method

After several attempts we have chosen the following procedure for the
mixing of additives to the polymer stock and the molding of the sample plaques.
A large quantity of polyethylene powder stock was prepared from NBS-SRM 1475,
Linear Polyethylene Whole Polymer, pellets by first dissolving in hot toluene,
and then followed by cooling. Most of the polyethylene precipitates out. The
precipitate was filtered and dried in a vacuum oven to remove the solvent.

To a quantity of the polyethylene powder stock, a specific amount of labeled
additive dissolved in a highly volatile solvent is mixed. The mixture is then
evaporated to dryness in a rotary evaporator under reduced pressures at relatively
low temperatures, and further dried in a vacuum oven. The mixture is then com-
pression molded in a hydraulic press operated at about 180°C.

Four sample plaques were prepared by the aforementioned techniques, i.e.,
by wetting the SRM 1475 polyethylene precipitate with hexane solution of ^{14}C-
labeled $C_{18}H_{38}$, followed by evaporation and compression molding. The four sample
plaques, designated as A, B, C and D respectively, are molded into two different
thicknesses from two powder mixes of different $C_{18}H_{38}$ additive levels as shown
in Table 4.

The plaques (50 X 125 mm) were molded with brass shim stocks of 0.76 (30 mil)
and 0.25 mm (10 mil) thickness sandwiched between two sheets of teflon. The
teflon sheets are used for the easy removal of the samples from the mold. The
finished plaques have nominal thicknesses of slightly less than 0.7 and 0.2 mm
respectively. The thickness at the edge is generally thicker than that in the
center. Part of the shrinkage is due to the large coefficient of expansion of
polyethylene. The depression of the teflon sheets may also contribute to the
apparent total shrinkage. The variation in the thickness can often reach ± 0.05 mm
(± 2 mil).

Table 4

Description of Polyethylene Samples

Sample	Thickness mm	Concentration of added $C_{18}H_{38}$, %	Specific Activity Mdpm/g
A	0.7	1	5
B	0.2	1	5
C	0.7	0.01	3.5
D	0.2	0.01	2

We have now obtained teflon coated top and bottom plates to replace the teflon sheets in order to eliminate some of the sources of shrinkage and thickness non-uniformity. Stainless steel shims will be used instead of the brass ones to eliminate possible contamination and reaction during the molding process.

Uniformity

Besides the non-uniformity in the thickness the samples are not too uniform in the additive distribution. The sample plaques were checked for the uniformity of the distribution of the added radioactive $C_{18}H_{38}$ by autoradiography. No-Screen X-ray film type NS-5T was used because of its speed. Exposure time in the order of 16 hours is sufficient to register the activities of these plaques. The distribution in the 0.7 mm plaques seems to be more uniform than that in the 0.2 mm plaques, the distribution is especially poor for the 0.01% $C_{18}H_{38}$ sample (D). Therefore sample (D) was cut up and compression molded again. The distribution, although still not uniform, was improved greatly as shown in Figure 11 . Typical microdensitometer scans across the width on these sample plaques are shown in Figure 12 , along with the scans of background of the film adjacent to the images of the plaques. The variation in the optical density levels are quite obvious, and can often reach 20% or higher.

Figure 11. Autoradiographs of Sample plaque D. Top: first molding. Bottom: second molding
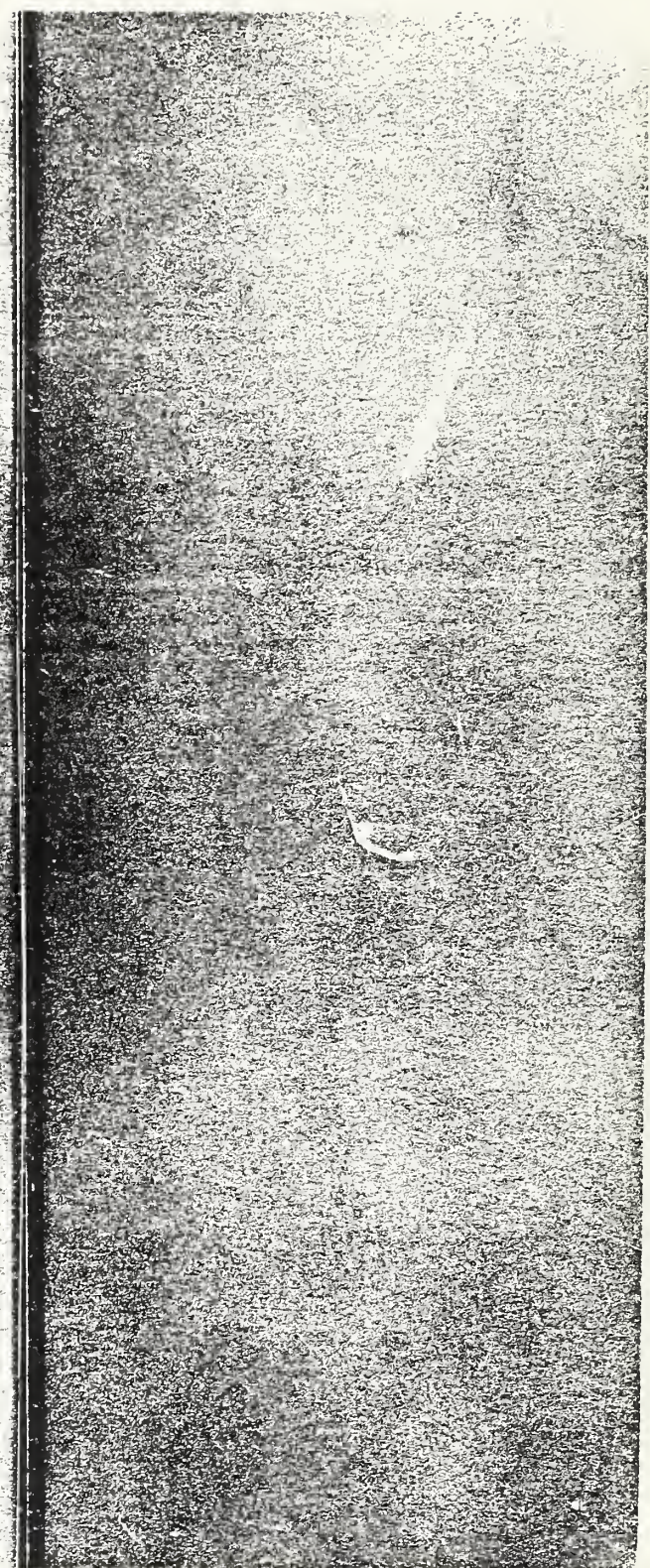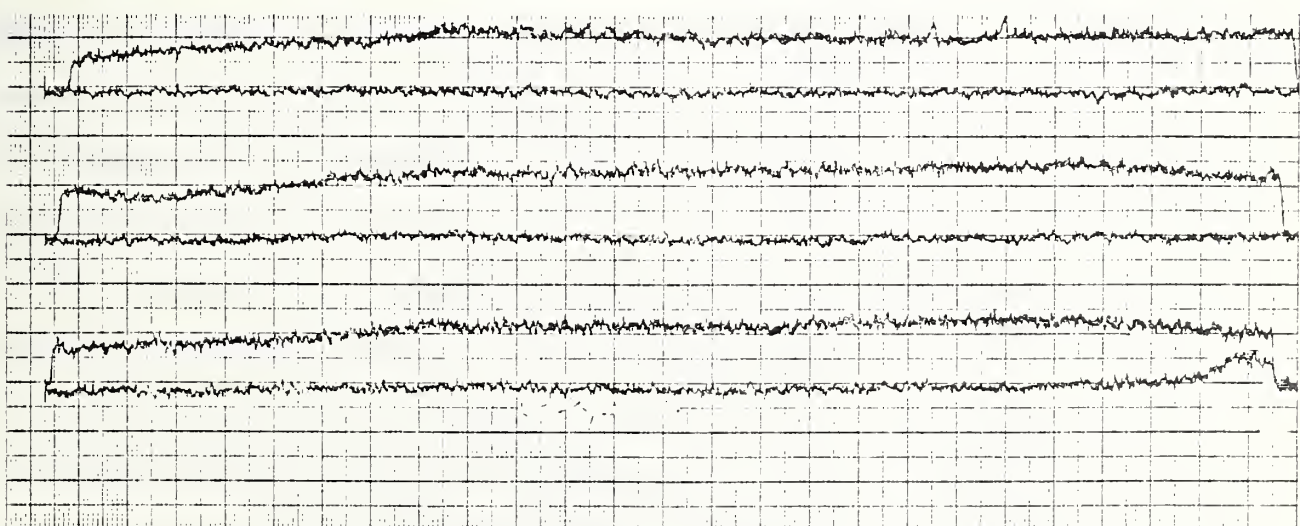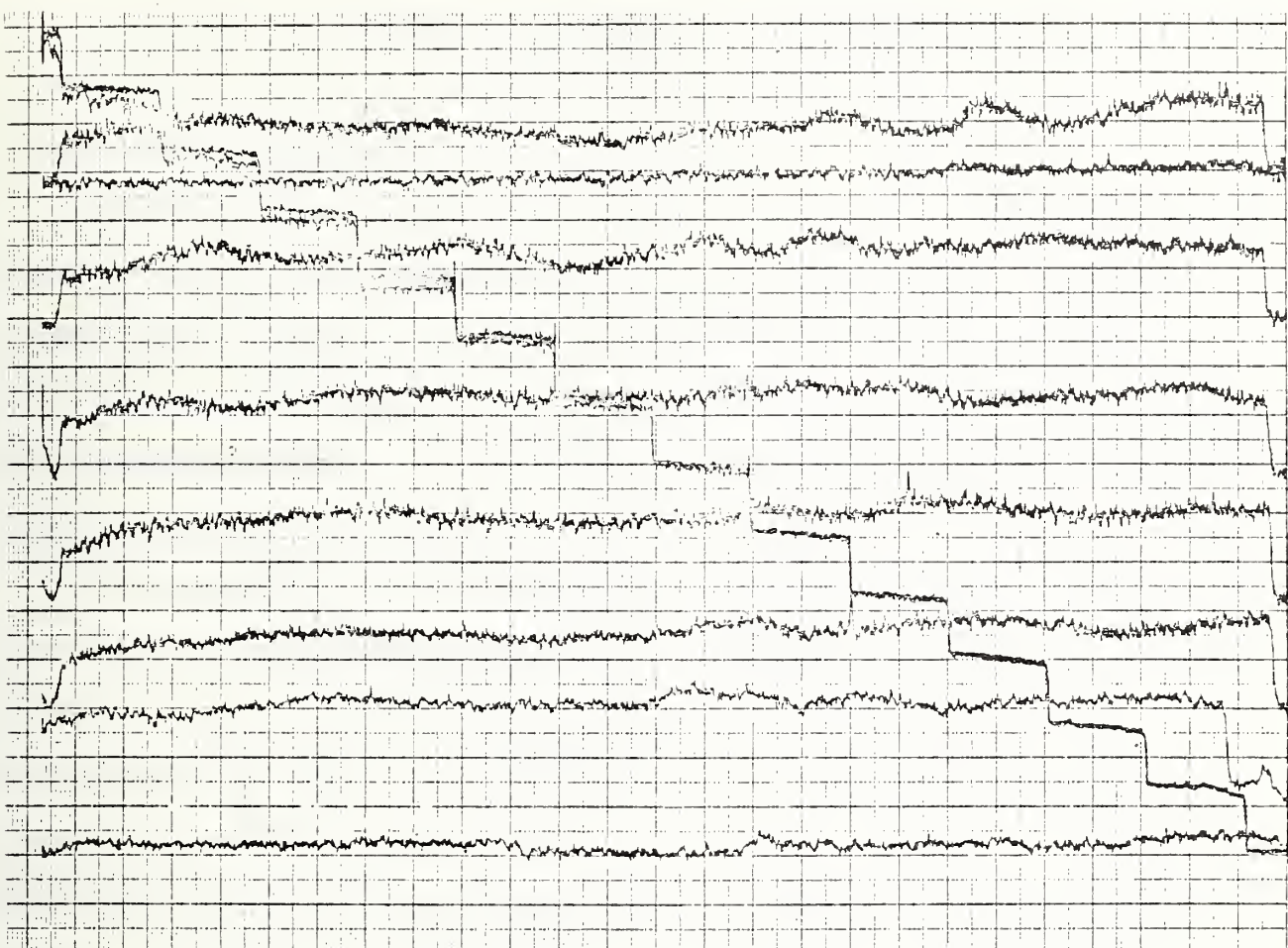
Figure 12. Microdensitometer scans of the Autoradiographs of Sample plaque D.
Top Curves: first molding. Bottom Curves: second molding. Steps:
Calibration strip.

LUMINESCENCE SPECTROSCOPY MEASUREMENTS

The migration of antioxidant from polymers will be studied by two types
of experiments: extraction experiments and concentration profile experiments.
In an extraction experiment, a plane sheet of polymer with uniform concentra-
tion of an antioxidant is immersed in a limited amount of well stirred solvent.
The migration of an antioxidant is then deduced from the change in antioxidant
concentration in the solution surrounding the plane sheet. The antioxidant
concentration can be determined either by fluorimetry at room temperature or
phosphorimetry at a lower temperature. If the diffusion coefficient for the
antioxidant is constant, it can be deduced from an extraction experiment. In
a concentration profile experiment, a plane sheet of polymer with uniform con-
centration of an antioxidant is immersed in a large volume of well stirred solvent.
The concentration profiles along the direction normal to the larger surfaces of the
sheet can be determined at various times by microfluorimetry after sectioning
the sheet. The diffusion coefficient of an antioxidant can then be deduced from
the concentration-distance curve.

Solution Concentration Measurements

In late FY 78, we made room-temperature fluorescence measurements on Irganox
1076 (n-Octadecyl-8-(3,5-di-t-butyl-4-hydroxyphenyl)-propionate) in hexane, Agerite
White (N, N'-di-8-naphthyl-p-phenylenediamine) in ethanol, BHA (3-t-Butyl-4-hydro-
xyanisole) in ethanol, and BHA in heptane. We found that, of these three antio-
oxidants, only Agerite White and BHA show room temperature fluorescence sufficiently
intense to be useful for trace analysis. In FY 79, we will develop a procedure to
follow the extraction of Agerite White or BHA from low density polyethylene. This
development entails principally the preparation of polyethylene films of about
0.025 cm containing an antioxidant, uniformly distributed and undegraded by the
preparation, the construction of an extraction device equipped with a cell for

making fluorescence measurements without exposing antioxidant to oxygen, and the establishment of an analytical working curve relating antioxidant concentration to fluorescence intensity.

Since, for most antioxidants, the phosphorescence is known to be more intense than room-temperature fluorescence, we plan in late FY 79 to begin the development of a procedure to follow the extraction of an antioxidant such as Santonox R (Bis(2-methyl-4-hydroxy-5-t-butylphenyl)sulfide), by phosphorescence measurements.

Concentration Profile Experiments

Figure 13 gives the block diagram of the microfluorometer used for our concentration profile experiments. The most noteworthy feature of the microfluorometer is a vertical illuminator equipped with a dichroic mirror with high reflectance for the exciting wave length and high transmission for other wavelengths (see Figure 14). The dichroic mirror thus reflects an intense exciting light into the objective and allows an intense fluorescent light to reach the eyepiece. In addition, a relatively dark background can be obtained since the dichroic mirror also deflects the exciting light that is reflected by the glass surfaces of the objective and by the cover glass or the sample. A barrier filter is used to eliminate the weak exciting light that passes the dichroic mirror.

Measurements have been made with our microfluorometer on solids of Agerite White, solids of Nonox WSP (Bis(2-hydroxy-3-α-methyl-cyclohexyl-5-methylphenyl)-methane), a high density polyethylene film containing 3100 ppm Irganox 1076, and a low density polyethylene film containing 1000 ppm Agerite White. We found that, or these three antioxidants, only Agerite White shows room-temperature fluorescence sufficiently intense to be useful for measurements with our microfluorometer. In FY 79, we shall develop a procedure for concentration profile measurements on low density polyethylene films containing Agerite White. This development

37
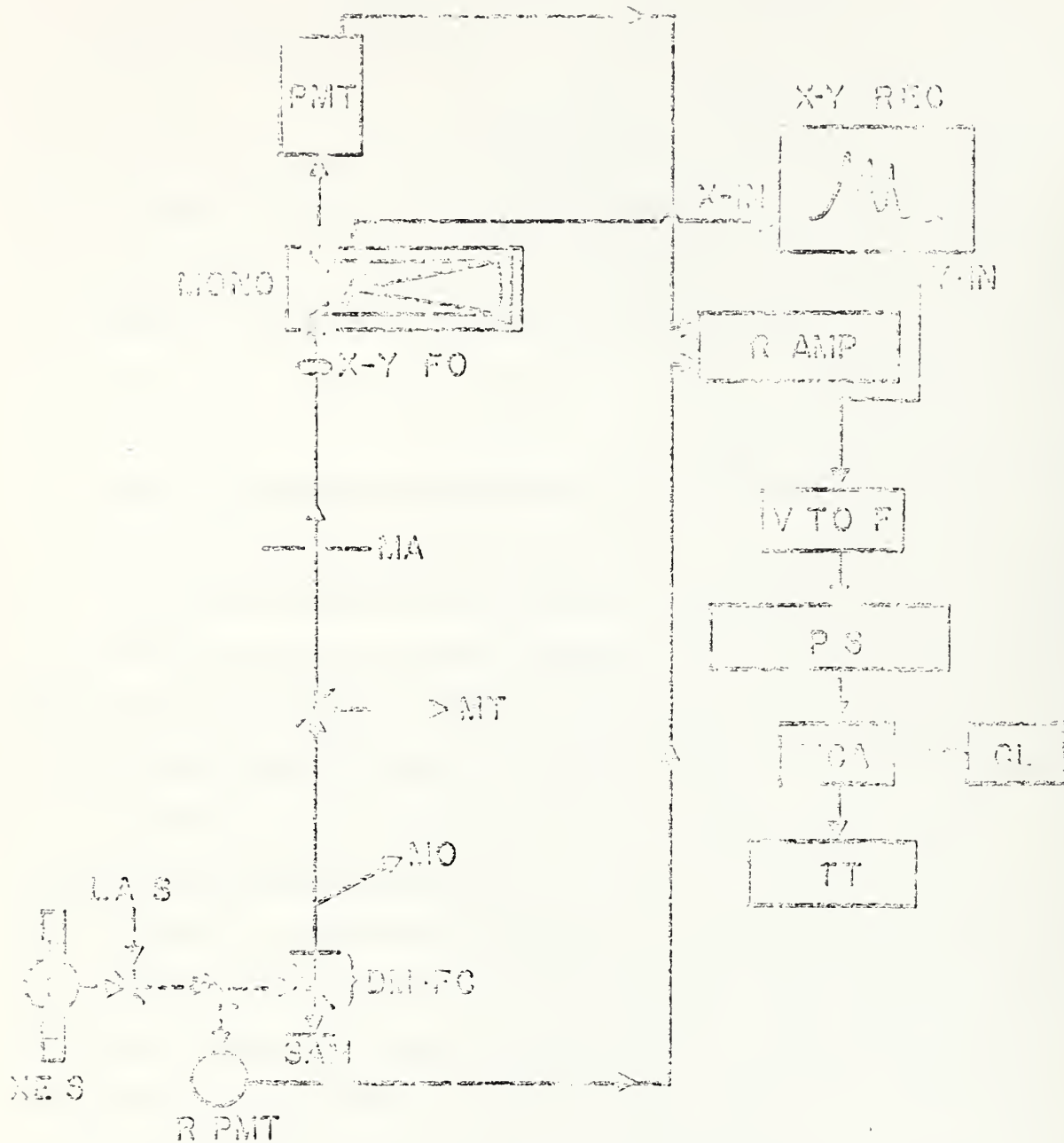
Figure 13. Block diagram of microfluorometer. XE S - xenon source; LA S - laser source; R PMT - reference photomultiplier tube; SAM - sample; DM-FC - dichroic mirror - barrier filter combination; MO - monocular; MT - measuring telescope; MA - measuring aperture; X - Y FO - x - y focusing optics; MONO - monochromator; PMT - photomultiplier; R AMP - ratio amplifier; X - Y REC - x - y recorder; V TO F - voltage to frequency converter; P S - pulse shaper; MCA - multichannel analyzer; TT - teletype; and CL - crystal clock.
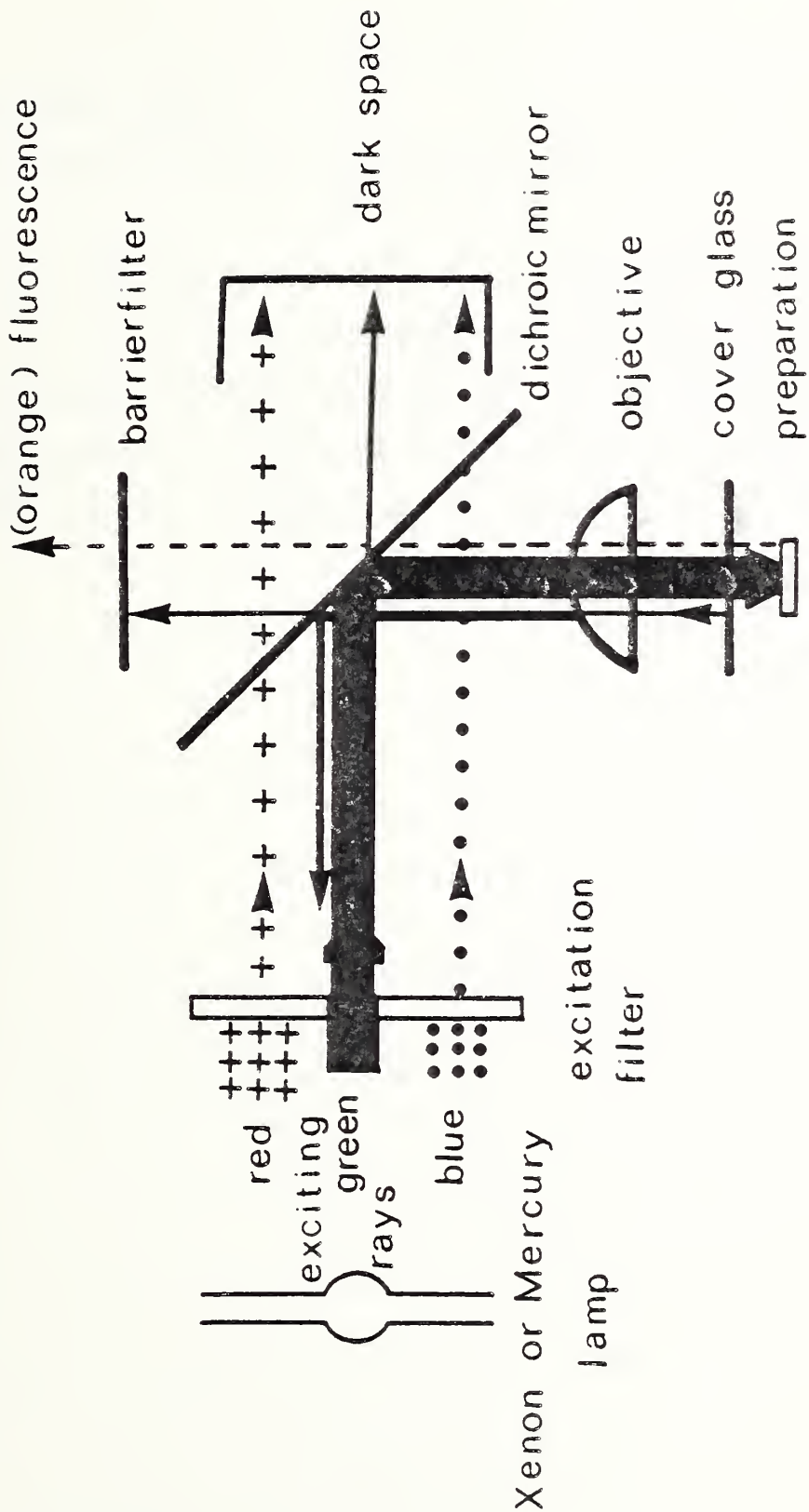
Fig. 14. Light path in a vertical illuminator equipped with a dichroic mirror(45°) with high reflectance for green light and high transmission for blue and red light(Taken from J. S. Ploem, Z. wiss. Mikrosk., 68, 129(1967))

will involve, in addition to the film preparation mentioned earlier, the sectioning of a film, the construction of a holder for the sectioned film, and the measurement of concentration profile maintained unperturbed by antioxidant degradation.

Because of the limitation of the available dichroic mirrors, our microfluorometer is not suitable for measurements on films containing BHA or Agerite superlite (mixture of polybutyrated bisphenol A) which is excited by light of shorter wavelengths than Agerite White. In late FY 79, we shall modify our microfluorometer to make it useful for measurements on films containing BHA or Agerite superlite.

RADIOACTIVITY COUNTING

Liquid Scintillation Counting

We have chosen the liquid scintillation technique to monitor the level of radioactivity. This method is capable of detecting relatively low levels of radioactivity with the background counts being in the order of 20-30 counts per minute (cpm). It is also free from effects of sample geometry. However, the radioactive material should be soluble in the counting cocktails or in solvents compatible with the counting cocktails. This method is a destructive testing, therefore the test material is not easily recoverable from the counting solution.

The general methodology is described in several books.[19,20] A commercial liquid scintillation counter with microprocessor control is used in this work.

In the determination of radioactivity in numbers of disintegration per minute (dpm) from the observed counts per minute, we have adopted the method of locating the upper edge of the pulse height distribution for the Compton electrons, generated in the counting solution by an external radioactive ^{137}Cs source, as the measure of the degree of quenching. This method provides a rather universal calibration curve of counting efficiency versus degree of quench over a very wide range of quenching conditions. With extensive testings, we have found that the ultimate precision in dpm for the counter operated in the above mentioned mode is of the order of 0.2%, even when the total counts are much greater than 10^6. In general, a precision of 0.5% can generally be realized. Thus at low counts the precision is limited by the counting statistics (although the actually observed precision is often about twice that indicated by Poisson statistics), however at high counts the precision is limited by the stability of the instrument and the reproducibility in the determination of the Compton edge or of the shift of the Compton edge

from an unquenched counting solution. Therefore we have generally used a limit of $2\sigma = 0.2\%$ (10^6 counts) and/or 10 minutes of counting time to terminate the counting process for routine work. A collection of repeated counts to increase the reliability of the results is usually recorded on a tape and then processed by the NBS central computing facilities.

Calibration of Liquid Scintillation Counter

The calibration results are listed in Table 5 and shown graphically in Figure 15. The results were obtained on a commercial unquenched standard, a commercial standard quenched set and on a variety of quenched solutions made from a National Bureau of Standards Standard Reference Material (NBS-SRM) 4222 and various commercial counting cocktails. The commercial unquenched and quenched set are sealed in glass vials and use $CC\ell_4$ as the quenching agent. All these standards are traceable to NBS-SRM Na_2CO_3 and are quoted with an uncertainty of 3%.

In calibrating the liquid scintillation counter by NBS-SRM 4222, Carbon-14 standard (Hexadecane), 14 samples were weighed out. The samples weighed from 0.02 to 0.1 g. The certified specific activity is $3.93_2 \times 10^4$ disintegration per second per gram (dps/g). To each of the samples, a certain amount of counting cocktail was added and then counted. To these, ethanol and counting cocktails in various ratio were added to vary the quenching levels and then counted. The liquid level in the counting vials varied from 0.5 ml to 20 ml. From previous experiments we have established that the liquid level in the counting vial, varying from 1 to 20 ml, does not effect the counting efficiency beyond the precision of the counting process.

The degree of quenching is represented by the so-called H#, which indicates a shift in the position of the Compton edge from that of an unquenched solution. The H# is a logarithmic representation of the energy spectrum where integer numbers from 0 to 1000 are used to indicate the energy level up to 2 MeV.

Table 5

Calibration of Liquid Scintillation Counter

H#	Efficiency	H#	Efficiency	H#	Efficiency

1. <u>Commercial Unquenched Standard (31500 dpm)</u>

0	0.963	0	0.956		

2. <u>Commercial Quenched Set (190300 dpm)</u>

19	0.957	19	0.958	20	0.959
75	0.933	80	0.929	80	0.929
147	0.871	155	0.864	152	0.867
200	0.790	210	0.774	206	0.785
217	0.756	228	0.758	224	0.748
248	0.676	265	0.646	253	0.666

3. <u>NBS-SRM 4222 (Carbon-14, hexadecane, $3.95_5 \times 10^4$ dps/g)</u>

EP		GP		HP	
<u>I. 86300 dpm</u>		<u>I. 67240 dpm</u>		<u>I. 257200 dpm</u>	
48	0.934	'69	0.927	65	0.926
55	0.931	55	0.937	54	0.936
89	0.913	91	0.913	85	0.920
116	0.889	113	0.897	109	0.901
141	0.867	136	0.880	130	0.884
168	0.838	162	0.852	157	0.858
191	0.799	182	0.820	180	0.824
<u>II. 112900 dpm</u>		<u>II. 154500 dpm</u>		<u>II. 112200 dpm</u>	
314	0.487	285	0.566	310	0.501
205	0.779	192	0.804	197	0.799
217	0.742	225	0.758	204	0.767

Table 5   (continued)

H#	Efficiency	H#	Efficiency
	NA		OCS

I. 120200 dpm		I. 51120 dpm	
323	.442	27	.934
192	.805	21	.936
205	.784	63	.924
217	.747	76	.916
		112	.889
		142	.865
		159	.843

II. 148100 dpm		II. 134100 dpm	
44	.942	309	.495
25	.948	182	.822
89	.919	192	.807
119	.897	208	.772
182	.824		

III. 105000 dpm		III. 162400 dpm	
278	.573	36	.937
303	.514	208	.770
146	.866	108	.897
171	.836		
212	.762		
259	.634		

IV. 187900 dpm		IV. 194600 dpm	
56	.933	48	.933
288	.574	285	.561
387	.241	418	.116
427	.111	457	.033
459	.031	349	.362
351	.349	282	.613
245	.679	269	.612
		238	.701
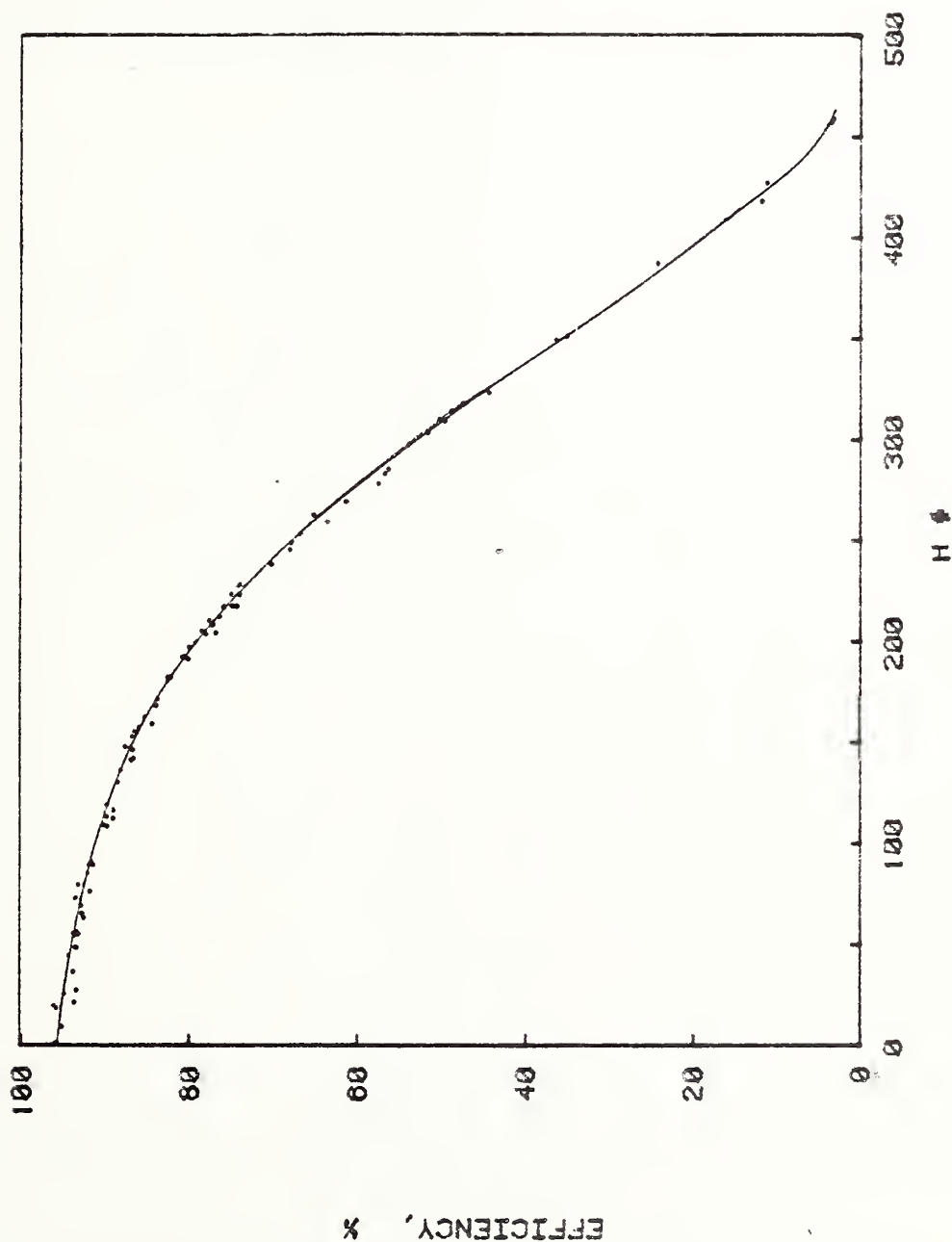
Figure 15. Calibration of the Liquid Scintillation Counter.
Efficiency versus Quench Level.

45

It is obvious from the composite graph, Figure 15, that regardless of the types of counting cocktails, ^{14}C sources, liquid levels in the counting vial and quenching agents used, the calibration curve for non-aqueous sample is quite universal in nature with a scatter of about 1% in counting efficiency which is well within the accuracy quoted or certified by the various standards.

Methods of Extraction

Two extraction methods were used, i.e., (1) continuous extraction into limited solvent volume and (2) discrete extraction simulating infinite solvent volume.

In method (1) an extraction vial of 40 ml in volume with a teflon valved cap is used, Figure 16. The solvent in the vial will only meet glass walls and teflon surfaces. A silicone rubber plug is situated above the valve and may be exposed to the solvent vapor only while an aliquot of 1 ml is taken through syringes from time to time. The plastic sample may sometimes be surrounded by a nichrome or stainless steel screen to prevent it from sticking to the walls or another sample if more than one piece is being extracted in the same vial or if the sample has lower density then the solvent.

In method (2), the plastic sample is immersed in about 10 ml of extracting solvent in a 20 ml counting vial. At specific times the sample is removed from the solvent, rinsed and placed in a vial with fresh solvent to repeat the extraction process.

Method (1) should be able to yield information about the equilibrium partition coefficient at infinite extraction time. However it suffers from rigid requirements of knowing accurately the ratio of aliquot versus total solution and of keeping track of materials lost during the sampling process for material balance purposes. As extraction time increases, there is only very small change in the concentration of extracted material in the solution, whereas the weighing or ratio error may persist. Therefore, the results at long time or high degree of extraction will show considerable degree of scatter.

Method (2) is much simpler in operation, but simulates a condition of migration into infinite media, and is relatively free from aforementioned experimental difficulties.

We may employ a third method: many plastic samples are placed in individual vials with solvents at similar surface to volume ratio. Each vial is then counted at different times (both the solution and the plastic sample for its residue activity).

Figure 16. Typical Extraction Vial.

48
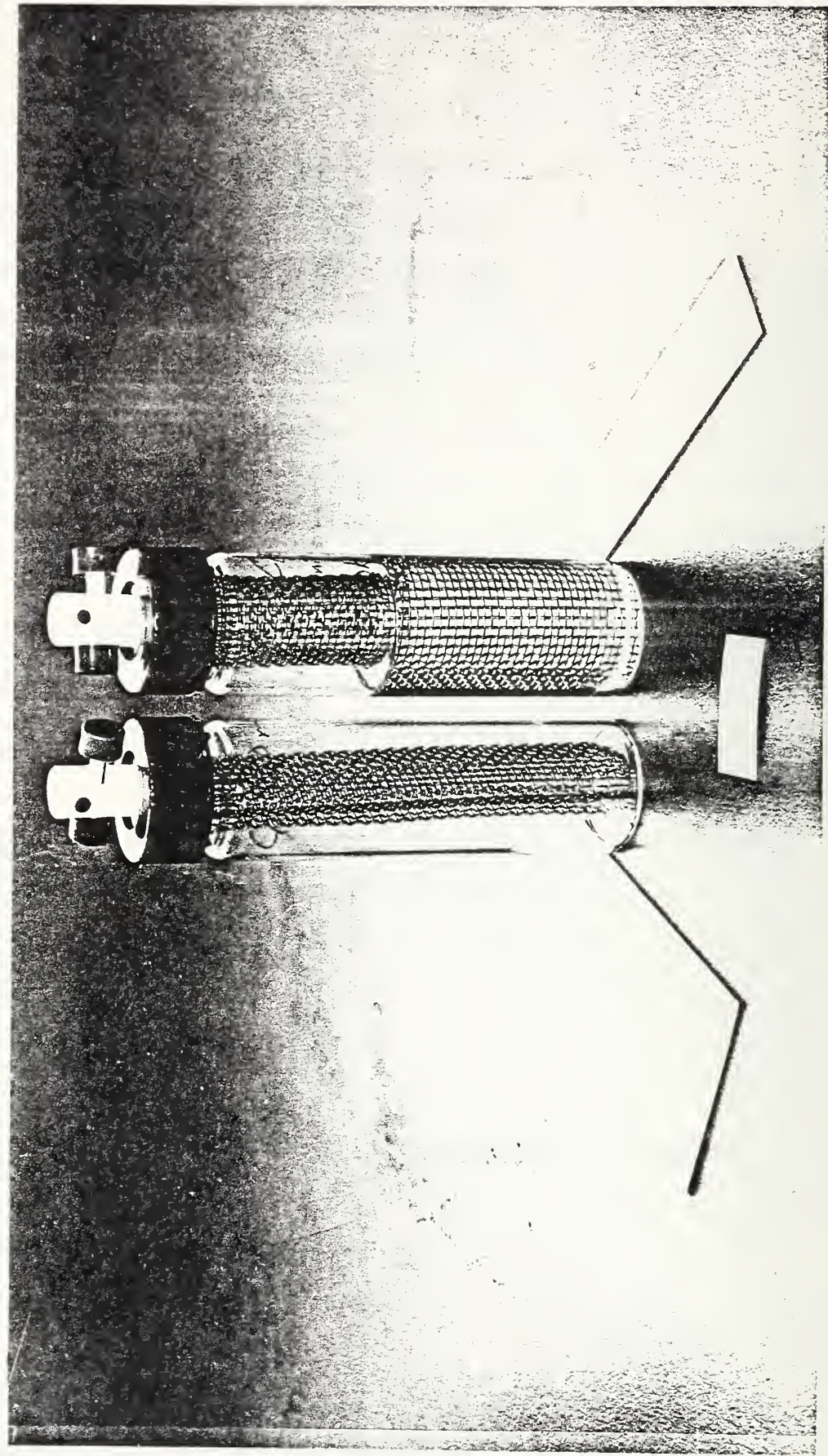
This method may be operationally simpler than that of Method (1). It yields similar results and has similar shortcomings to those of Method (1). Furthermore, additional scattering of the results may arise from the non-uniformity of the sample.

For all the methods mentioned the extraction vials may be shaken by a wrist-action shaker in a temperature environment chamber, or placed in a temperature controlled aluminum block on a shaking table as shown in Figure 17 . When the extraction process is ended, the residual radioactivity remaining in the polyethylene sample is extracted by dissolving the sample in toluene at high temperatures. We found that the single crystals or precipitates of polyethylene in the counting vial does not effect the counting efficiency beyond the normal scattering of the counting results.

Results of Extraction

The experimental results on the extraction of labeled $C_{18}H_{38}$ from polyethylene are listed in Table 6 and summarized in Table 7.

The experiments are coded by two letters followed by a number to facilitate easy identification. The first letter denotes the sample plaque designation as that in Table 4. The second letter denotes the extracting solvent, e.g.. E for ethanol, H for heptane, O for octadecane and W for water. The number denotes the test number of the sample-solvent combination.

The results are expressed in terms of M_t/M_O, where M_O is the original amount of labeled $C_{18}H_{38}$ in the polyethylene, and M_t is the cumulative amount of labeled $C_{18}H_{38}$ extracted at time t.

In Method (1) the amount extracted between time t-1 and t is obtained by

$$A_t = \{[(N_t/E_t)/W_{a,t}] - [(N_{t-1}/E_{t-1})/W_{a,t-1}]\}W_{s,t} \qquad (51)$$

where A is the activity increment, N the count rate, E the efficiency of counting, W_a the weight of aliquot and W_s the weight of total solution. In Method (2) the
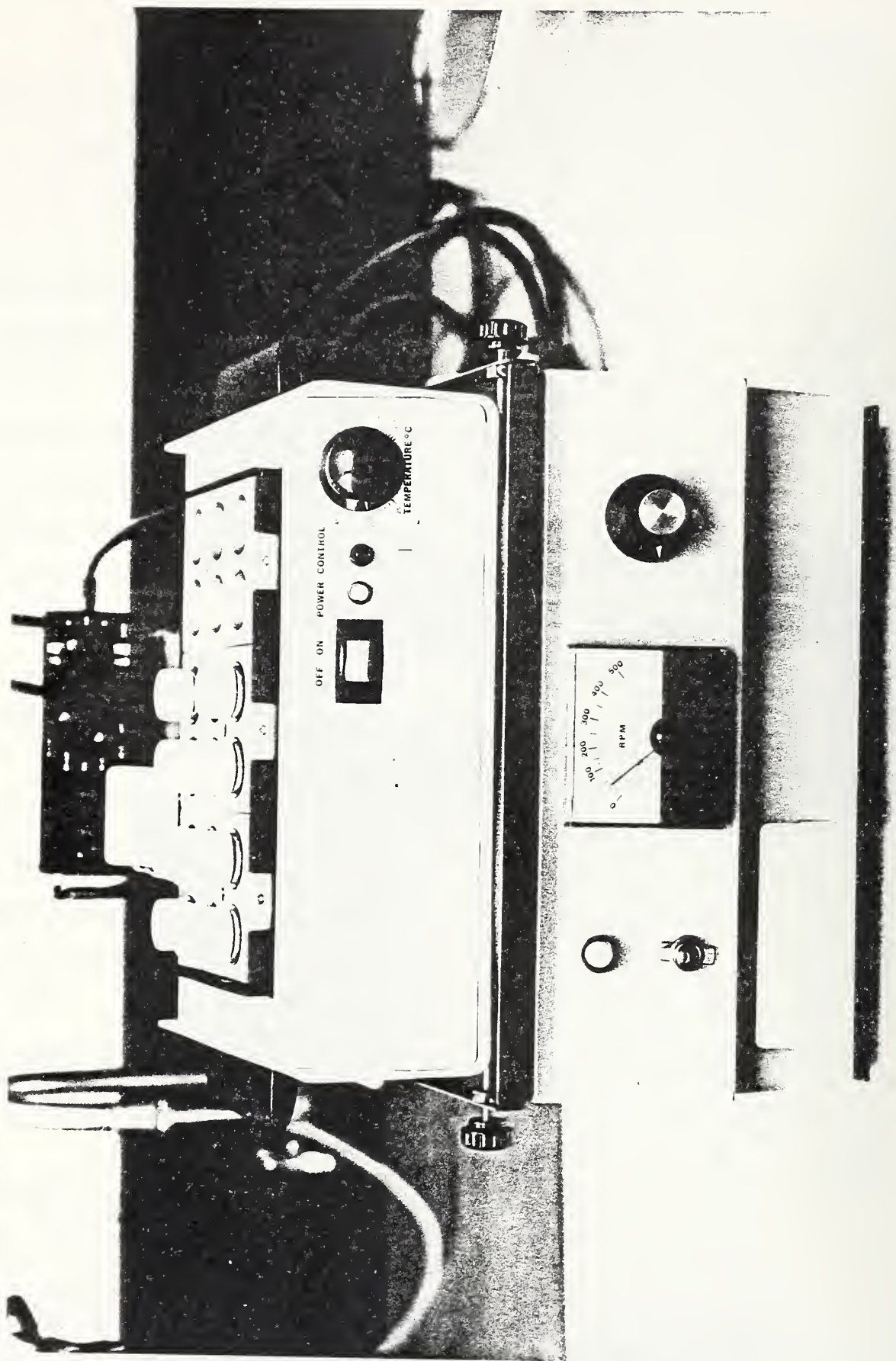
Figure 17. Typical Set up for Extraction Experiment

Table 6

Migration of $C_{18}H_{38}$ from Polyethylene

t hours	$\dfrac{M_t}{M_O}$	t hours	$\dfrac{M_t}{M_O}$	t hours	$\dfrac{M_t}{M_O}$

I. Into Heptane at 24°C

AH1		AH2		BH1	
0.1	0.046	0.025	0.026	0.017	0.086
16	0.836	0.05	0.039	0.033	0.124
23	0.891	0.1	0.053	0.067	0.183
40	0.932	0.25	0.083	0.133	0.28
70	0.955	0.5	0.115	0.25	0.458
136	0.964	1	0.163	0.5	0.683
216	0.969	2	0.242	1	0.804
308.5	0.972	4	0.378	2	0.866
357.5	0.975	8	0.662	4	0.904
665.5	0.974	28	0.902	6	0.919
		72	0.947	22	0.950
		151	0.962	30	0.955
		244.5	0.968	94	0.968
		293.5	0.970	148	0.972
		437.5	0.97	216	0.974
		462	0.974	286.5	0.975
		511.5	0.974		
		578.5	0.975		

CH1				DH1	
0.033	0.008			0.033	0.015
0.067	0.015			0.067	0.026
0.133	0.020			0.133	0.041
0.25	0.029			0.25	0.063
0.5	0.039			0.5	0.108
1	0.056			1	0.202
2	0.086			2	0.342
4	0.128			4	0.477
8	0.196			20	0.693
27.25	0.467			28	0.732
71.25	0.663			92	0.817
150.5	0.787			146	0.838
243.75	0.834			196	0.85
292.75	0.848			289	0.861
316.75	0.853			460	0.873
460.75	0.869			692.5	0.885
510.75	0.873				
603.75	0.878				
775	0.887				
1008	0.894				

Table 6   (continued)

t	$\frac{M_t}{M_0}$	t	$\frac{M_t}{M_0}$
hours		hours	

II.   Into Heptane at 60°C

AH3		AH4	
0.25	0.265	0.25	0.26
0.5	0.382	0.5	0.378
1	0.576	1	0.572
2	0.860	2	0.859
4	0.968	4	0.968
8	0.982	8	0.982
24	0.986	24	0.986
48	0.988	48	0.988
120	0.990	120	0.990
168	0.991	168	0.991

III.   Into Ethanol at 24°C

BE1		BE2	
1	0.114	0.083	0.016
3	0.16	0.167	0.023
19.5	0.335	0.33	0.035
51.5	0.487	0.67	0.052
116	0.639	1	0.069
195	0.735	2	0.109
288	0.778	4	0.166
337	0.799	8	0.237
387	0.816	24	0.367
505	0.832	48	0.485
648	0.857	78	0.578
820	0.855	216	0.720
1220	0.883	409	0.809
1556	0.900	745	0.865
		1081	0.902

IV.   Into Octadecane at 60°C (B01)

B01	
0.25	0.687
0.5	0.922
1	0.978
2	0.984
4	0.987
8	0.990
24	0.992
48	0.993
127	0.994
168	0.995

Table 7

Summary of Extraction of $C_{18}H_{38}$ from Polyethylene

Sample	Weight g	M_0 Mdpm/g	ℓ(nom.) mm	C_0(nom.) wt% $C_{18}H_{36}$	t °C	Solvent	D_i cm²/s	Solvent Absorption %
AH1	0.449	5.03	0.7	1	24	H	(1×10^{-8})	4.5
AH2	0.165	5.20	0.7	1	24	H	7×10^{-9}	5.1
AH3	0.138	5.10	0.7	1	60	H	7×10^{-8}	4.4
AH4	0.150	5.14	0.7	1	60	H	7×10^{-8}	5.2
BE1	0.075	5.21	0.2	1	24	E	(2×10^{-10})	1.0
BE2	0.041	5.18	0.2	1	24	E	8×10^{-11}	1.0
BH1	0.043	4.91	0.2	1	24	H	9×10^{-9}	3.6
BO1	0.160	5.16	0.2	1	60	O	(3×10^{-8})	5.1
CH1	0.160	3.51	0.7	0.01	24	H	1×10^{-9}	4.3
DH1	0.054	2.13	0.2	0.01	24	H	2×10^{-10}	2.0

Solvents = E - Ethanol, H - Heptane, O - Octadecane

Thickness ℓ = the variation in the thickness is generally within $\pm$ 0.05 mm.

Solvent Absorption = measured right after the sample was removed from the solvent

activity extracted between t and t-1 is simply the total activity in the extracting solution, i.e., $A_t = N_t/E_t$.

In Method (3) M_t/M_o is obtainable directly from each vial, thus

$$M_t/M_o = A_{s,t}/(A_{s,t} + A_{r,t})$$

where A_s is the activity in the solution and A_r the residue activity in the polymer.

The initial D_i is estimated from the approximate expression of

$$\frac{M_t}{M_\infty} = 4\left(\frac{Dt}{\pi \ell^2}\right)^{\frac{1}{2}} \tag{52}$$

where D is the diffusion constant, t the time, ℓ the thickness and M_∞ the amount extracted at infinite time. Substitution of M_o for M_∞ should make less than 10% error (cf. section on the discussion of the results).

The amount of solvent absorbed was obtained by blotting the rinsed test specimen at the last measurement with filter papers and weighing immediately. Adjustments have also been made to the weight loss due the loss of the migrant.

Data on the extraction of $C_{18}H_{38}$ from polyethylene, BW1, is not presented here, because of the inconclusiveness of the result. The radioactivity in the aqueous extract is very close to that of the background even after 2-months of extraction at 24°C.

As all the results are listed and shown here in terms of M_t/M_o, it is some-times more convenient to express them in terms of the FDA's expression for extrac-tives in terms of ppm (µg of extractives per ml of solvent or per 0.1 in^2 of polymer surface area). To do this one may convert the M_t/M_o values by a factor expressing the original concentration of the extractives in 10^{-7}g per square inch of surface area. By approximating the density of polymer as 1 g/cm^3, the factor is 0.32 X 10^{-6} $C_o\ell$, where C_o is the concentration of the additive in weight fraction and ℓ is thickness in cm.

DISCUSSION

The experimental results are grouped together to show the effects of thickness, additive concentration in the polymer, temperature and solvent. Three time scales, i.e., $\log_{10} t$, $t^{\frac{1}{2}}$, and $t^{-\frac{1}{2}}$, are used to plot the results with each scale emphasizing a different time domain. Figure 18 shows the corresponding scale in t versus the three scales. For all the subsequent graphs, the dashed lines in graphs A and B denote the extension of a linear $t^{\frac{1}{2}}$ dependence, whereas the dashed lines (where n is an integer) denotes the factor for the coordinates as 10^n, whereas in C denote the extension of a linear $t^{-\frac{1}{2}}$ dependence.

Figure 19 and 20 show the effect of 0.7 and 0.2 mm nominal thicknesses for AH1, AH2 and BH1 at 1% $C_{18}H_{38}$ concentration, and for CH1 and DH1 at 0.01% $C_{18}H_{38}$, respectively. Over most of the ranges, M_t/M_o for BH1 is about four times that of AH2, with a thickness ratio of BH1 : AH2 = 1 : 3.5. The initial diffusion constants, D_i estimated from the initial portions of the extraction experiments, for AH2 and BH1 are in good agreements with the thickness variation as per Eq. (52). Therefore initially either the rate or the amount of additive migration per unit surface area should be the same regardless of the sample thicknesses. At long times, when most of the additive has been extracted, the total amount migrated per surface area will be proportional to the thickness. Only qualitative agreements may be drawn from the results of CH1 and DH1.

The effect of concentration varying from 1% to 0.01% of added $C_{18}H_{38}$ is shown in Figure 21 and 22 for AH1, AH2 and CH1 at 0.7 mm thickness, and for BH1 and DH1 at 0.2 mm thickness, respectively. Over most of ranges there is only a change by a factor of 3 in the M_t/M_o for a hundred fold change in the added $C_{18}H_{38}$ for the 0.7 mm samples. Decreasing the concentration by a factor of 100 seems to decrease D_i by a factor of 10. However there appears a 10 fold change in the amount migrated at short times between the 0.2 mm samples BH1 and DH1.
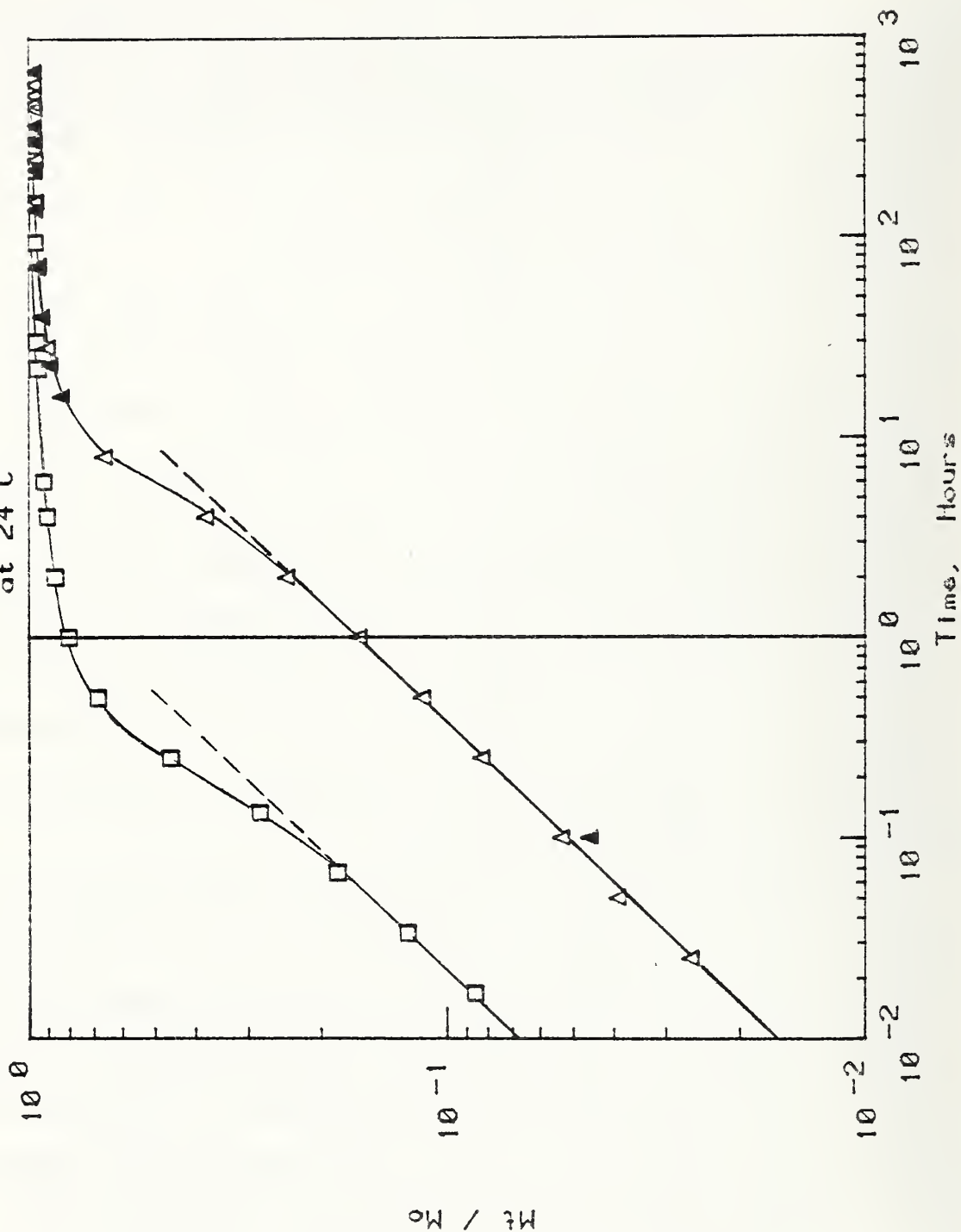
Figure 19 A. Migration of $C_{18}H_{38}$ from Polyethylene – 1% $C_{18}H_{38}$ Sheets into C_7H_{16}
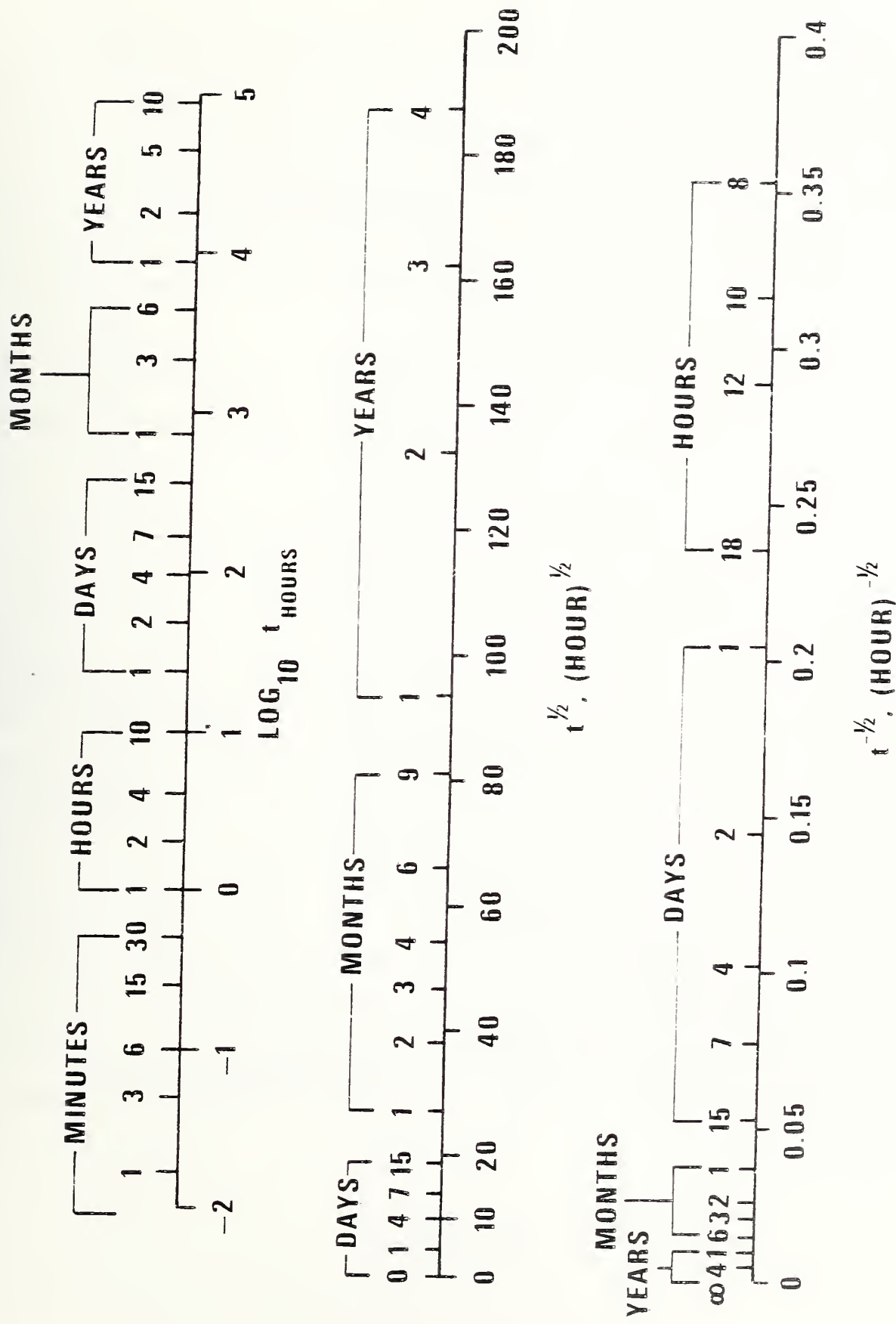
Figure 18. Comparison of Time Scales

It appears that the results from the experiment DH1 or the sample D is somewhat peculiar. Unlike AH2, BH1 and CH1, even the initial portion of the DH1 extraction curve does not have a $t^{\frac{1}{2}}$ dependency. It also absorbs least amount of solvents, C_7H_{18} (Table 7). If one artificially brings the initial DH1 curve up so that it has a $t^{\frac{1}{2}}$ dependency and that its initial diffusion constant for DH1 is similar to that of CH1, then the new curve will also indicate a 3-fold change in M_t/M_o or a 10-fold change in D_i.

The effect of temperature is shown in Figure 23. A 36^oC temperature increment from 24 to 60^oC increases D_i by a factor of 10 or the amount migrated by a factor of 3 at short t.

Changing from non-polar solvent to polar solvent from C_7H_{16} to ethanol decreased the D_i by a factor of 100 or the amount extracted by a factor of 10 at short times as shown in Figure 24.

At this time the results on B01, Figure 25, may not be compared directly with other results collected for the effect of a single variable. However if we assume the migration of $C_{18}H_{38}$ has the same temperature dependency as that of $C_{18}H_{38}$ into C_7H_{16} then the amount migrated into $C_{18}H_{38}$ is about 2/3 of that migrated into C_7H_{16} at the same temeprature under otherwise the same conditions.

In comparing the two extraction methods, i.e., continuous extraction with aliquot taken at different times and discrete extraction·with new solvent each time, the differences are very small even at large t as shown in Figure 19 and 21 (C) for AH1 and AH2 and in Figure 24 (C) for BE1 and BE2. A set of duplicate measurements, AH3 and AH4, was made at 60^oC with virtually identical results as shown in Figure 23.
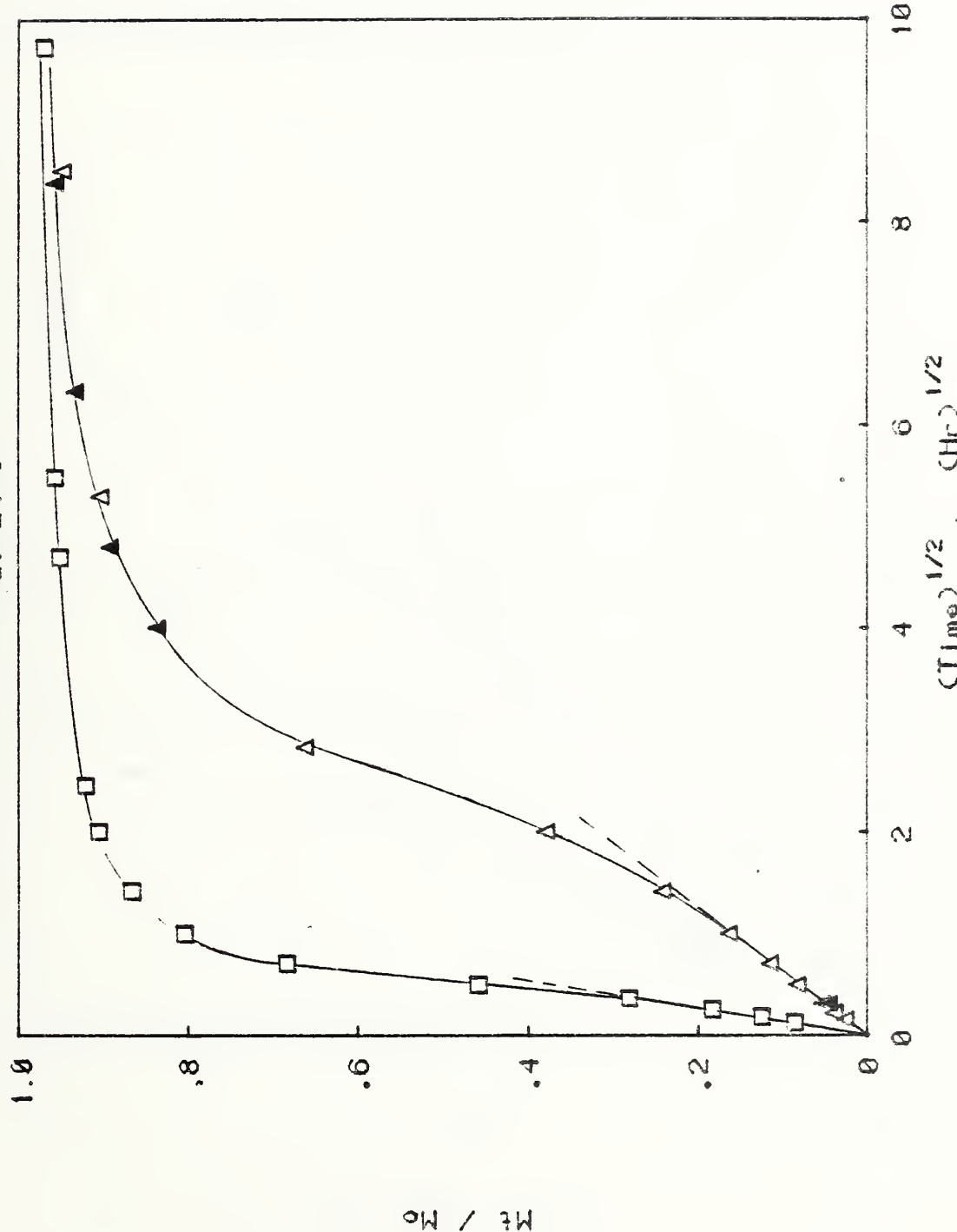
Figure 19 B. Migration of $C_{18}H_{38}$ from Polyethylene – 1% $C_{18}H_{38}$ Sheets into C_7H_{16}

at 24°C. ℓ=0.7 mm: $\triangle$H1, $\triangle$H2. ℓ=0.2 mm: $\square$BH1
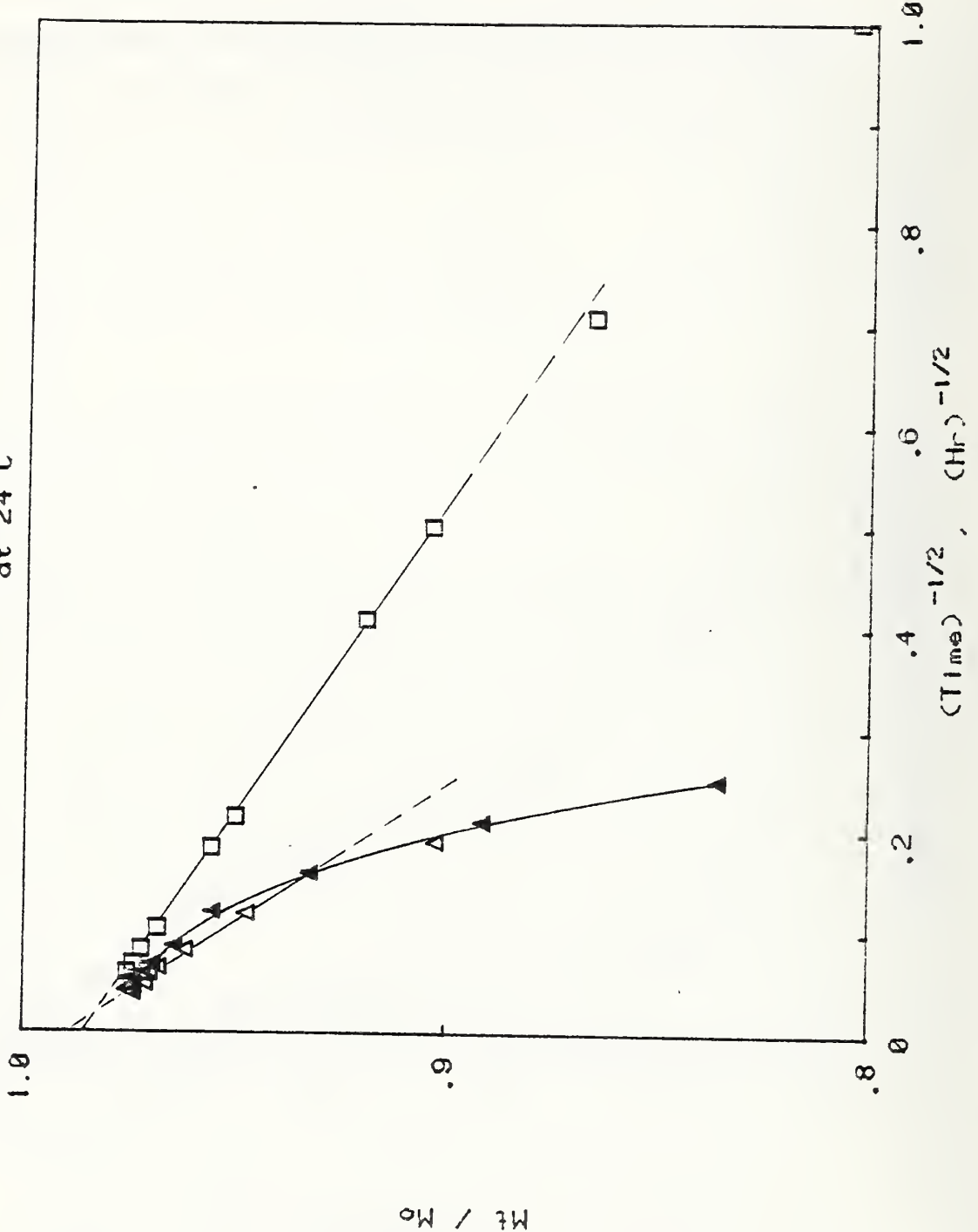
Figure 19 C. Migration of $C_{18}H_{38}$ from Polyethylene – 1% $C_{18}H_{38}$ Sheets into C_7H_{16} at 24°C. $\ell=0.7$ mm: $\triangle$ AH1, $\sqrt{}$ AH2. $\ell=0.2$ mm: $\square$ RH1
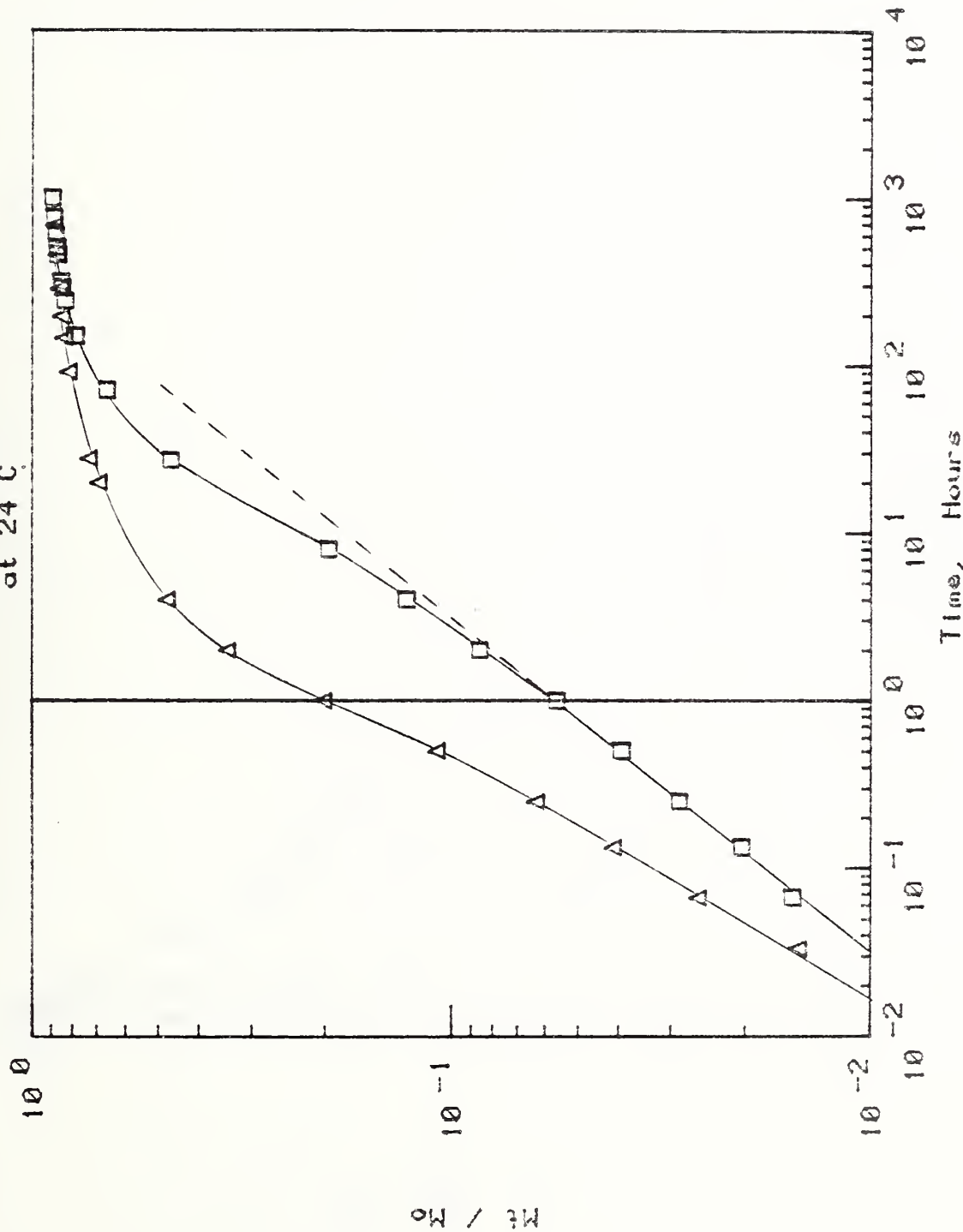
Figure 20 A. Migration of $C_{18}H_{38}$ from Polyethylene - 0.01% $C_{18}H_{38}$ Sheets into
C_7H_{16} at 24°C. $\ell=0.7$ mm; $1:CH1$. $\ell=0.2$ mm; $\ell:.DH1$

61
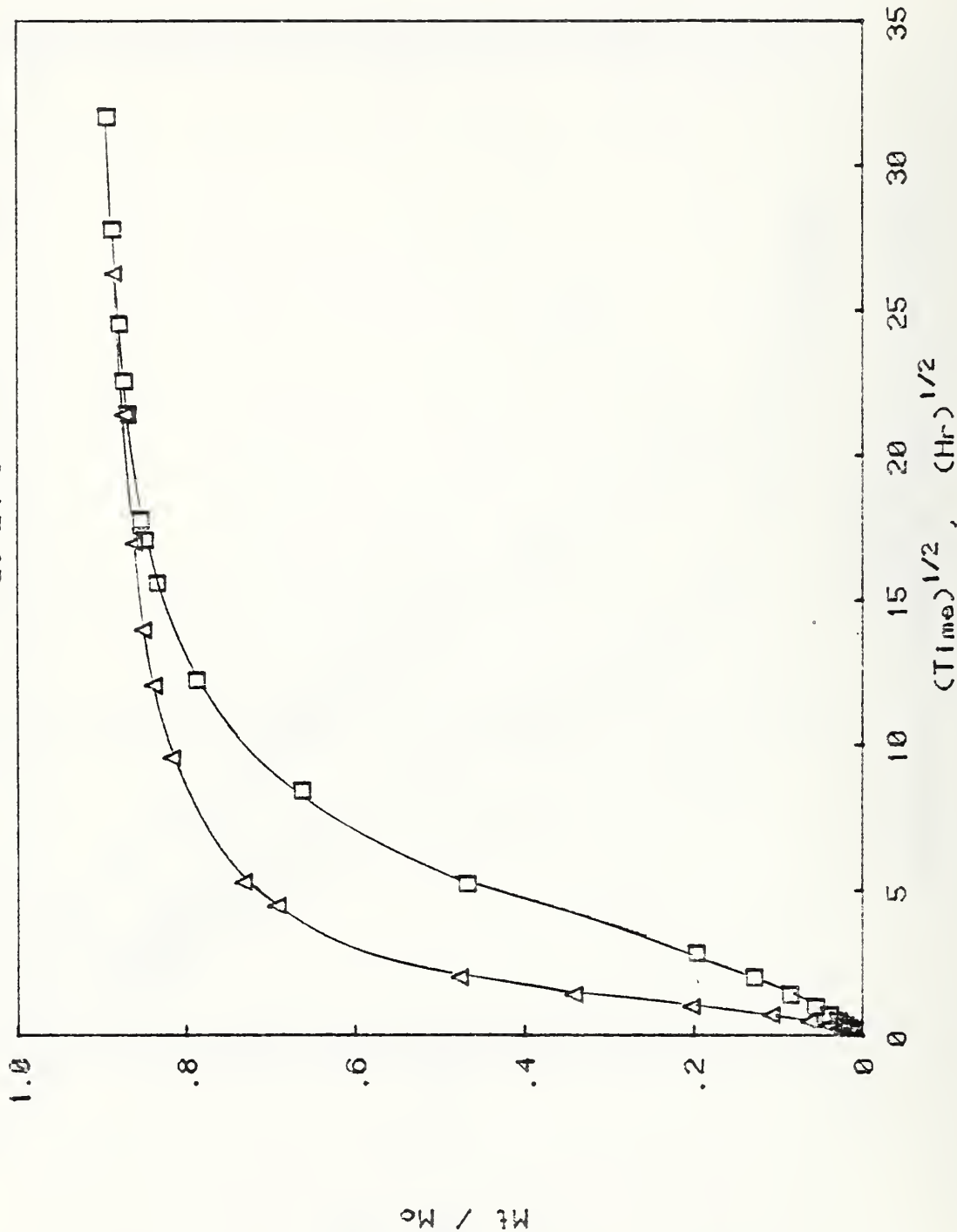
Figure 20 B. Migration of $C_{18}H_{38}$ from Polyethylene - 0.01% $C_{18}H_{38}$ Sheets into
C_7H_{16} at 24°C. $\ell=0.7$ mm:⎓CH⎓. $\ell=0.2$ mm:△DH△
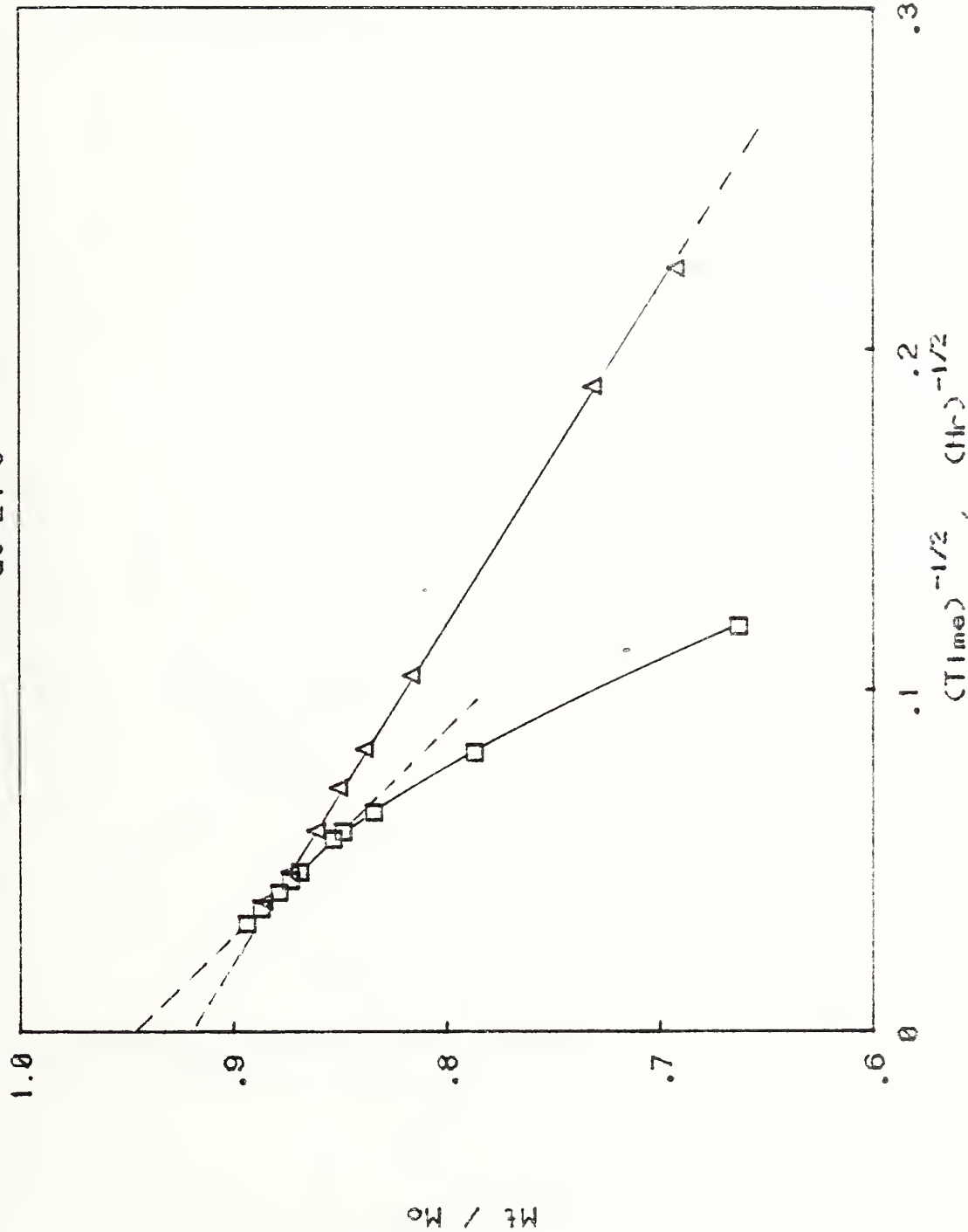
Figure 20 C. Migration of $C_{18}H_{38}$ from Polyethylene – 0.01% $C_{18}H_{38}$ Sheets into

C_7H_{16} at 24°C. $\ell=0.7$ mm: △IIt; $\ell=0.2$ mm: △MIL
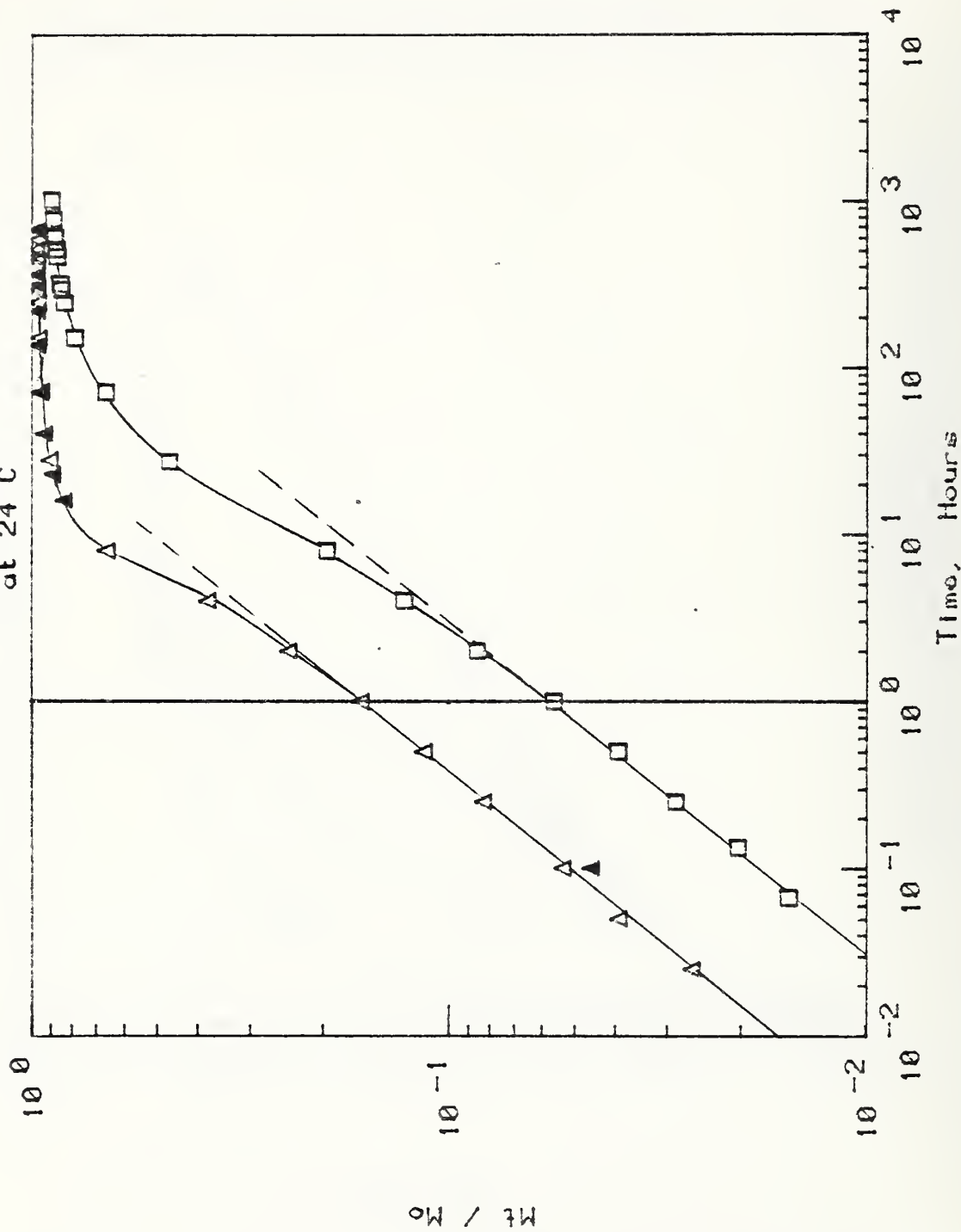
Figure 21 A. Migration of $C_{18}H_{38}$ from 0.7 mm Polyethylene Sheets into C_7H_{16}

at $24^{\circ}C$. $C_O=1\%$: $\triangle$ AH1, $\triangle$ AH2. $C_O=0.01\%$: $\square$ CH1
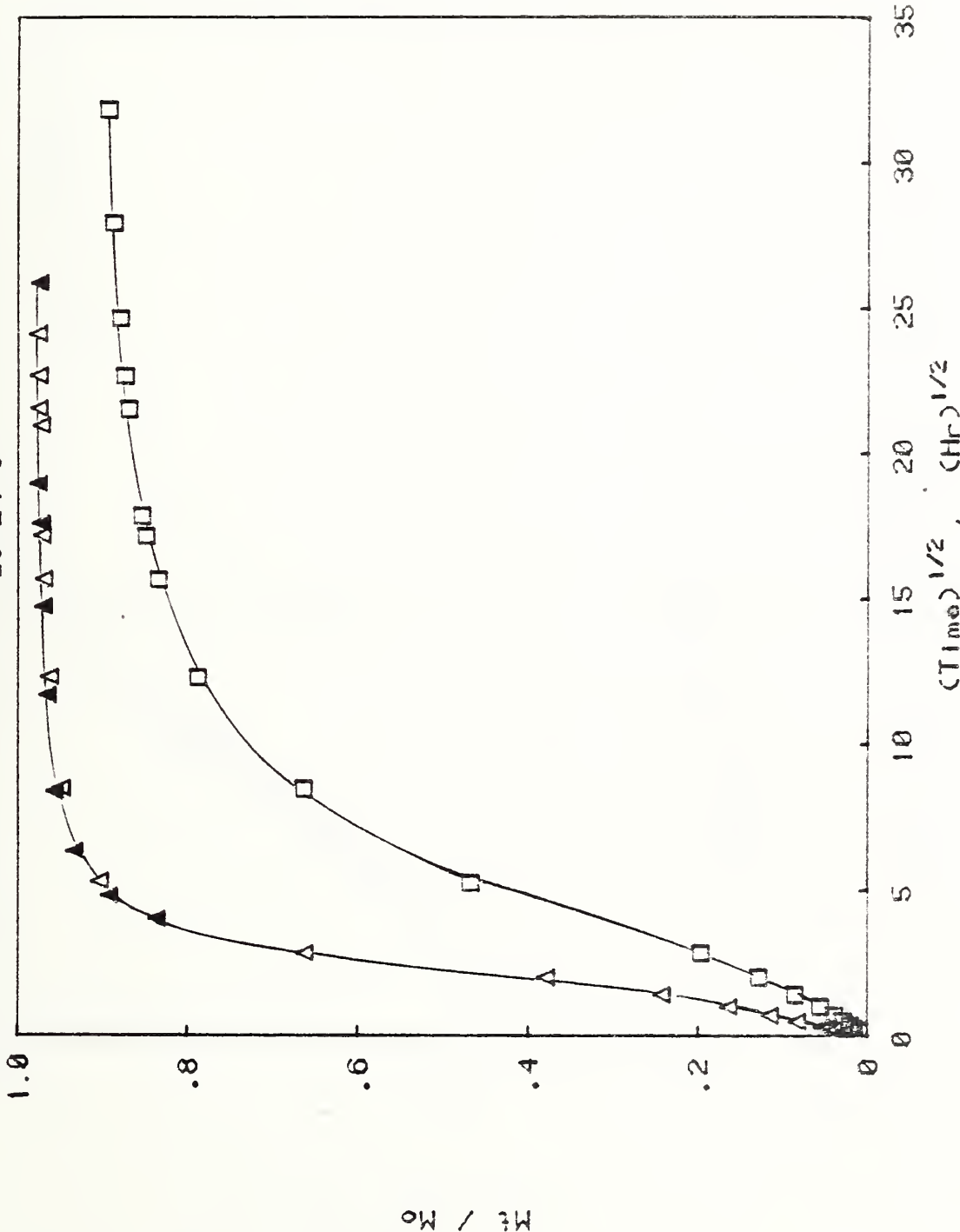
Figure 21 B. Migration of $C_{18}H_{38}$ from 0.7 mm Polyethylene Sheets into C_7H_{16}

at 24°C. $C_0 = 1\%: $ AH, AP. $C_0 = 0.01\%:$ CH
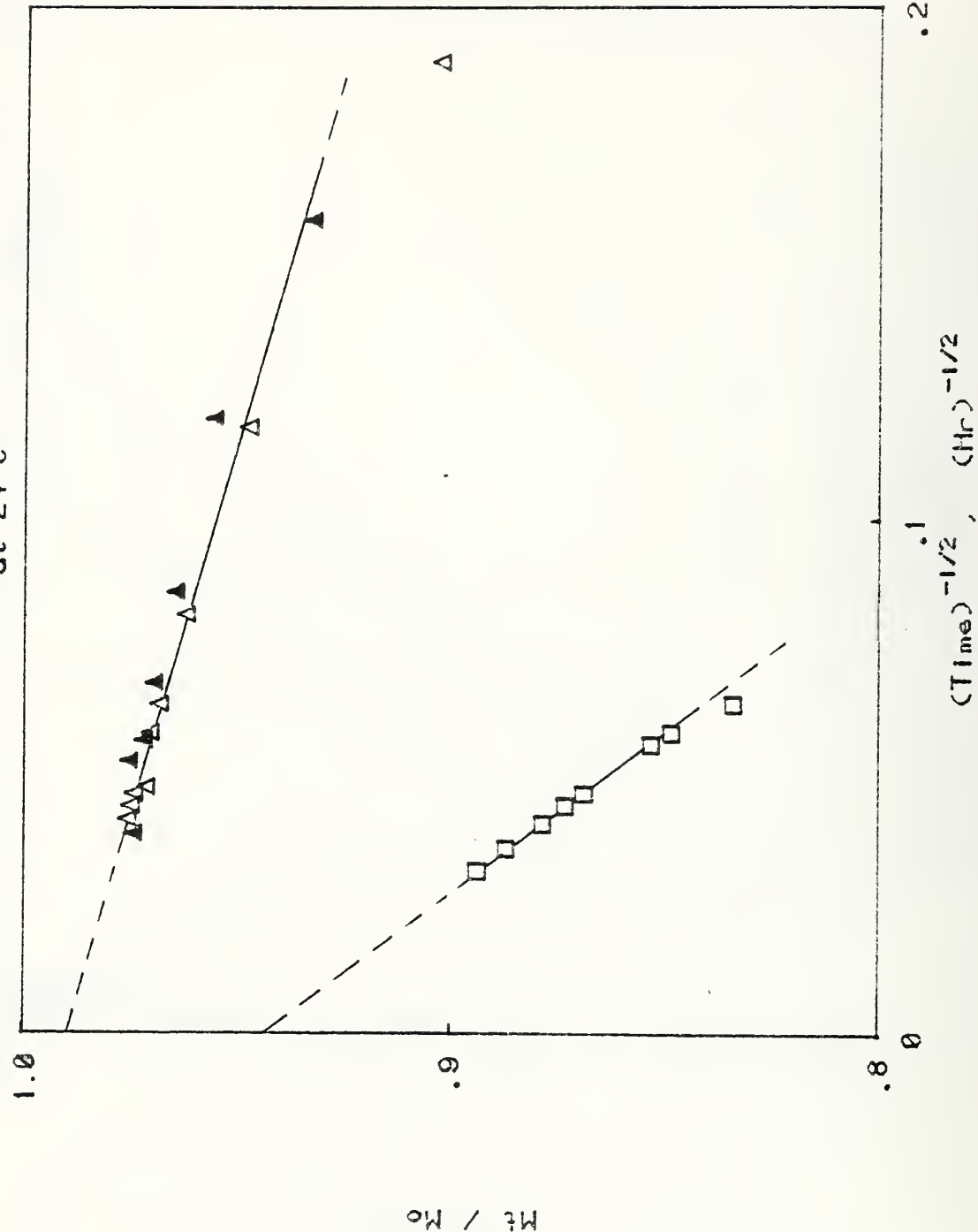
Figure 21 C. Migration of $C_{18}H_{38}$ from 0.7 mm Polyethylene Sheets into C_7H_{16}

at 24°C. $C_0=1\%: \triangle \triangle H2, \triangle \triangle H2$. $C_0=0.01\%: \square H1$
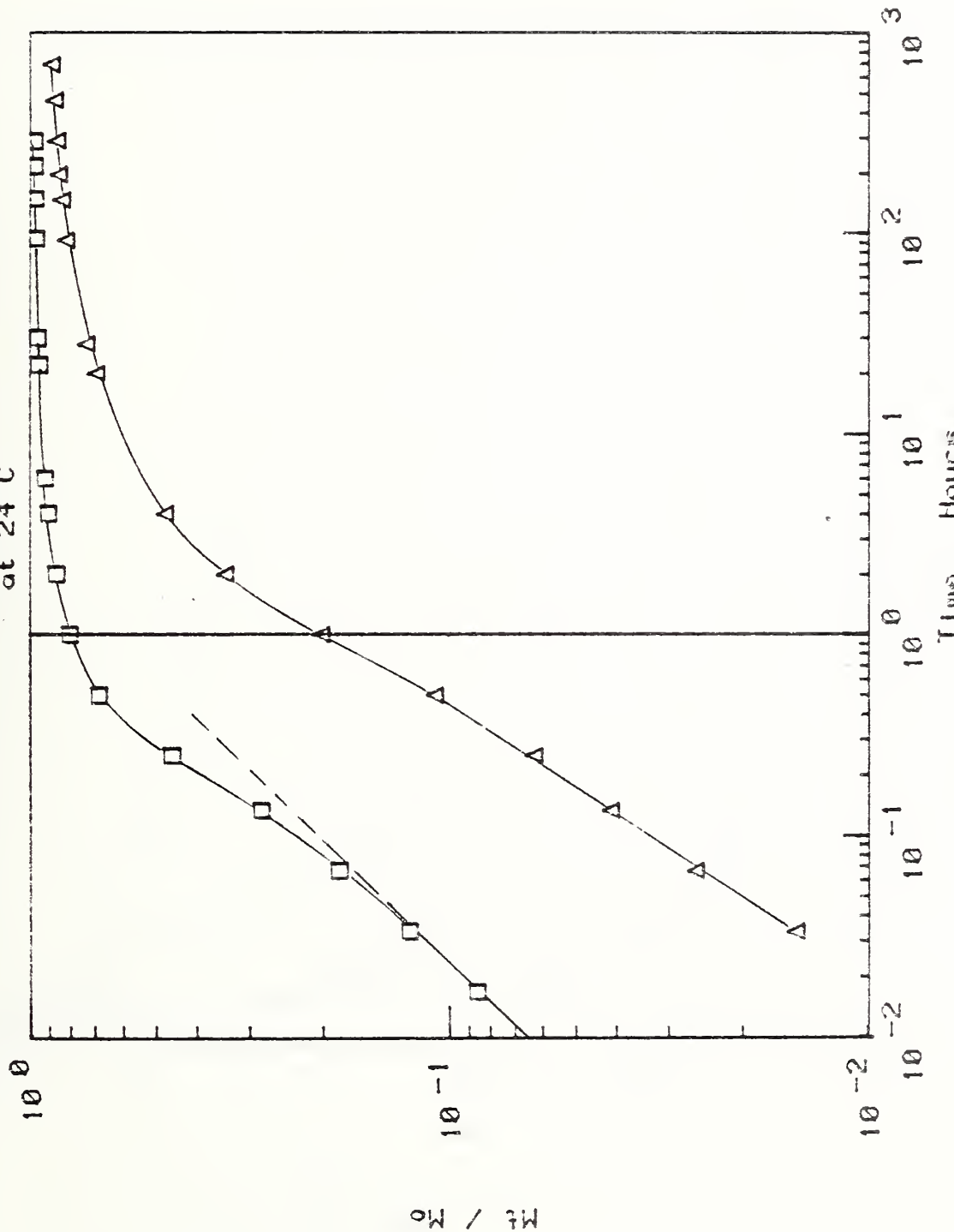
Figure 22 A. Migration of $C_{18}H_{38}$ from 0.2 mm Polyethylene Sheets into C_7H_{16}

at 24°C. $C_o = 1\%$: 1·BHT. $C_o = 0.01\%$: ·BHT

Migration of n-C18H38 from Polyethylene
into C7H16
at 24 C

$(Time)^{1/2}$, $(Hr)^{1/2}$

Mt / Mo
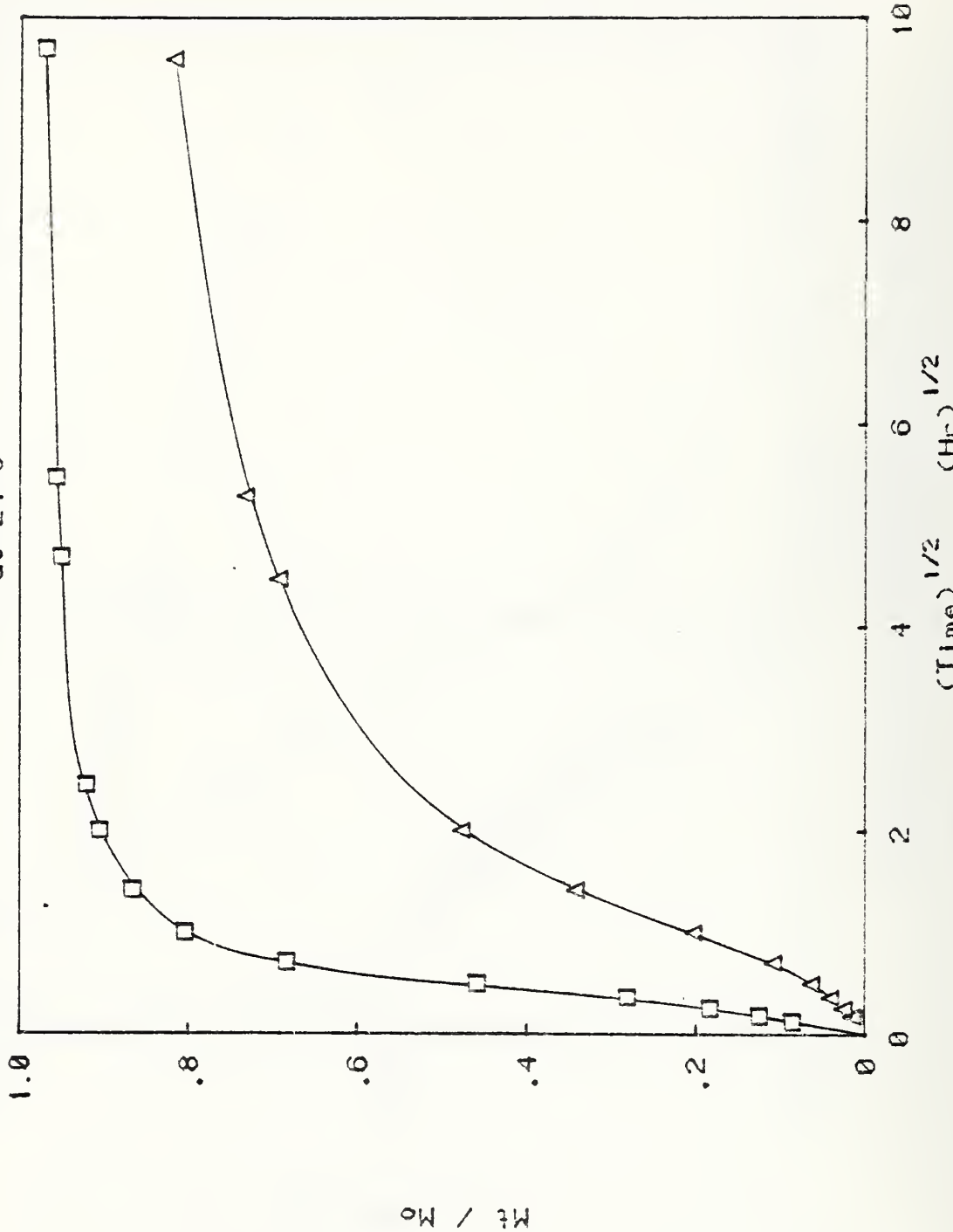
Figure 22 B. Migration of $C_{18}H_{38}$ from 0.2 mm Polyethylene Sheets into C_7H_{16}

at 24°C. $C_O=1\%$:☐BHT. $C_O=0.01\%$:△BHT.

68

Migration of n-C18H38 from Polyethylene
into C7H16
at 24 C
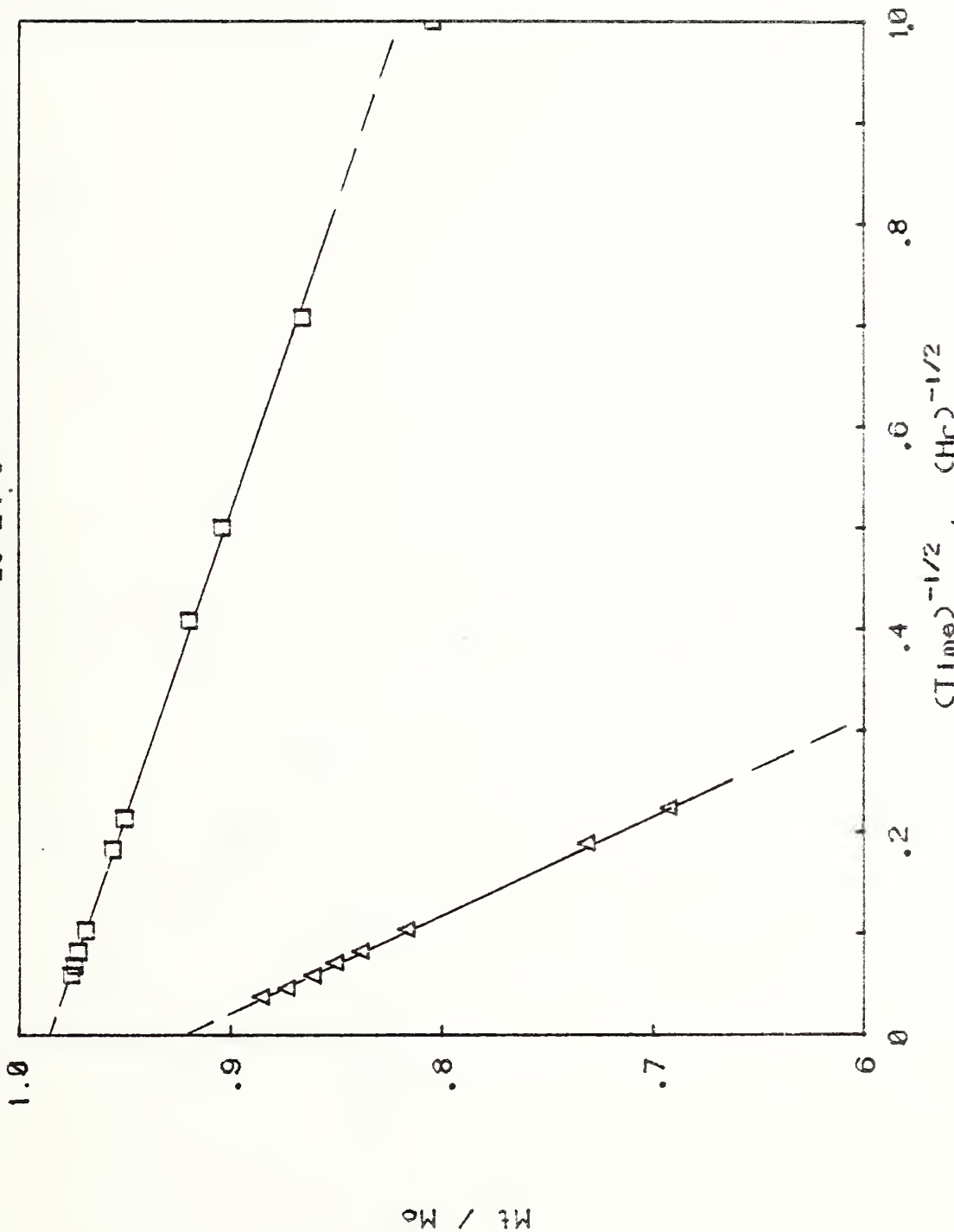
Figure 22 C.   Migration of $C_{18}H_{38}$ from 0.2 mm Polyethylene Sheets into C_7H_{16}

at 24°C. C_o=1%: BHI. C_o=0.01%: BHI
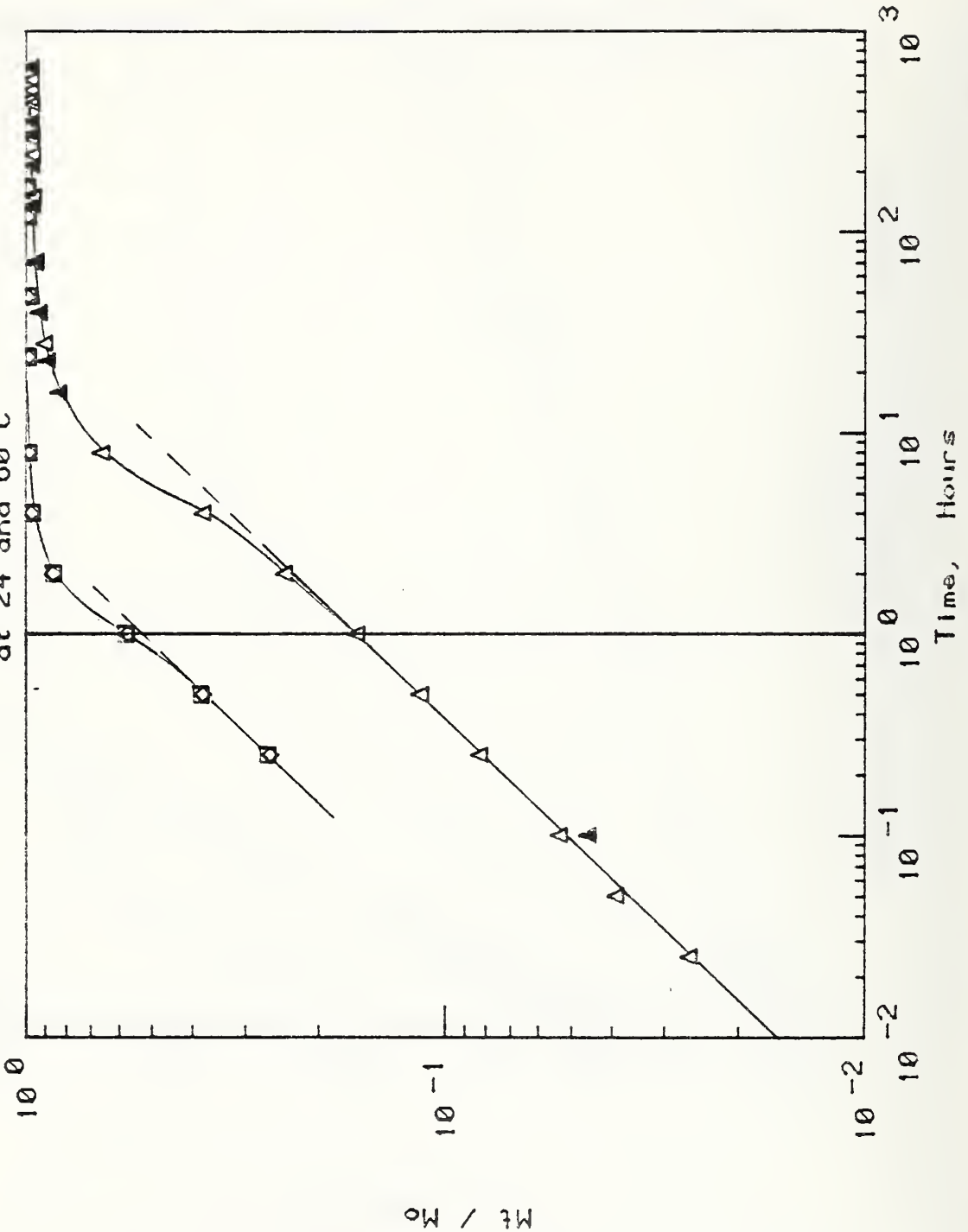
Figure 23 A. Migration of $C_{18}H_{38}$ from 0.2 mm Polyethylene - 1% $C_{18}H_{38}$ Sheets

into C_7H_{16}. 24°C: △ AH1, ◁ AH2. 60°C: ▷ AH3, ▶ AH4.
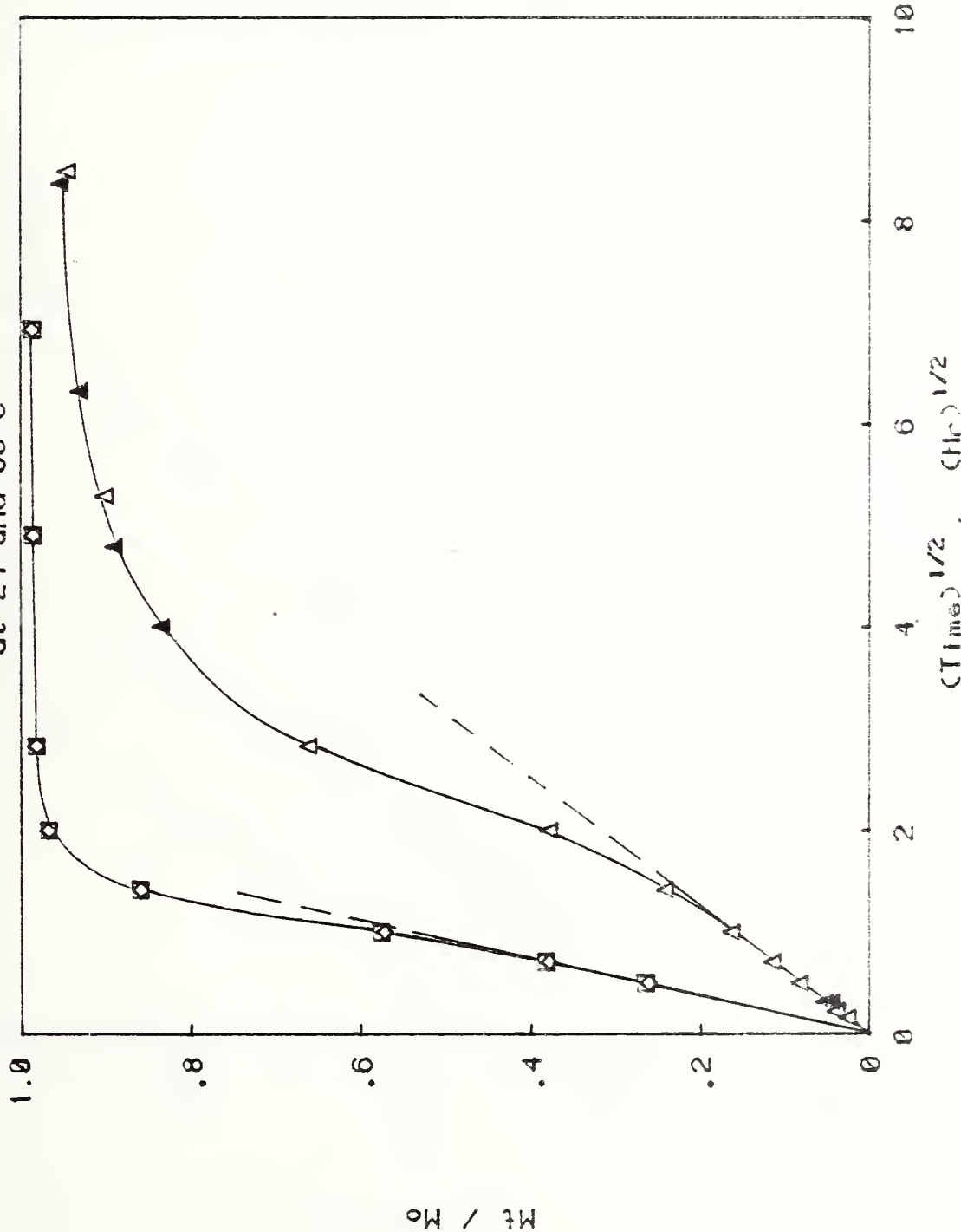
Figure 23 B. Migration of $C_{18}H_{38}$ from 0.2 mm Polyethylene – 1% $C_{18}H_{38}$ Sheets into C_7H_{16}. $24°C$: ▲ △H1, △H2. $60°C$:■H3, ◇H4.

Figure 23 C. Migraton of $C_{18}H_{38}$ from 0.2 mm Polyethylene - 1% $C_{18}H_{38}$ Sheets into C_7H_{16}. 24°C: $\triangle$ AH1, $\triangle$ AH2. 60°C: $\square$ AH3, $\diamondsuit$ AH4.
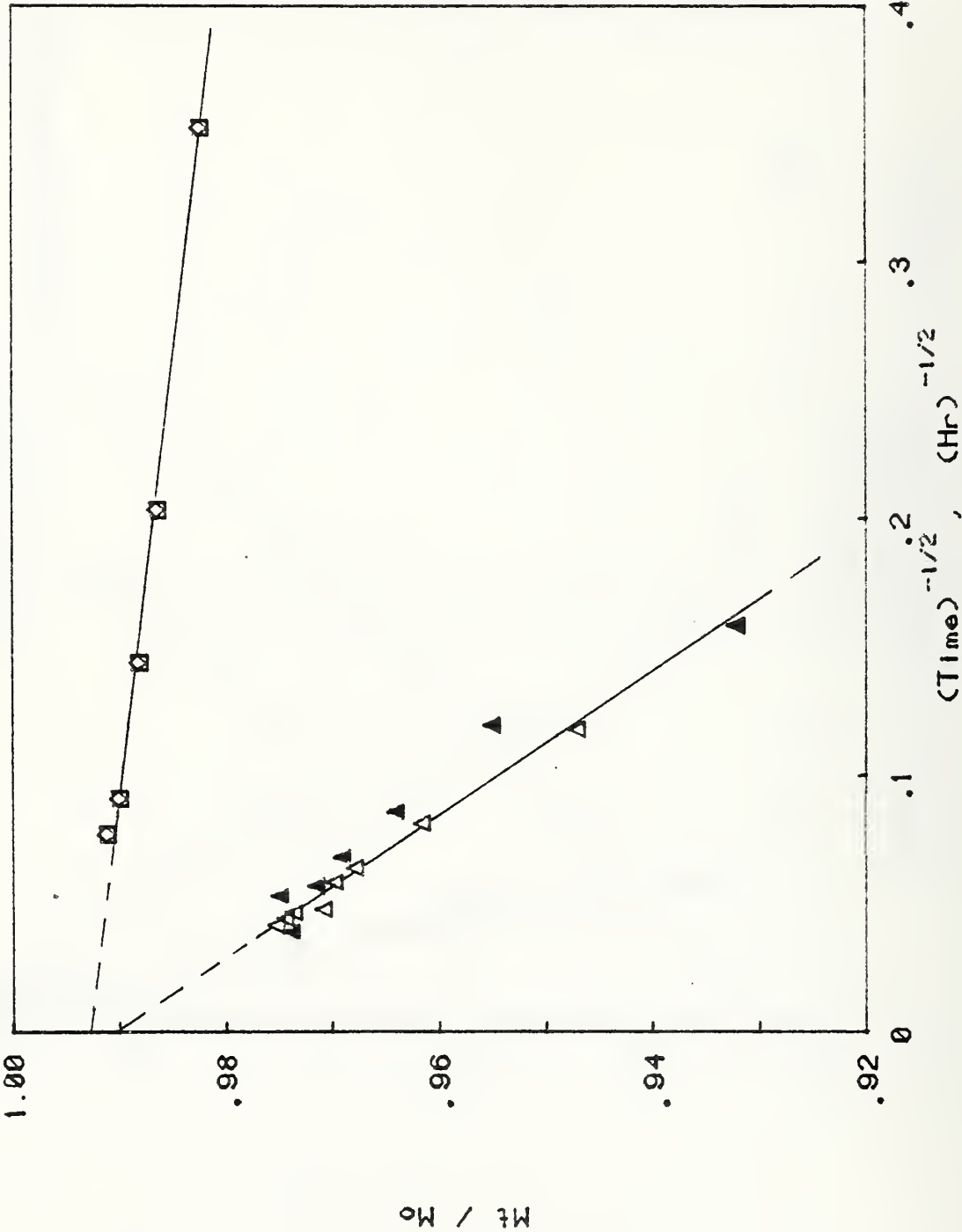
Figure 24 A. Migration of $C_{18}H_{38}$ from 0.2 mm Polyethylene - 1% $C_{18}H_{38}$ Sheets
at 24°C. Into C_7H_{16}: □ BEl. Into Ethanol: △ BEl, ◇ BE2.

Migration of n-C18H38 from Polyethylene
into C7H16 and Ethanol
at 24 C
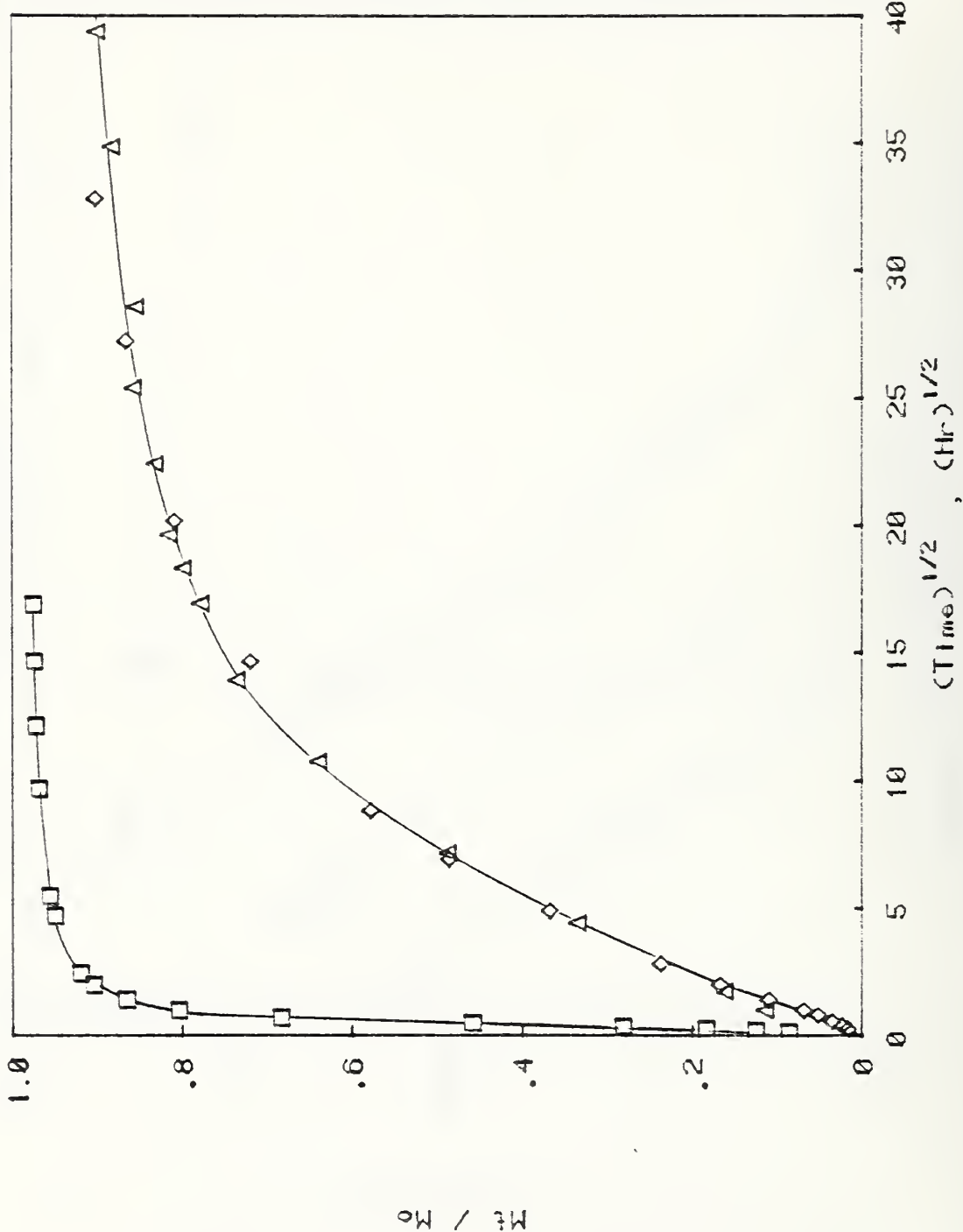
Figure 24 B. Migration of $C_{18}H_{38}$ from 0.2 mm Polyethylene – 1% $C_{18}H_{38}$ Sheets at 24°C. Into C_7H_{16}: □ Run. Into Ethanol: △ BEt, ◇ B12.

74
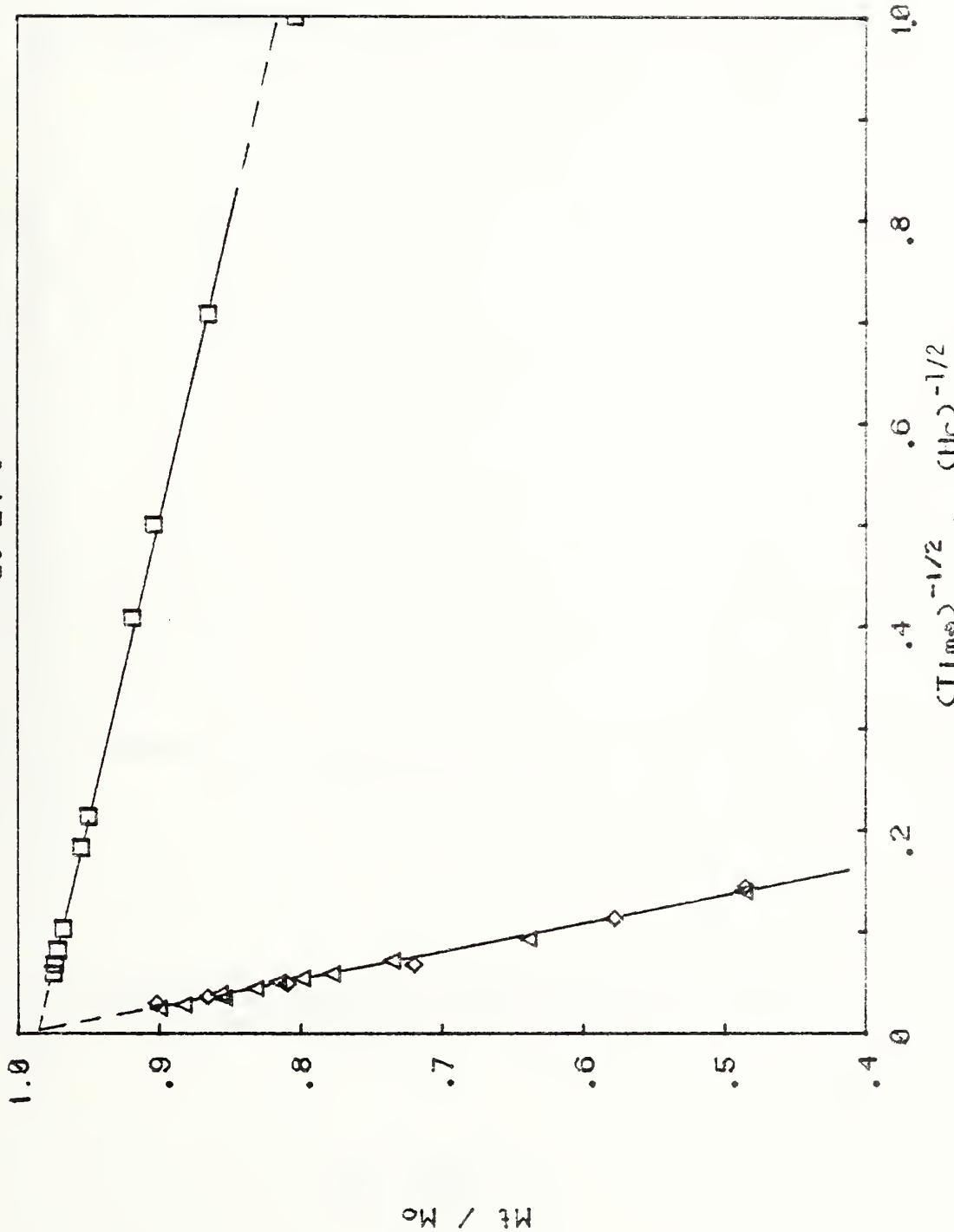
Figure 24 C. Migration of $C_{18}H_{38}$ from 0.2 mm Polyethylene – 1% $C_{18}H_{38}$ Sheets at 24°C. Into C_7H_{16}: BH1. Into Ethanol: BE1, BE2.
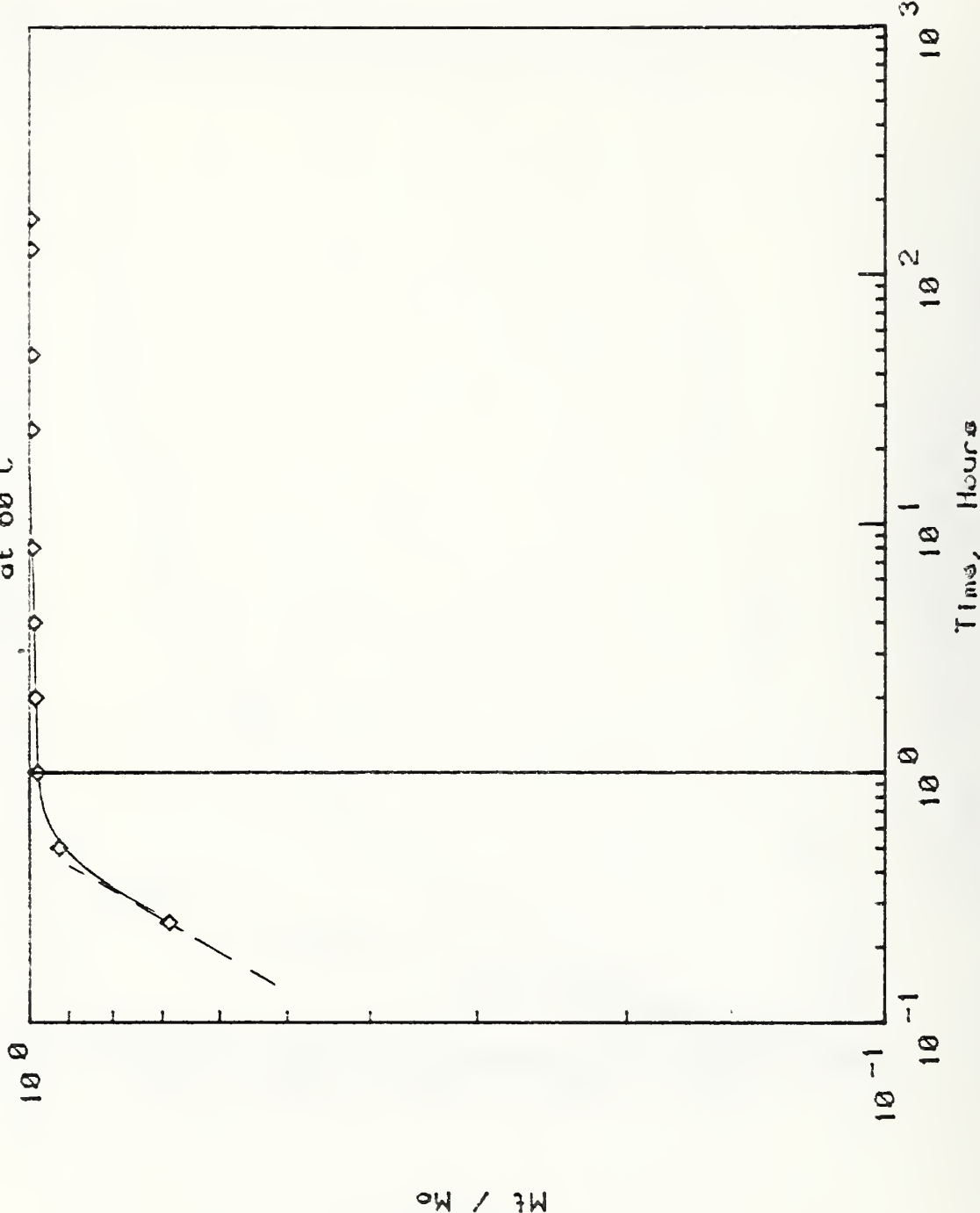
Figure 25 'A. Migration of labeled $C_{18}H_{38}$ from 0.2 mm Polyethylene – 1% $C_{18}H_{38}$

Sheets into unlabeled $C_{18}H_{38}$ at 60°C.
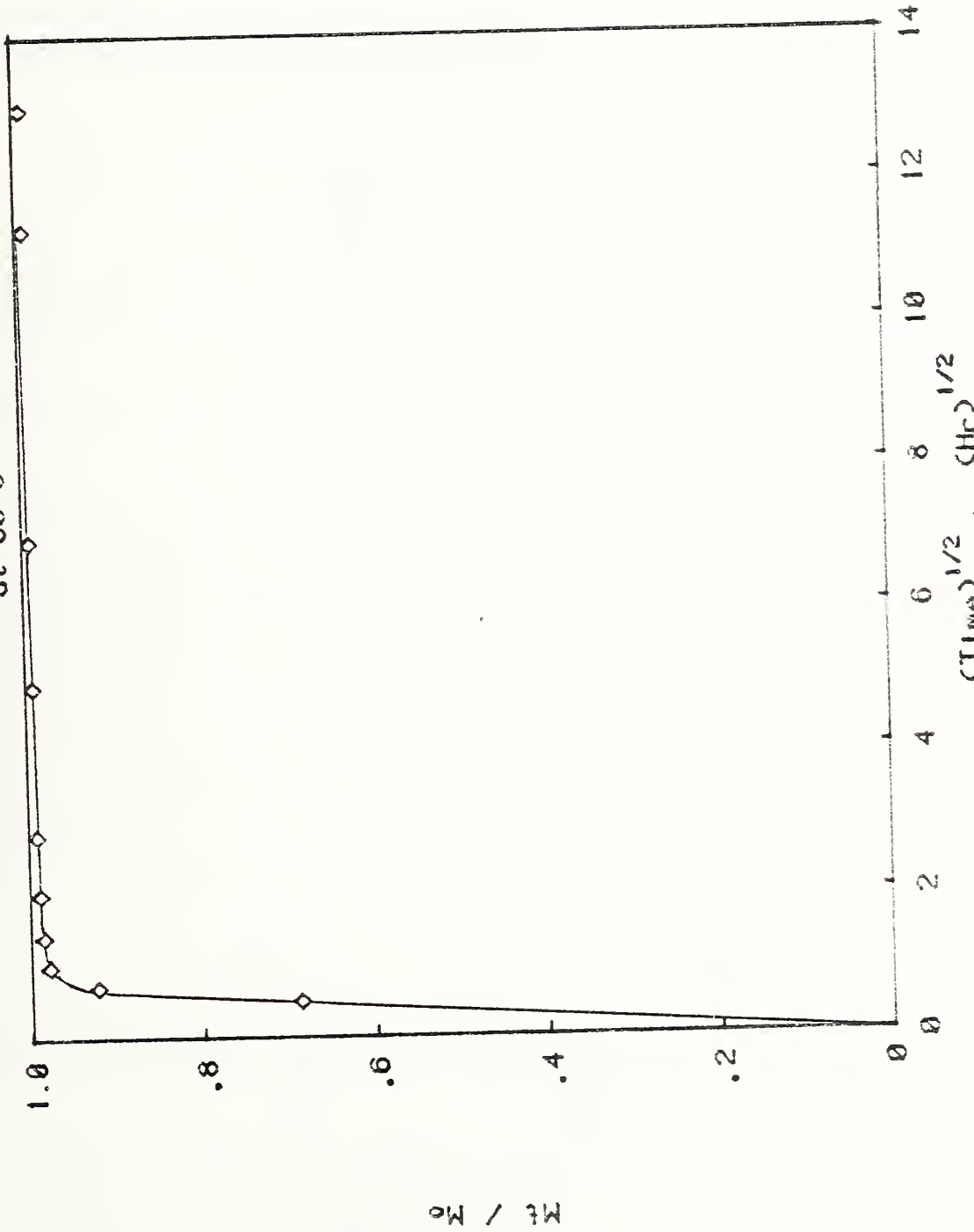
Figure 25 B. Migration of labeled $C_{18}H_{38}$ from 0.2 mm Polyethylene – 1% $C_{18}H_{38}$

Sheets into unlabelled $C_{18}H_{38}$ at 60°C.

77
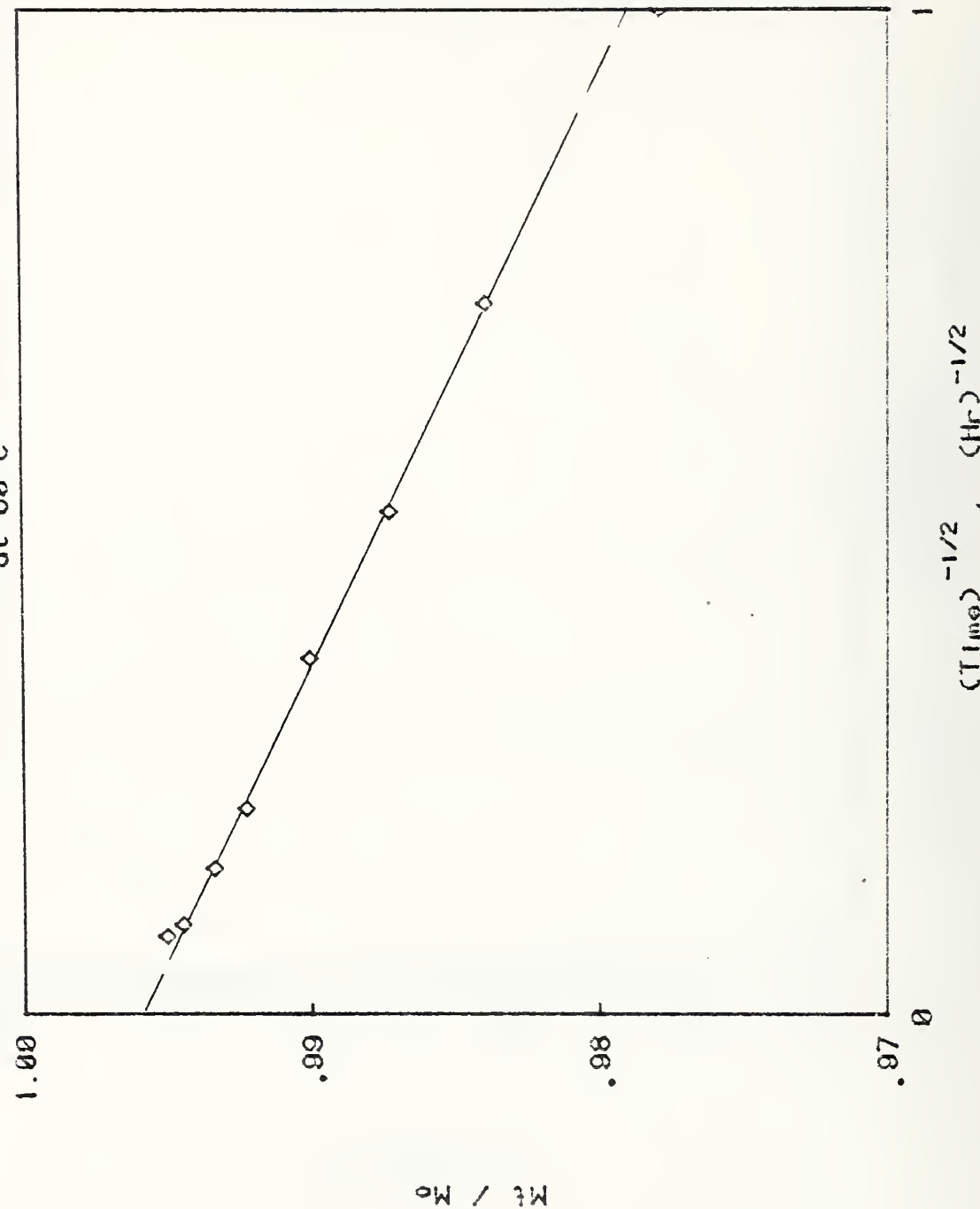
Figure 25 C. Migration of labeled $C_{18}H_{38}$ from 0.2 mm Polyethylene - 1% $C_{18}H_{38}$

Sheets into unlabeled $C_{18}H_{38}$ at 60°C.

Figure 26 A and B show the migration behavior as calculated from a solution for the diffusion from a plane sheet with the assumption that the diffusion coefficient is concentration independent and that the sheet does not swell

$$\frac{M_t}{M_\infty} = 1 - \frac{8}{\pi^2} \sum_{n=0}^{\infty} \frac{1}{(2n+1)^2} \exp\left[-D(2n+1)^2 \pi^2 t/\ell^2\right] \tag{53}$$

At $M_t/M_\infty \lesssim 0.5$, M_t/M_∞ is proportional to $t^{\frac{1}{2}}$. Thus the initial diffusion constant may be estimated by the approximation for short times, Eq. (52). At long times

$$\frac{d}{dt}\left[\ln(M_\infty - M_t)\right] = \frac{D\pi^2}{\ell^2} \tag{54}$$

Therefore the plot of $\ln(1 - M_t/M_\infty)$ versus t at $M_t/M_\infty > 0.5$ is highly linear, as shown in Figure 27. The behavior at long times, or as M_t/M_∞ approaches 1, as calculated from the series solution is shown in Figure 26 C and D for M_t/M_∞ versus $1/t^{\frac{1}{2}}$. It seems that when the time scale is expressed in $1/t^{\frac{1}{2}}$, the approach of M_t to M_∞ is quite sudden. The experimental results, Figure 19-25 (C), however seem to indicate a strong linear $1/t^{\frac{1}{2}}$ dependence at long times, and this linearity may start to appear in some cases when M_t/M_∞ is about 0.5. Thus the above mentioned solution is not sufficient to describe the overall behavior of these experiments. The difference may be due to swelling by solvent, concentration dependent diffusion constants and perhaps edge effects.

Additional general conclusion may be drawn from the limited set of the extraction data:

(1) No "blooming" of additives was observed in these experiments. This was indicated in Figures 19-25 (B) where the extraction curves can be extrapolated through the origin at t=0. An intercept at positive values of M_t/M_0 at t=0 would indicate the presence of blooming. This observation is expected for oligomers at moderate concentration, as they should be highly
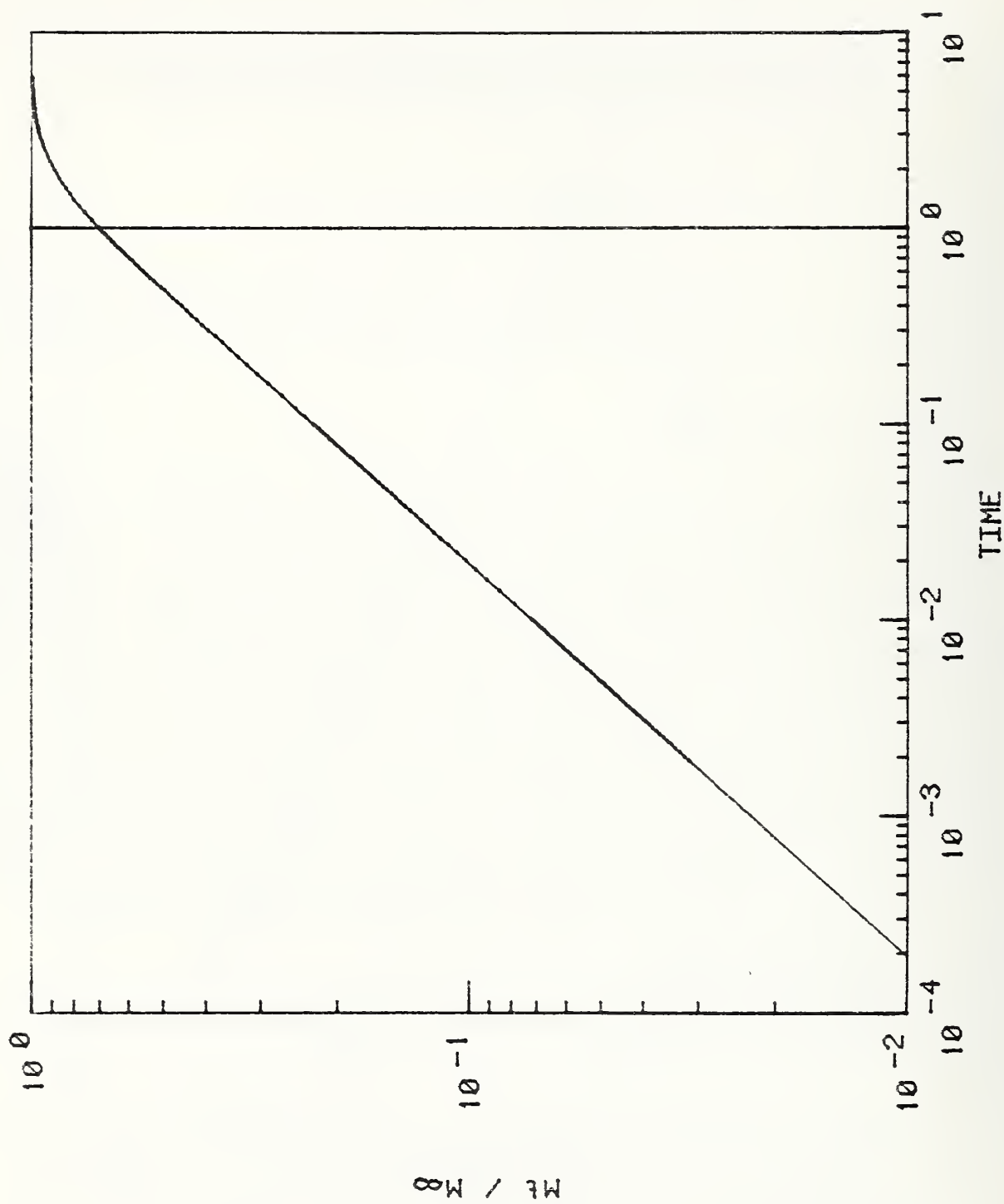
Figure 26 A. Calculated Diffusion Curves M_t/M_∞ versus $\log(4D_{II}^2 t/\ell^2)$.
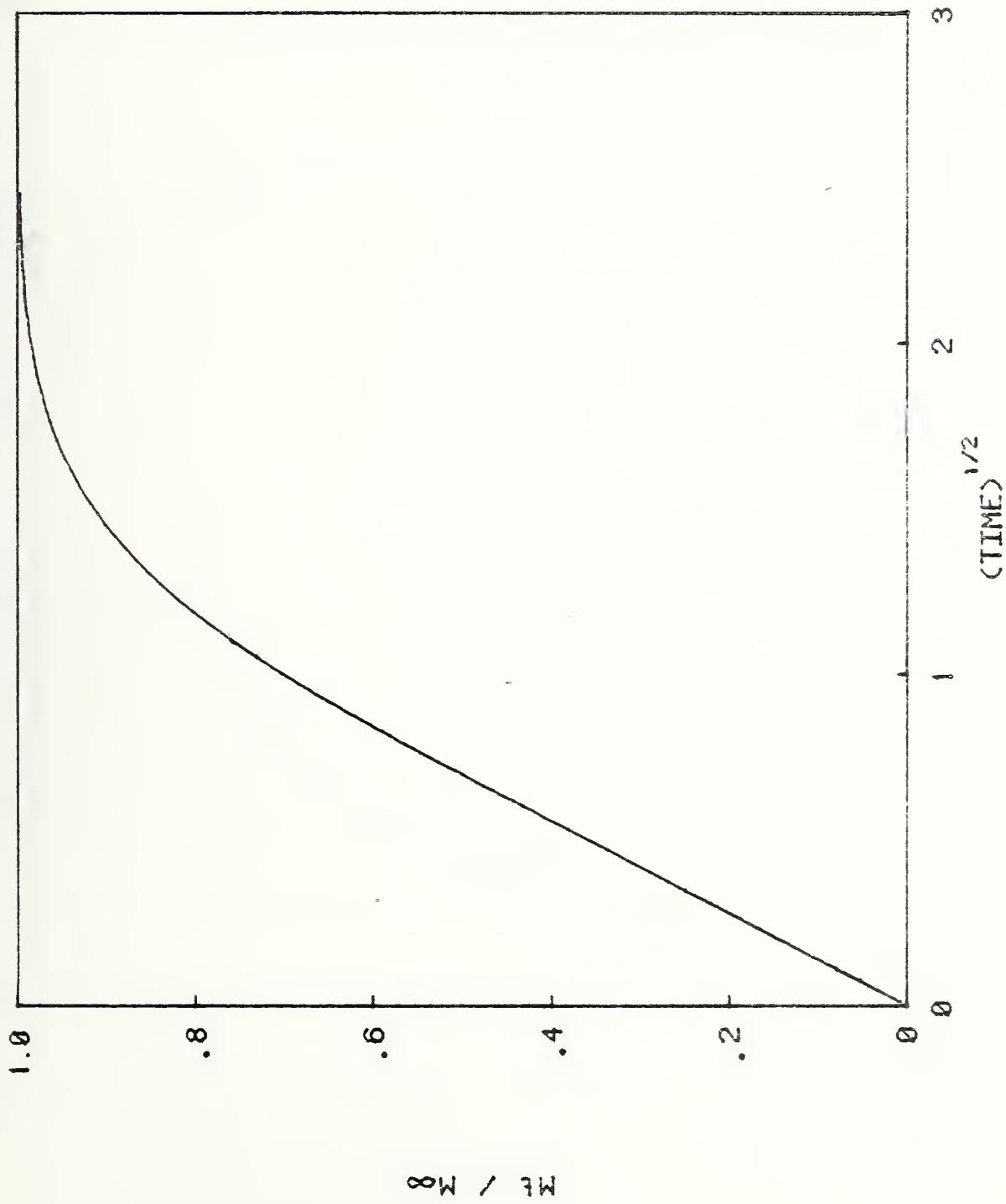
Figure 26 B. Calculated Diffusion Curves M_t/M_∞ versus $(D_H t/\ell^2)^{1/2}$.
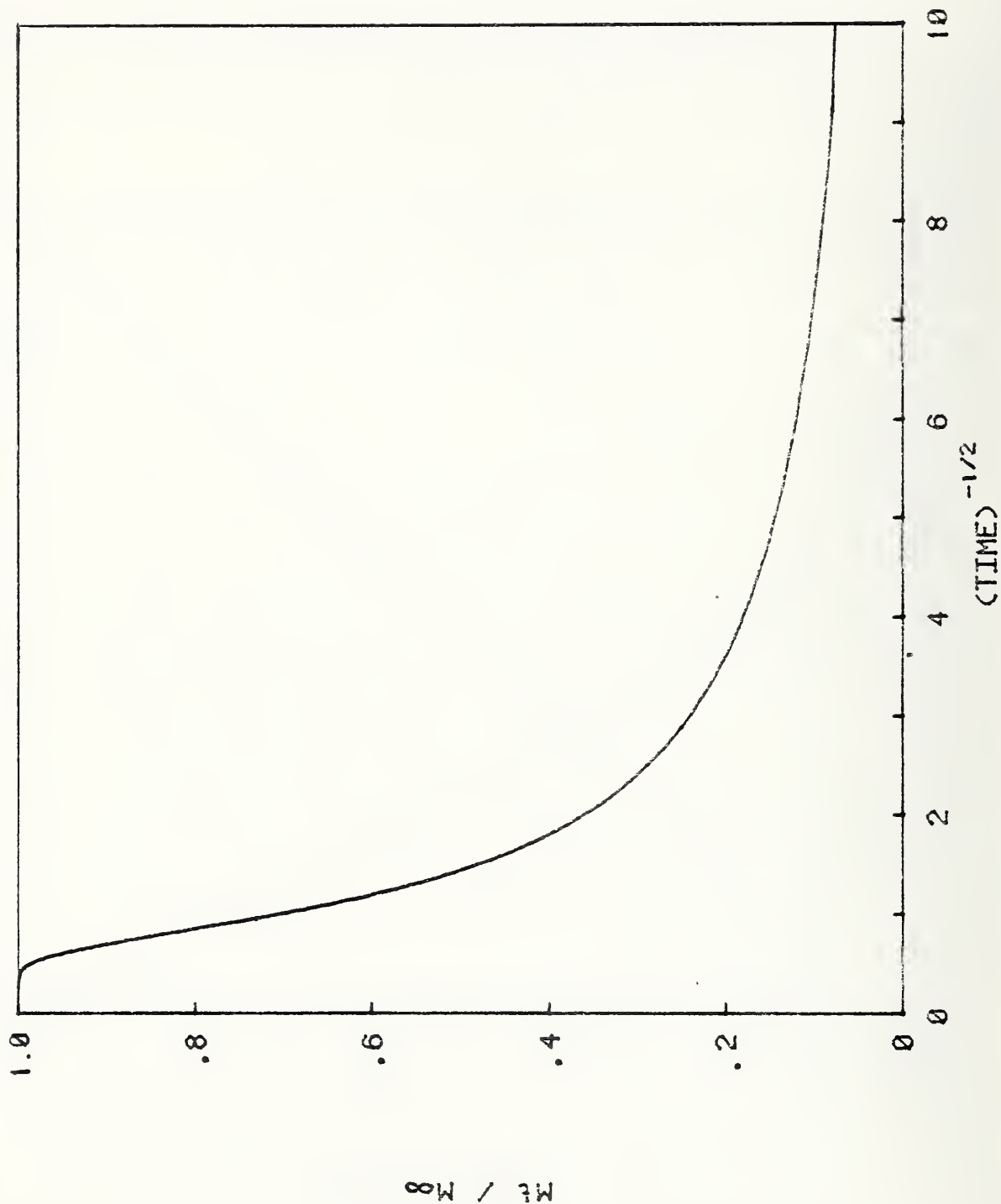
Figure 26 C. Calculated Diffusion Curves M_t/M_∞ versus $1/(4D\pi^2 t/\ell^2)^{\frac{1}{2}}$.
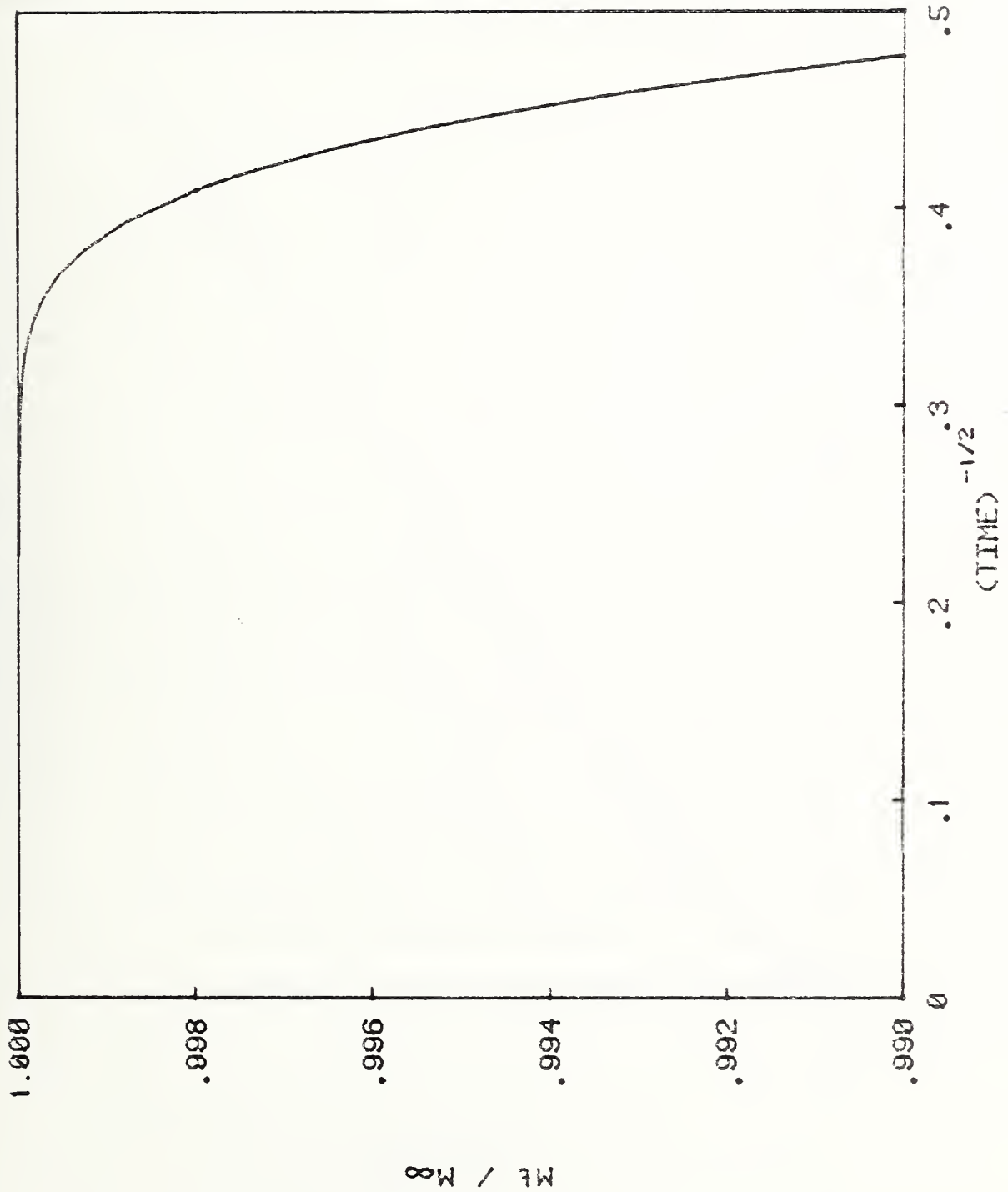
Figure 26 D. Calculated Diffusion Curves M_t/M_∞ versus $1/(4D_\Pi^2 t, \psi^2)^{1/2}$.
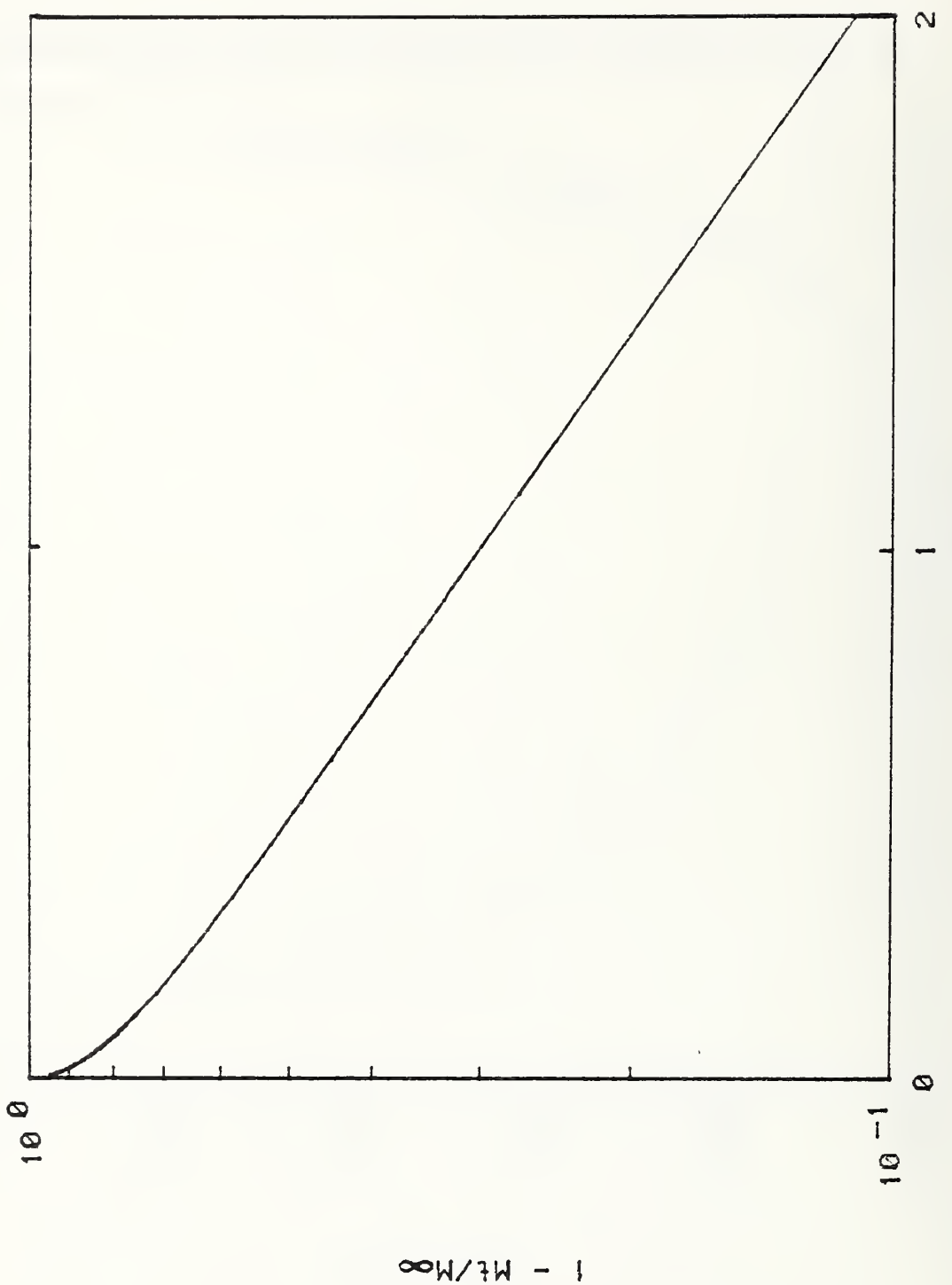
Figure 27. Calculated Diffusion Curves Log($1-M_t/M_\infty$) versus $4D\pi^2t/\ell^2$.

84

compatible in the polymer matrices.

(2) The initial migration kinetics obeyed Fickian behavior, i.e., $M_t \propto t^{1/2}$. This
behavior may be seen as a slope of $d \log(M_t)/d \log t = 1/2$ in Figures 19-25
(A) and a linear portion at small t for M_t vs $t^{1/2}$ in Figures 19-25(B). How-
ever this behavior only lasted to $M_t/M_O \sim 0.2$, or less for these experiments.

(3) There is an apparent enhancement of the diffusion of the additive molecules
by solvent penetration or swelling of the polymer, as seen in Figure 19-25
(B). The behavior cannot be fully described by Eq. (53) and Figure 26, nor
by some simple model described in section II of this report. In Table 7
we see that the amount of solvent absorbed by the test pieces at long times
are generally in the order of 4-5%, with the exception of DH1, for heptane
or octadecane either at 24 or at 60°C. The amount of ethanol absorbed
seems to balance out the weight loss of $C_{18}H_{38}$ of 1%.

Separate weight uptake measurements on unlabeled polyethylene plaques also
indicated a leveling off of weight gain at 4% C_7H_{16} at 24°C after 4 to 48
hours. Approximately 95% of the absorbed C_7H_{16} may be driven off in 24
hours by air·drying or by vacuum evaporation. The remaining 5% of the absorbed
solvent takes much longer time to come out. The weight uptake of octadecane
at 37°C is about 4.5% at 24 hours and about 5% after 500 to 1000 hours.
The time when the polymer reaches saturation swelling by the solvent seems
to correspond to the time with maximum increase in the extraction rate.

(4) When t is large, M_t/M_O vs. $1/t^{1/2}$ plots generally give a linear appearance
as in Figure 19-25 (C). These plots thus yield a reasonable estimate of
M_∞. We used M_O, the initial total amount of additive in the polymer, to
normalize the results here instead of the customary M_∞, the amount desorbed
at infinite time. For the case $d \ln(M_\infty - M_t)/dt \approx -D_O \pi^2/\ell^2$ at large t, it would
take a fitting procedure and some judgment in order to estimate the D_O or
M_∞ values. M_O is more readily available in higher precision than the extra-

85

polated value of M_∞. In most experiments, except for AH1 and BE1, M_0 and M_∞ should be identical. However it is obvious from Figure 19-25 (C) that M_∞ is about 99% of M_0 for the 1% $C_{18}H_{38}$ samples and about 93-94% of M_0 for the 0.01% $C_{18}H_{38}$ samples. One of the likely explanations is that a small portion of the oligomer additive gets incorporated in the crystalline portion of the polyethylene and thus migrates at much slower rates and behaves differently from the additive in the amorphous portion of the polyethylene. Therefore it is rather difficult for the experiments described here to yield any reasonable estimate of the equilibrium partition coefficients for systems favoring the solvents.

(5) The average labeled $C_{18}H_{38}$ content for all samples derived from both sample plaques A and B with sample sizes greater than 1.5 cm X 1.5 cm, is within 1% of 5.15 Mdpm/g—with the exceptions that AH1 and BH1 are about 3-5% off. Both plaques A and B were molded from the same 1% $C_{18}H_{38}$ - polyethylene powder mix. This indicates a relatively uniform sample on a macroscopic scale. The labeled $C_{18}H_{38}$ concentrations in sample plaques C and D are very much different, even though both plaques were molded from the same 0.01% $C_{18}H_{38}$ - polyethylene powder mix.

IV. REFERENCES

1. Flory, P.J., "Principles of Polymer Chemistry", Cornell Univ. Press, Ithaca, N. Y. 1953.

2. Tompa, H., "Polymer Solutions", Academic Press, New York 1956.

3. Flory, P.J. and Rehner, J., J. Chem. Phys., (1943), 11, 521.

4. Rogers, C.E., Stannett, V., and Szwarc, M., J. Phys. Chem., (1959), 63, 1406.

5. Kwei, K.P. and Kwei, T.K., J. Phys. Chem., (1962), 66, 2146.

6. Flory, P.J., Orwoll, R.A., and Vrij, A., J. Amer. Chem. Soc., (1964), 86, 3515.

7. Flory, P.J., J. Amer. Chem. Soc., (1965), 87, 1833.

8. Eichinger, B.E. and Flory, P.J., Trans. Faraday Soc. (1968), 64, 2035.

9. Flory, P.J., Discuss. Faraday Soc., (1970), 49, 7.

10. Sanchez, I.C. and Lacombe, R.H., J. Phys. Chem., (1976), 80, 2352, 2568.

11. Sanchez, I.C., "Polymer Blends", D.H. Paul and S. Newman, editors, Academic Press, N. Y., 1978, Ch. 3.

12. Sanchez, I.C. and Lacombe, R.H., J. Poly. Sci., Polymer Letters Ed., (1977), 15, 71.

13. Sanchez, I.C. and Lacombe, R.H., Macromolecules, 11, 1145 (1978).

14. Bueche, F., J. Chem. Phys., 21, 1850 (1953)

15. Turnbull, D. and Cohen, M.H., ibid, 31, 1164 (1959).

16 Westlake, J.F. and Johnson, M., J. Appl. Pol. Sci., 19, 319 (1975).

17 Crank, J., "Mathematics of Diffusion", Oxford University Press, London (1975).

18 Wagner, H.L., and Verdier, P.H., Editors, NBS Special Publication 260-42, "The Characterization of Linear Polyethylene SRM 1475" (1972)

19 Wang, C.H., Willis, D.L. and Loveland, W.D., "Radiotracer Methodology in the Biological, Environmental and Physical Sciences." Prentice Hall, 1975.

20 Meame, K.D. and Homewood, C.A., "Liquid Scintillation Counting". John Wiley and Sons, 1974

APPENDIX A

Molecular parameters for low molecular weight fluids can be estimated from a known heat of vaporization ΔH_v, a vapor pressure P, and a liquid specific volume v_ℓ all at the same temperature T:

$$r = \frac{\Delta H_v/RT - \ln(v_g/v_\ell)}{1 + (\tilde{v}-1)\ln(1-\tilde{\rho})} \qquad (A.1)$$

$$T^* \equiv \varepsilon^*/R = (\Delta E_v/R)/r\tilde{\rho} \qquad (A.2)$$

$$\rho^* = 1/\tilde{\rho}v_\ell \qquad (A.3)$$

$$v^* = M/r\rho^* \qquad (A.4)$$

$$P^* = RT^*/v^* \qquad (A.5)$$

The reduced density $\tilde{\rho}$ required above satisfies the following equation which must be numerically evaluated:

$$[2\Delta E_v/RT - \ln(v_g/v_\ell)][\tilde{\rho} + \ln(1-\tilde{\rho})] - [\Delta E_v/RT - 1]\tilde{\rho}\ln(1-\tilde{\rho}) = 0 \qquad (A.6)$$

where ΔE_v is the energy of vaporization and v_g is the specific volume of the gas phase.

In deriving the above results we assumed that P was low enough so that the vapor phase could be treated as an ideal gase and that $v_g >> v_\ell$. Under these conditions the entropy of vaporization ΔS_v is given by

$$\Delta S_v/R = \Delta H_v/RT = r[1+(\tilde{v}-1)\ln(1-\tilde{\rho})] + \ln(v_g/v_\ell) \qquad (A.7)$$

and

$$\Delta E_v = \Delta H_v - RT = r\tilde{\rho}/\tilde{T} \qquad (A.8)$$

Using equations (A.7) and (A.8), r and $\tilde{T}$ can be eliminated in the equation of state (12) to obtain (A.6) with $\tilde{P} = 0$.

For a binary solution the only unknown parameter is ΔP^* or Δ (see text). There are variety of experimental methods by which this parameter can be determined. One of the simplest methods is to use solution densities. The equation of state for the solution is formally identical to that for a pure fluid (see Eq. 25) except that the reducing parameters, T^*, P^*, and ρ^* are compostion dependent (see reference 13). At atmospheric pressure $\tilde{P} \simeq 0$, and the equation of state can be solved for T^* which is a function of ΔP^*:

$$T^*(\Delta P^*) = - T[\ln(1-\tilde{\rho}) + (1-{}^1/r)\tilde{\rho}]/\tilde{\rho}^2 \qquad (A.9)$$

Thus measurements of density will yield values of T^* and ΔP^*.

In Appendix B a brief description is given on how liquid densities can be accurately determined on a digital densimeter.

Appendix B

Densities of solutions and solvents are being determined by comparison with standard density fluids in a Mettler/Paar vibrating cell type densimetry system. The densimetry system consists of two external vibrating cells connected to a dual channel processing unit.

For temperature control, thermostat fluid is pumped from an external constant temperature both through the thermal control cylinders of the two cells connected closely in series. With the present temperature control system, the temperature of the thermostat fluid can be selected to within $0.01^\circ C$ and controlled with a variation of less than $\pm 0.01^\circ C$ by a thermistor control sensor and a proportional controller. The effects of small variations in temperature on the density data were suppressed by operating the densimeter in its optional phase-locked-loop mode, in which the oscillation frequency of the cell containing the solution is continuously compared with the oscillation frequency of a second cell containing either a standard density liquid or a solvent of the solution system under investigation. The second cell functions as a time interval standard that responds sympathetically to the same small variations in the thermal environment.

The density measurements in the present report were conducted at temperatures indicated by a copper-constantan thermocouple and a potentiometer which demonstrated a sensitivity of $0.003^\circ C$. The calibration of the thermocouple-potentiometer combination is traceable to a Mueller bridge and a platinum resistance thermometer which in turn had been subjected to a certified calibration in the NBS Thermometry Section. The hot junction of the thermocouple was stationed in the temperature indication tube of that densimeter cell containing the fluid of density to be determined. The uncertainty in indicated temperature was estimated to be $\pm 0.01^\circ C$. Plans are under consideration to improve both control and indication of temperature for future density determinations.

The secondary density standard liquids were standardized by comparison in the densimeter with two primary density standard fluids, the lighter of which was the ambient air of the laboratory, and the heavier primary density standard was a sample of xylene. The density of the air was computed from its temperature in the densimeter cell and the absolute barometric pressure. The density of the primary standard xylene had been determined by Schoonover [1,2] from its buoyancy on high purity silicon single crystals at a series of nine temperatures from $10^\circ C$ to $23^\circ C$. On the basis of

[1] Bowman, H.A., Schoonover, R.M., and Carroll, C.L.
"A Density Scale Based on Solid Objects",
J.Res. Nat. Bur. Stand. (U.S.), 78A 13 (1974)

[2] Bowman, H.A., Schoonover, R.N., and Carroll, C.L.,
"The Utilization of Solid Objects as Reference
Standards in Density Measurements",
Metrologia 10 117 (1974)

these measurements Whetstone et al (3) have reported an expression for density of the primary standard xylene versus temperature as

$$0.884671 - 0.00086147 \ (T, \ deg \ C)$$

with a standard deviation of 1.2×10^{-6} in the fit of density to temperature.

89

Subsequent measurements by Greer [4,5], using the magnetically suspended buoy method, very closely duplicated the thermal density coefficient and indicated it to be linear in the temperature interval from 14°C to 47°C. This value for the thermal density

[3] Whetsone, J.R., Cameron, J.M.,
    Carroll, C.L., and Gallagher, W.H.
    NBS Internal Report 77-1533 (September 1978)

[4] Greer, Sandra C., private communication

[5] Greer, S.C., and Hocken, R.,
    "Thermal Expansion Near a Critical Solution Point",
    J.Chem.Phys. 63 5067 (1975)

coefficient will also be used with the secondary density standard xylene.

The densities of a substantial reserve of two secondary standard liquids, heptane and xylene, were determined at 35°C in the densimeter calibrated with air and the sample of primary density standard xylene:

Sec. Den. Std.	, gcm^{-3} 35.00°C	$\frac{d}{dt}$, gcm^{-3} deg^{-1}
Heptane	0.672157	-0.000840
Xylene	0.854254	-0.00086147

The thermal density coefficient tabulated above for the secondary density standard heptane is quoted by Riddick and Bunger [6] to be applicable in the temperature interval from 0°C to 50°C, and it will be used as a provisional value until either superseded or substantiated by determinations within the present project.

[6] Riddck, J.A., and Bunger, W.B., page 87 in
    "Techniques of Chemistry, Vol. II Organic Solvents -
    Physical Properties and Methods of Purification" 3rd
    (1970) Wiley-Interscience, New York

Mathematical Analysis of Additive Extraction with Solvent Absorption

The plastic is in the shape of a sheet of thickness 2ℓ containing an initial concentration of the additive of c_0. Let s be the position coordinate in the sheet with the surfaces at $x = \ell$ and $x = -\ell$. Then the concentration of the additive is given by the solution of

$$\frac{\partial c}{\partial t} = \frac{\partial}{\partial x}\left(D\frac{\partial c}{\partial x}\right) \qquad (C-1)$$

for the boundary conditions

$$c = c_0 \text{ at } t = 0,\ -\ell < x < \ell \qquad (C-2)$$

$$c = 0 \text{ at } x = \ell \text{ and } -\ell \text{ for } t > 0 \qquad (C-3)$$

In addition to the additive diffusing out of the sheet, the surrounding liquid will diffuse into the sheet. At zero time, its concentration will be 0.
The liquid concentration at the side of the sheet is C_∞ and its diffusion coefficient is D_s. Then by Crank[?]

$$\frac{C_s}{C_\infty} = H = \sum_{n=0}^{\infty} (-1)^n \left[\text{erfc}\frac{(2n+1)\ell-x}{2\sqrt{D_s t}} + \text{erfc}\frac{(2n+1)\ell+x}{2\sqrt{D_s t}}\right] \qquad (C-4)$$

Substituting eqs. 46 and C-4 in eq. C-1 gives

$$\frac{\partial c}{\partial t} = D_0\frac{\partial}{\partial x}\left[(1+KH)\frac{\partial c}{\partial x}\right] \qquad (C-5)$$

where $K = kC_\infty/D_0$ \qquad (C-6)

The concentration of the additive is thus given by the solution of eqs. C-5, C-2 and C-3.
We transform to the reduced variables

$$T = D_0 t/\ell^2 \qquad (C-7)$$

$$X = x/\ell \qquad (C-8)$$

$$C = c/c_0 \qquad (C-9)$$

The eqs. 6 and 7 may be written

$$H = \sum_{p=1}^{\infty} (-1)^{p-1}\left[\text{erfc}\frac{p-0.5-X/2}{\sqrt{TD_s/D_0}} + \text{erfc}\frac{p-0.5+X/2}{\sqrt{TD_s/D_0}}\right] \qquad (C-10)$$

where $p = n + 1$

$$\frac{\partial C}{\partial T} = \frac{\partial}{\partial X}\left(F\ \frac{\partial C}{\partial X}\right) \tag{C-11}$$

where $F = 1 + KH$ $\tag{C-12}$

The boundary conditions eq. C-2 and C-3 become

$C = 1$ at $T = 0$ $\tag{C-13}$

$C = 0$ at $X = 1$ and -1 $\tag{C-14}$

In order to solve eq. C-11 by finite differences, intervals ΔX and ΔT are used, so that,

$X = (I - 1)\Delta X$ $\tag{C-15}$

$T = (J - 1)\Delta T$ $\tag{C-16}$

We choose 2M intervals for X so

$\Delta X = 1/M$ $\tag{C-17}$

By symmetry

$C(X,T) = C(-X,T)$ $\tag{C-18}$

or

$C_{I-2,J} = C_{I,J}$ $\tag{C-19}$

The boundary conditons eqs. C-13 and C-14 are

$C_{I,1} = 1$ $\tag{C-20}$

$C_{M+1,J} = C_{-M+1,J} = 0$ $\tag{C-21}$

By eqs. C-10, C-15 and C-16

$$H_{i,j} = \sum_{p=1}^{\infty} \mathrm{erfc}\left[\frac{p-0.5}{[(J-1)\Delta T D_s/D_o]^{\frac{1}{2}}} - \frac{(I-1)\Delta X}{2}\right] +$$
$$\sum_{p=1}^{\infty} \mathrm{erfc}\left[\frac{p-0.5}{[(J-1)\Delta T D_s/D_o]^{\frac{1}{2}}} + \frac{(I-1)\Delta X}{2}\right] \tag{C-22}$$

The Crank-Nicolson finite difference approximation to eq. C-11 is

$(C_{I,J+1} - C_{I,J})/\Delta T = [C_{I+1,J}(F_{I+1,J} + F_{I,J}) - C_{I,J}(F_{I+1,J} + 2F_{I,J} + $

$F_{I-1,J}) + C_{I,J}(F_{I,J} + F_{I-1,J}) + C_{I+1,J+1}(F_{I+1,J+1} + F_{I,J+1}) - C_{I,J+1}(F_{I+1,J+1}$

$+ 2F_{I,J+1} + F_{I-1,J+1}) + C_{-1,J+1}(F_{I,J+1} + F_{I-1,J+1})]/[4(\Delta X)^2]$ $\tag{C-23}$

Eq. C-23 is rearranged to give

$A_{I,J}C_{I-1,J+1} + B_{I,J}C_{I,J+1} + E_I C_{I+1,J+1} = G_{I,J}$ $\tag{C-24}$

92

$$A_{I,J} = F_{I+1,J+1} + F_{I-1,J+1} \tag{C-25}$$

$$B_{I,J} = -(F_{I+1,J+1} + 2F_{I,J+1} + F_{I-1,J+1} + R) \tag{C-26}$$

$$E_{I,J} = F_{I+1,J} + F_{I,J+1} \tag{C-27}$$

$$G_{I,J} = -(F_{I,J} + F_{I-1,J})C_{I-1,J} + (F_{I+1,J} + 2F_{I,J} + F_{I-1,J} - R)C_{I,J}$$

$$- (F_{I+1,J} + F_{I,J})C_{I+1,J} \tag{C-28}$$

$$R = 4(\Delta X)^2/\Delta T \tag{C-29}$$

For $I = 1$ and M, eq. C-25 must be modified for the boundary conditions eq. C-19, C-23 and C-24 to be

$$B_{1,J}C_{1,J+1} + (A_{1,J} + E_{1,J})C_{2,J+1} = G_{1,J} \tag{C-30}$$

$$A_{M,J}C_{M-1,J+1} + B_{M,J}C_{M,J+1} = G_{M,J} \tag{C-31}$$

The distributions of the concentration of the additive in the plastic sheet is computed as follows: For $J = 1$ ($T = 0$), $C_{I,1} = 1$ by eq. C-13. Eqs. C-24, C-30 and C-31 give linear simultaneous equations for the concentrations at $J + 1$ in terms of concentrations at J. Solving these equations for $J = 1, 2, 3$ etc. give the concentration distribution versus J or T.

For the case that the liquid diffuses as a front, shown in Fig. 3, the concentration of the liquid is given by

$$\frac{C_s}{C_\infty} = H = \frac{x - \ell + w\sqrt{t}}{\sqrt{t}} \qquad \text{for } x > \ell - \sqrt{t}$$

$$= 0 \qquad \text{for } 0 \leq x \leq \ell - w\sqrt{t} \tag{C-32}$$

We define the reduced value

$$U = w/\sqrt{D_o}$$

Then Eq. C-32 is written

$$H = \frac{X + U\sqrt{T} - 1}{U\sqrt{T}} \qquad \text{for } X < 1 - U\sqrt{T}$$

$$= 0 \qquad \text{for } 0 < X < 1 - U\sqrt{T} \tag{C-33}$$

The calculation is then the same as previously with Eq. C-33 replacing Eq. C-10.

Appendix D

Let diffusion occur in a polymer exposed to a temperature that varies with time, t. The diffusion constant $D(t)$ will then also vary with time. Diffusion will be controlled by the equation

$$\frac{\partial C}{\partial t} = D(t)\frac{\partial^2 C}{\partial X^2} \qquad \text{(D-1)}$$

where C is the concentration of the additive in the polymer. As shown by Crank,[17] substituting

$$w = \int_0^t D(t^1)dt^1 \qquad \text{(D-2)}$$

gives

$$\frac{\partial C}{\partial w} = \frac{\partial^2 C}{\partial X^2} \qquad \text{(D-3)}$$

Now consider diffusion in the polymer exposed to the constant temperature T_e. The diffusion equation is then

$$\frac{\partial C}{\partial t} = D(T_e)\frac{\partial C^2}{\partial X^2} \qquad \text{(D-4)}$$

By the substitution

$$v = tD(T_e), \qquad \text{(D-5)}$$

the diffusion equation D-4 gives

$$\frac{\partial C}{\partial v} = \frac{\partial^2 C}{\partial X^2} \qquad \text{(D-6)}$$

At the equivalent test temperature, the diffusion given by the solution of Eq. D-6 is required to be the same as if the polymer was exposed to a varying test temperature which is given by the solution of Eq. D-4. Because the equations are of the same form, their solutions will be equal if

$$w = v \qquad \text{(D-7)}$$

Substituting Eqs. D-2 and D-5 in Eq. D-7 gives the condition

$$D(T_e) = \frac{1}{t}\int_0^t D(t^1)dt^1 \qquad \text{(D-8)}$$

The diffusion constant varies with temperature by the relationship

$$D = D_o \exp(-E/RT) \tag{D-9}$$

Substituting Eq. D-9 in Eq. D-8 gives Eq. 50.

Let the polymer be exposed to a constant temperature T_1 for a time ft and a constant temperature T_2 for a time $(1-f)t$. Substituting in Eq. 3, the integral may be evaluated to give Eq. 49.

The equations D-1 and D-4 apply to diffusion in a plane sheet. However, as mentioned in Reference 17, the same results may be similarly derived for diffusion in a plane sheet, cylinder or sphere.

NBS-114A (REV. 9-78)

U.S. DEPT. OF COMM. BIBLIOGRAPHIC DATA SHEET	1. PUBLICATION OR REPORT NO.	2. Gov't. Accession No.	3. Recipient's Accession No.

4. TITLE AND SUBTITLE "Models for the Migration of Paraffinic Additives in Polyethylene"	5. Publication Date
	6. Performing Organization Code

7. AUTHOR(S) L. E. Smith, I. C. Sanchez, S. S. Chang, and F. L. McCrackin	8. Performing Organ. Report No.

9. PERFORMING ORGANIZATION NAME AND ADDRESS NATIONAL BUREAU OF STANDARDS DEPARTMENT OF COMMERCE WASHINGTON, DC 20234	10. Project/Task/Work Unit No.
	11. Contract/Grant No.

12. SPONSORING ORGANIZATION NAME AND COMPLETE ADDRESS (Street, City, State, ZIP) Same as Item 9	13. Type of Report & Period Covered Annual 10/1/77 - 9/30/78
	14. Sponsoring Agency Code

15. SUPPLEMENTARY NOTES

☐ Document describes a computer program; SF-185, FIPS Software Summary, is attached.

16. ABSTRACT *(A 200-word or less factual summary of most significant information. If document includes a significant bibliography or literature survey, mention it here.)*

General physical models of the migration of low molecular weight species in polymer matrices are needed to provide a basis for the efficient regulation of plastics used in food contact applications. This report presents the first year's progress on a project containing both theoretical and experimental elements aimed at producing such models. Using a modified equation of state approach, models have been developed for estimating the equilibrium partitioning of a diffusant in a polymer at a temperature above its glass transition in contact with a finite volume of solvent. Some possible new approaches to a diffusion theory based on volume fluctuations were outlined. Model calculations using diffusion equations have been made for the extraction of additives from polymers with concomitant solvent absorption and for finding a constant extraction temperature equivalent to migration under varying temperature conditions. The migration of an oligomer, ^{14}C-labeled octadecane, from high density linear polyethylene into various solvents at different temperatures was measured in order to elucidate the effects of thickness, temperature, concentration and solvent. Deviations from ideal Fickean kinetics in the experimental results may be attributed to the strong influence of swelling of the polymer on the migration rates and to the possible incorporation of a small portion of the oligomer in the crystalline phase of the polymer.

17. KEY WORDS *(six to twelve entries; alphabetical order; capitalize only the first letter of the first key word unless a proper name; separated by semicolons)*

Additives; diffusion; food additives; indirect additives; migration; models; regulation.

18. AVAILABILITY	☒ Unlimited	19. SECURITY CLASS (THIS REPORT)	21. NO. OF PRINTED PAGES
☐ For Official Distribution. Do Not Release to NTIS		UNCLASSIFIED	
☐ Order From Sup. of Doc., U.S. Government Printing Office, Washington, DC 20402, SD Stock No. SN003-003-		20. SECURITY CLASS (THIS PAGE)	22. Price
☐ Order From National Technical Information Service (NTIS), Springfield, VA. 22161		UNCLASSIFIED	

USCOMM-DC